Técnico Lisboa

Techno-economic assessment of semi-submersible FOWT concepts

Tomás Norton de Matos Cortes

Thesis to obtain the Master of Science Degree in

Mechanical Engineering

Supervisors: Prof. José Alberto Caiado Falcão de Campos
Dr. Marco Aurélio Araújo Alves

Examination Committee

Chairperson: Prof. Carlos Frederico Neves Bettencourt da Silva
Supervisor: Dr. Marco Aurélio Araújo Alves
Member of the Committee: Prof. Luís Manuel de Carvalho Gato

November 2019

Acknowledgments

Fistly, I'd like to sincerely express my gratitude to both my supervisors, prof. Falcão de Campos and dr. Marco Alves, for their wise guidance and teaching.

A mention to WavEc workers who have always manifested availability and willingness to share their knowledge. To Juan Portillo who has gently given some of his time for clarifying some issues regarding Hydrodyn.

I also want to acknowledge Diogo Líbano Monteiro and Mafalda Almeida e Brito for their valuable help regarding the writing process.

To "Os Selvagens", with whom this Master degree's challenges have been shared.

To all those exceedingly enthusiastic and committed professors with whom I've had the chance to learn throughout my IST years.

To my family and friends for their unconditional support throughout my life and specially during the thesis-making period.

I also want to praise "Rainha da Tese" for the many graces provided in the last six months.

Abstract

The objective of the present thesis is to assess the possibility of a more accurate and trustful methodology regarding the annual energy production estimation of a floating wind turbine. The conventional approach is to integrate the turbine's power curve along a given Weibull wind distribution. The alternative proposed involves the use of numerical simulations with the OpenFAST code. Furthermore, an economic sensitiveness analysis is performed, with a suitable model from WavEC.

An introduction to the renewable energies field is presented, which ends tilting towards a discussion on present challenges and endeavours regarding the wind power industry. Special focus is attributed to its floating offshore sector.

The numerical tool is explored through the analysis of the set of modules that constitute it. The goal is to reach a more accurate and confident framing of the final results through the evaluation of the computer-implemented models and assumptions considered. Following, consistency tests are carried out in order to numerically check the model's validity.

Finally, the energy topic is dealt with and compared for the two suggested approaches. An economic analysis aiming at assessing the LCOE's sensitiveness to some determining factors is also presented. Such study also allows an insight into the relevance of the numerical approach proposed.

Resumo

O objectivo desta tese é o de aferir a possibilidade de tornar o cálculo da energia produzida anualmente por uma turbina eólica flutuante mais fidedigno. Ao método mais convencional de integração da curva de potência da turbina numa dada distribuição de Weibull de vento propõe-se uma alternativa baseada em simulações numéricas realizadas com o código OpenFAST. Procede-se, também, a uma análise de sensibilidade económico-financeira recorrendo a um modelo disponibilizado pelo WavEC.

Apresenta-se uma introdução ao panorama das energias renováveis, convergindo numa mostra e debate dos actuais desafios e desenvolvimentos relacionados com a indústria eólica, com especial foco no sector marítimo flutuante.

Procede-se a uma análise da ferramenta numérica através do estudo dos vários módulos que a constituem. Trata-se duma avaliação dos modelos implementados e hipóteses consideradas, a fim de obter um enquadramento dos resultados finais mais preciso e, por isso mesmo, mais confiante. Acto contínuo, testes de consistência são feitos a fim de consolidar a validade do modelo usado.

Finalmente, a problemática da energia é abordada e comparada, recorrendo aos dois métodos em diálogo. De seguida, apresenta-se um exercício de análise económica pretendendo aferir a sensibilidade do custo de energia em relação a alguns factores determinantes. Este permite também avaliar a relevância da abordagem numérica proposta.

Palavras-chave: Energias renováveis, estiamtiva de produção de energia, turbinas eólicas flutuantes, métodos numericos, análise económica

Contents

List of Tables

List of Figures

Nomenclature

A_∞	Infinite frequency added mass matrix
A_{wave}	Wave amplitude.
C_D	Normalized viscous drag coefficient.
C_{hydros}	Linear hydrostatic restoring matrix.
d	Water depth.
D	Diameter.
$dF^{viscous}$	Infinitesimal viscous force.
F_{aero}	Aerodynamic force.
$\hat{f}_{exc}$	Complex wave excitation force per unit wave amplitude.
F_{exc}	Excitation force.
F_{hydro}	Hydrodynamic and Hydrostatic force.
F_{hydrod}	Hydrodynamic force.
F_{hydros}	Hydrostatic force.
F_{platf}	Total platform force.
F_{rad}	Radiation force.
F_{RD}	Radiation memory effect force
g	Gravitational constant.
H_s	Significant wave height.
K	Kernel of the convolution.
k	Wave number or stiffness.
m	Mass.
P_{ext}	Extracted power
$\overline{P}_{wave}$	Average energy flux per unit wave crest length
$\ddot{q}$	Acceleration vector
q	Displacement vector
$\dot{q}$	Velocity vector
r	Discount rate.
t	Time.
T_e	Energy period.
T_{gen}	Generator torque

U	Wind speed
V_o	Displaced volume of water at platform undisplaced position.
w_{gen}	Generator angular velocity
Φ_D	Diffraction complex potential
Φ_E	Excitation complex potential
Φ_I	Incident wave complex potential
Φ_R	Radiation complex potential
α	Power law exponent
α	Angular acceleration modulus.
β	Angular resolution of a stepper motor.
η	Efficiency.
η	Free surface elevation
λ	Wave wavelength
ξ	Damping ratio
ρ	Density.
ω	Wave frequency
ω_d	Damped frequency
ω_n	Natural frequency

Glossary

2D	Two-Dimensional
3D	Three-Dimensional
AEP	Annual Energy Production
BFOW	Bottom Fixed Offshore Wind
BFW	Bottom-Fixed Wind
CAE	Computer Aided Engineering
CAPEX	Capital Expenditures
CM	Center Of Mass
COB	Center Of Buoyancy
DECEX	Decommissioning Expenditures
DOF	Degree Of Freedom
FAST	Fatigue, Aerodynamics, Structures and Turbulence
FOW	Floating Offshore Wind
FOWT	Floating Offshore Wind Turbine
FW	Floating Wind
HAWT	Horizontal Axis Wind Turbine
HOM	High-Order Method
JONSWAP	Joint North Sea Wave Project
LCOE	Levelized Cost of Energy
LOM	Low Order Method
MSL	Mean Sea Level
NREL	National Renewable Energy Laboratory
OC4	Offshore Code Comparison Collaboration Continuation
OHVS	Offshore High Voltage Station
OPEX	Operational Expenditures
PV	Photo-Voltaic
RD	Research and Development
RPM	Revolutions per Minute
SWL	Sea Water Level
TRL	Technology Readiness Level

TSR	Tip-Speed Ratio
VIV	Vortex Induced Vibration
WACC	Weighted Average Cost of Capital
WAMIT	Wave Analysis Massachusetts Institute of Technology
WavEC	Wave Energy center

Chapter 1

Introduction

1.1   Socio-economic and political framework on renewable energy

Undeniably, environment awareness and a responsible energetic resource exploration,commercialization and utilization is on the forefront of the global political, social and economic agenda. International groups, organizations, institutions as well as governments are increasingly more committed to take serious action in regard to a clean energy transition, to replace fossil fuels and to preserve earth's fragile equilibrium.

Many protocols have been signed, such as the Kyoto protocol, 1997 and the Paris Agreement, 2016, though many others have preceded these. The means to pursuit their goals have started to come into action. The European Union, for example, has established a 32% renewable energy target for 2032, with a possible increased revision of that value, due to the expected decrease in the cost of renewable technologies [1]. At the same level, civil societies are more and more conscious about the issues raised by disordered, simply cost-driven answers to societies energetic demands. By pressuring their representatives and leaders not to ignore such problems, they constitute themselves as important change-drivers.

Moreover, factors such as economy, social justice and social well being, among others, also play a role in this discussion, thus broadening it far from a simply "ecological" (in the strict meaning of the term) frame.

In order to fulfil the above mentioned long-term objectives, the interest in renewable sources of energy has boosted enormously. Specially after the oil shortages of the 1970's, wind energy appeared as a strong appealing alternative for the oil-dependent economies. Thus, wind-powered energy increasingly became an important electricity source. For example, in the U.S.A., the share of electric energy generated from wind increased from around 1% in 1990 to almost 7% in 2018. China has currently the world's largest wind electricity generation capacity [2]. In Europe, in 2018, 14% of the energetic demand was met by wind energy [3].

Figure 1.1 presents the generalized world trend concerning renewable power installed capacity is presented. As it can be seen, both onshore wind as well as solar photovoltaic have soared their numbers while the other technologies have more or less kept their capacity. An important remark is due to offshore

wind. Barely neglectful in the first decade analysed, it has dramatically soared in less than ten years. Indeed, a growth of over thirteen fold took place from 2008 to 2017 [4].
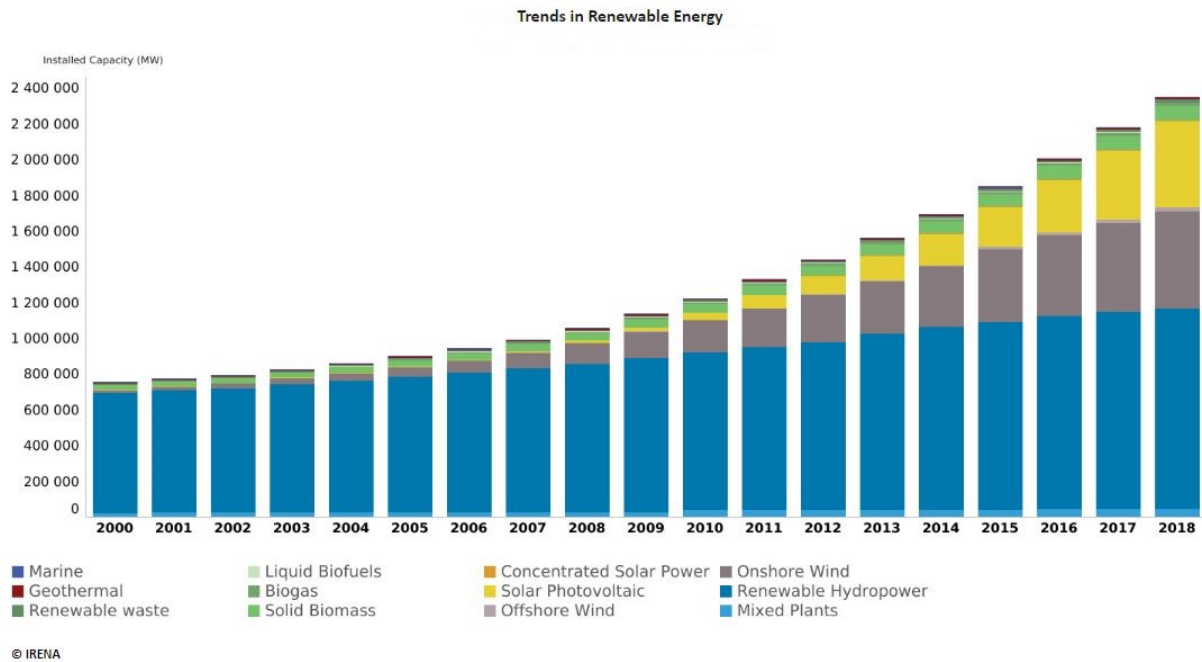
Figure 1.1: Renewable installed capacity growth in [5]

1.2 Offshore wind energy

A technological overview and an acknowledgement of the state of the art of the offshore wind industry is presented in this section.

1.2.1 Technological framework and state of the art

With regard to extracting energy from wind power in offshore conditions, there are two possibilities: either through bottom-fixed turbines or by means of a turbine coupled to a floating structure which is kept in place with a mooring system. The main constraint that defines which of these two is used is water depth. In fact, sea bed-attached structures cannot be used in waters deeper than about 40 to 50m [6]. However, the average depth of installed structures is much lower: Indeed, for farms under construction in 2018, it was 27,1 m [7]. This already represents an increase, if compared with an average depth of 16 m for turbines operating in 2013 [8]. On the other hand, floating devices can be used in water depths of up to 300 m, having the potential to reach up to 700 m [8]. Naturally, the deeper and farther away from the coast the wind farm is set up, the more expensive it will tendentiously be (as there are other factors driving cost). As an example, the average distance of operational wind farms from shore in 2013 was of only 29 km [8].

Figure 1.2 presents an overview of the main configurations of turbine foundations for offshore wind.
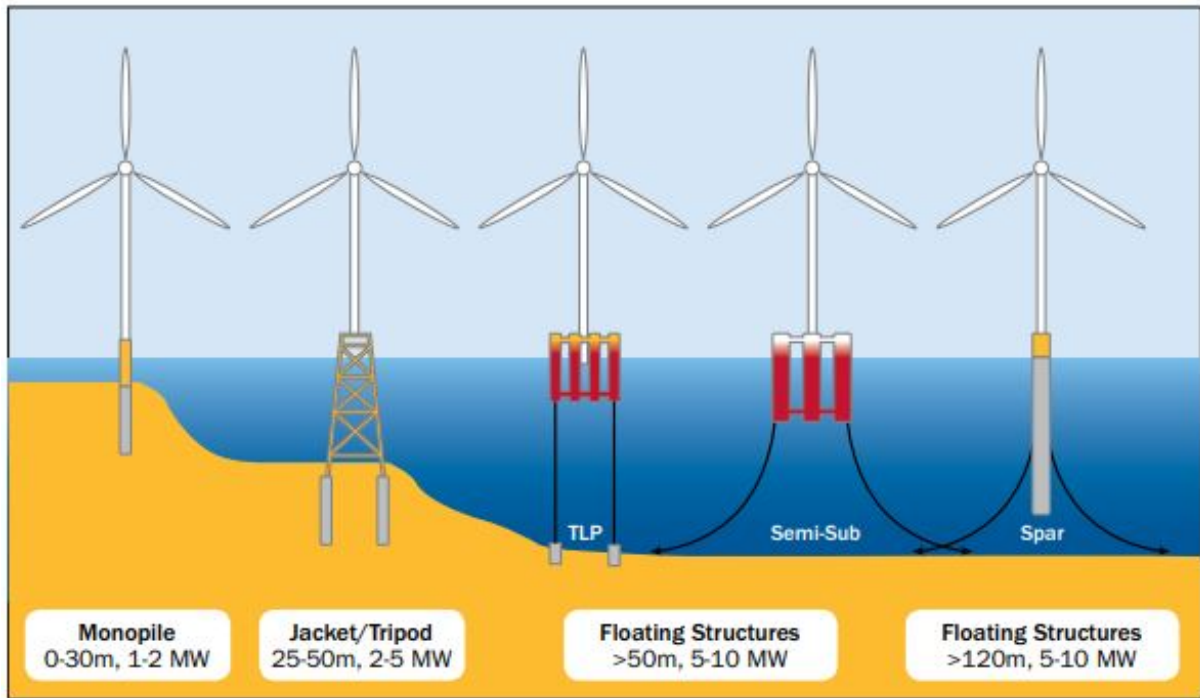
Figure 1.2: Typical offshore wind structures in [6]

As it may be seen in the graph that follows, the average rated power (as well as height and all other dimensions, consequently) has been steadily increasing for the last 20 years, reaching a value of 7 MW. The biggest turbine in the world to be deployed offshore, the V164-8.8 MW from MHI Vestas Offshore Windhas been connected in 2018 [7]. A 10 MW from MHI Vestas turbine is already available for sale [9].
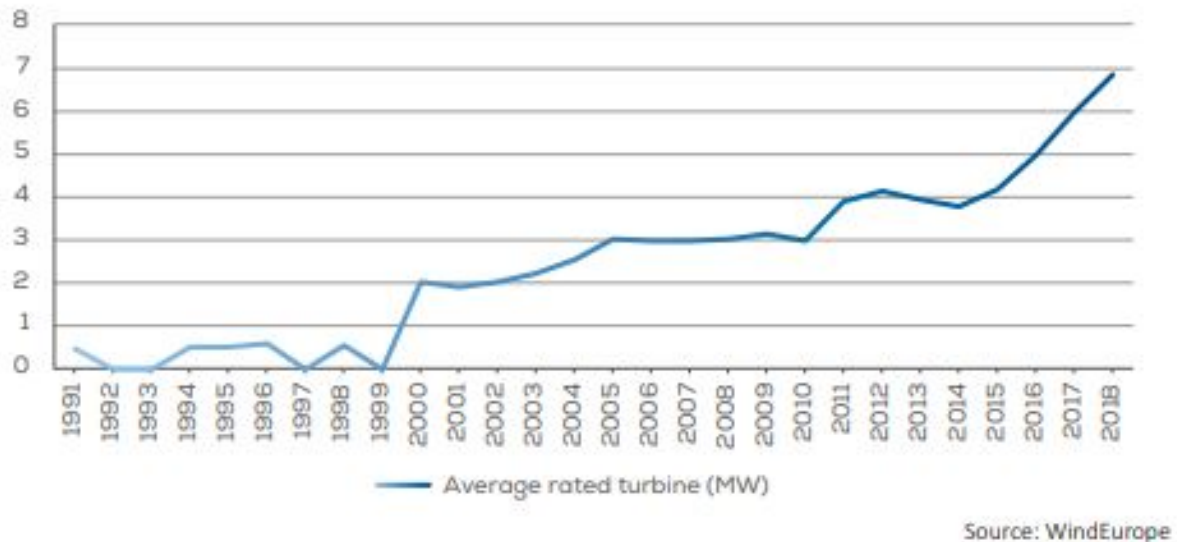
Figure 1.3: Yearly average of newly installed offshore wind turbine rated capacity (MW), in Europe, in [7]

At present, the mainstream turbine concept being used is a upwind three-bladed rotor. Two-bladed variants as well as downwind systems are being studied as potential alternatives, although there are almost no such wind turbines being used [10]. They have some advantages: theoretically, downwind

rotors do not need a yaw mechanism as they weathervane alone. The rotor, as it has less restriction on bending deformation, can be made lighter and thus, cheaper. The setback is that the shade from the tower influences negatively the wind field from which the rotor extracts energy [11]. An interesting example of such concept is provided by X1 Wind which is developing a disruptive floating wind system [12]. As far as two-bladed wind turbines are concerned, they present two main advantages: they have one less blade, thus reducing the material involved and the cost of manufacturing. Their assembly is also easier when compared with the three-bladed standard (this is especially relevant for offshore sites) [10]. Nautica Windpower is an exemple of a company developing a two-bladed downwind solution [13].

Nowadays, most of the offshore wind energy is extracted using turbines attached to the sea bed. In fact, there was in Europe, in 2017, a total installed capacity of 16387 MW [4] (regarding offshore wind). Not a single MW came from a commercial FOWT (floating offshore wind turbine). If pre-commercial FOWT's are taken into account (30MW Hywind project and 25 MW WindFloat Atlantic, with commissioning dates of 2017 and 2020, respectively [14]), they would still represent less than 0,5% of the total capacity installed at sea.

However, floating offshore wind is increasingly looked upon as a potential alternative, as much of the world wind resources are located in areas only accessible to such concepts. This also brings up new challenges and difficulties that are to be discussed later.

1.2.2   Discussing onshore, bottom-fixed and floating offshore wind

There are a lot of important reasons for offshore wind to become a very attractive source of energy, not to say almost mandatory if Europe and other countries are to achieve its ambitious clean energy goals. A brief discussion between onshore and offshore wind, followed by the pros and cons of FOW and BFOW is presented in this section.

Pros and cons of onshore and offshore wind

First of all, offshore wind is stronger, more constant (both in intensity and in direction) and less turbulent than onshore [15]. This has dramatic implications, if taken into account that wind power is proportional to the cube of wind speed and that turbines are optimized for a given wind speed. Thus, the more constant the wind speed is, the more efficient will be the turbine assigned to a specific site. These two factors alone (increased intensity and constancy) are very much the main drivers for developing offshore solutions. In fact, this is what is driving the industry to increasingly build turbines with higher rated power for the offshore market.

For instance, in 2018 the average onshore wind capacity factor was of only 22%, while offshore wind's was around 37% [3].

Offshore wind has a much smaller negative social, cultural and environmental impact (in some cases visual hazards are absolutely eliminated). Though care is obviously needed when assessing offshore projects (specially for wildlife-related issues), the benefits when compared with the onshore industry are patent. In fact, Denmark conducted an environmental assessment in two of the biggest offshore wind

farms in the world [16] and [17], proving many concerns related with such projects are not considerable. Although the report is cautious as to the long-term solidity of its remarks, it even noted beneficial outcomes from the wind farms due to reefs growth around the structures.

Another important advantage over onshore wind is the vast area availability. Although this pro is specially patent in FOW, to some extent it is also true for BFW: Onshore wind is limited to very specific sites such as big plains, deserts or mountains. As far as the optimization of farms layout in mountains is concerned this is an huge setback. Indeed, each turbine location is very limited to the mountain shape, not being possible to dispose them solely based on a wind direction/optimal production criteria. Wake problems are thus much more prone to affect onshore wind farms energy outputs than offshore deployments.

Other relevant factor is electricity offer/production-demand phase. This point is somehow dependent on geographical and meteorological conditions of each site. Nevertheless, offshore wind blows stronger during the day matching high demand from the the network and consumers. On the other hand, onshore wind is more intense at night, when electric demand is lower, thus complicating its use [18]. Moreover, in many coastal cases where the majority of the global population lives, the proximity to major electrical network lines represent another advantage, as that part of the infrastructure is already set up.

One of the downsides of offshore wind, however is its cost. More robust structures, more complex installation, more hazardous operating and maintenance conditions make the LCOE of offshore wind less competitive than onshore. BFOW's LCOE is currently, in average the double of onshore wind's [19]. However, due to improvements in technology, know-how and optimized procedures, it's expected that the LCOE of BFOW will be less than that of onshore wind, in a few years [20]. As far as FOW is concerned, the costs are still much higher, not being yet commercially competitive. The cost drivers are manifold and site-dependent, having many influential factors. The scope of this brief discussion is merely to assess the current general cost situation, and not to deeply evaluate specific cost-related factors of both technologies (such as grid connections, distances, logistics,...).

Finally, there's an important point to underline which is the experience and expertise gained throughout the years. The first onshore wind electricity generators were set in the end of the 19th century, more than 100 years ago...[21]. The first offshore wind farm, on the contrary, has been set in 1991, less than 30 years ago. It has only been decommissioned in 2017 [22]. It doesn't exist any commercial FOWF at present. This figures, by themselves, indicate the difference regarding industrial experience between the different solutions. This raises issues concerning lack of experienced human resources. However successful some offshore wind concepts might have already proven, they still lack the same degree of confidence and trust, built upon decades of industrial involvement, studies, research and improvements, that the onshore concepts enjoys.

Motivation for FOW

All that has been previously described,though in relation to offshore wind as a general field, applies to FOW in particular. The questions is: why, then, is there any interest in FOW if it's more expensive, technically more complex and risky? There are, indeed, advantages and there is a need to study, develop

and invest in floating concepts.

Firstly, FOW permits a much higher flexibility regarding the site choice as the depth constrain is very much weakened (this is important because many zones can be critical in regard to some factors: fisheries, ecology, ship lanes,...). Some wind farms are set very far away from the coast (what increases the costs and complexity of the project, regarding production, installation and maintenance) because the near-to-coast sites are not suitable for BFOW. If FOW was to be used, then the distance between the farm and the onshore power station could be much shorter, reducing costs. In some countries, FOW might even be the unique solution due to deep sea beds (as in Portugal). This issue, wind vs depth, will be explored later.

COUNTRY / REGION	SHARE OF OFFSHORE WIND RESOURCE IN +60m DEPTH	POTENTIAL FOR FLOATING WIND CAPACITY
Europe	80%	4,000 GW
USA	60%	2,450 GW
Japan	80%	500 GW
Taiwan	-	90 GW

Figure 1.4: Potential for floating offshore wind in [14]

As can be seen in figure 1.4, the vast majority of offshore wind potential is located in sites for which BFOW is neither technological nor economical viable. Thus, opening an opportunity window for FOW, which is the only concept that might unlock those huge energy resources, is a necessary condition if wind is to play an important role in the future's global energy mix.

1.2.3 FOW challenges and drawbacks

As with almost all renewable energy solutions, predictability and readiness to produce is a major concern. Wind is perhaps the most affected technology in this respect. In fact, as wind is not controllable, it is difficult to perfectly match production offer with demand, leading to restrictions regarding the potential extent of eolic share in a nation's energy mix and challenges to manage the installed capacity [23]. There are meteorological forecasts to help managing wind power production but even these are not 100% trustful, leading to difficulties and eventually some randomness (having said this, the offshore wind is still better than onshore, as concluded previously and increased number of turbines and geographical dispersion tends to damp this variability concern!). Low capacity factors also constitute an important setback (the reasons for such low capacity factors, are different from those of conventional power plants: they are dependent on wind availability, while conventional power plants have barely no restrictions but for their operators' strategy and will).

But certainly the most challenging issue concerning FOW is its cost. FOW is in its infancy and therefore currently has high costs, particularly for early prototype and pre-commercial arrays. However,
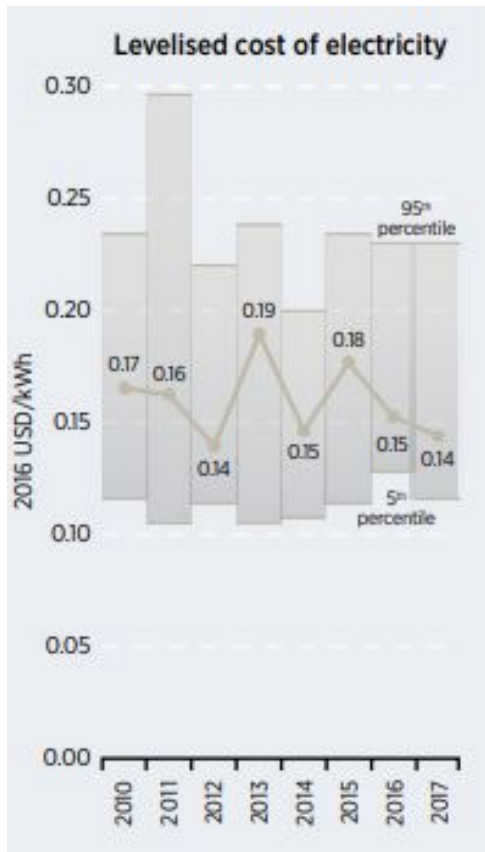
(a) BFOW wind LCOE's evolution
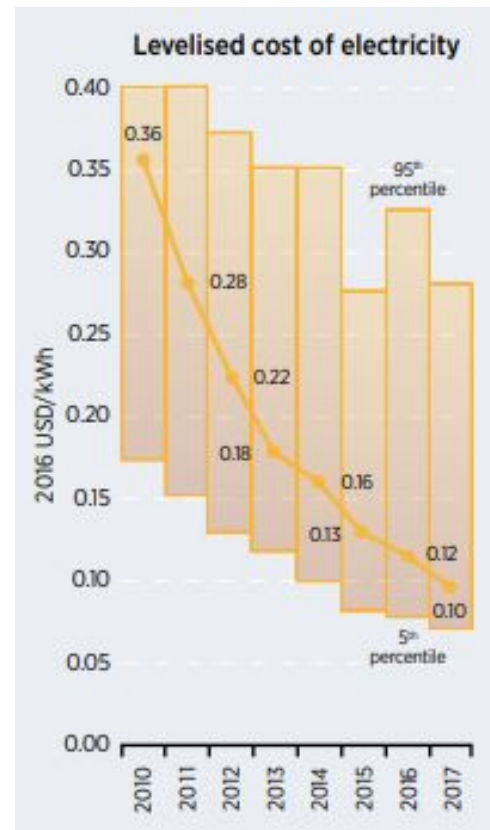
(b) Solar PV LCOE's evolution

Figure 1.5: Comparison of offshore wind and solar PV's LCOE reduction, from [19]

early prototypes do not reflect the true costs that can be expected with mass deployment, once designs have been optimised to reduce structural weight, introduce novel component technologies, improve installation methods, adopt serial fabrication processes, and benefit from scale effects more generally [24].

In fact, another difficulty in the upcoming years is related with competitive renewable energy sources, mainly solar PV. In fact, solar PV's LCOE, as per 2017, is 40% cheaper than offshore wind's [19]. But even more suggestive than present day LCOE's is their evolution.

This figures doesn't mean offshore wind industry has not the capacity to reduce the costs involved in its power production, but simply that it is behind solar PV industry. Nevertheless, as the world is urging for new renewable energy sources, such competitive lag might be crucial for the long term development and growth of the offshore wind business. And a LCOE's reduction is always a consequence of more investment and trust, what shoes an inclination of renewable energy investors towards such technology, strengthening its growth momentum.

Although this is expected to change in the future, as previously stated, the current "status quo" makes the concepts too expensive to be economically attractive and draw investors.

Due to a lack of experience, operational proofs and certainties, this technology is looked as financially risky and very expensive, and government subsiding mechanism to launch floating projects are scarce(which is what is needed in a fresh industry to launch it) [24]. This prevents its growth, minimizing

7

companies interest and will to invest, what again slows down the business emergence. Hence, it's necessary a political compromise and a stable regulatory framework while keeping and increasing the existing funding. All in all, the investment risk drives off public and private funding.

There are risk and concerns related to the environment. These are, nevertheless, expected to be less important than on BFOW and onshore wind (due to the higher freedom in choosing the FOWT's placement, allowing to pick less fragile and susceptible zones). The potential environmental problems are related with increased noise levels, risk of collisions, changes to benthic and pelagic habitats, alterations to food webs, and pollution from increased vessel traffic or release of contaminants from seabed sediments.[8]

1.2.4   Growing trend and the sector's dynamism

In fact, although there are not fully commercial projects on the run, many countries are investing in pre-commercial/research endeavours, many of them being multi mega-watt. If taken into account how recent these are, and how there was not almost any multi mega-watt and multi-turbine floating wind farm a few years ago, the growth is particularly striking. To illustrate such claim, figure 1.6 provides some of the most important FW projects to come into existence in the following years, in Europe.

Wind Farm Name	Country	Capacity (MW)	Commissioning date
Hywind Scotland	United Kingdom	30	2017 (in operation)
Windfloat Atlantic	Portugal	25	2019
Flocan 5 Canary	Spain	25	2020
Nautilus	Spain	5	2020
SeaTwirl S2	Sweden	1	2020
Kincardine	United Kingdom	49	2020
Forthwind Project	United Kingdom	12	2020
EFGL	France	24	2021
Groix-Belle-Ile	France	24	2021
PGL Wind Farm	France	24	2021
EolMed	France	25	2021
Katanes Floating Energy Park -Array	United Kingdom	32	2022
Hywind Tampen	Norway	88	2022

Figure 1.6: Some pre-commercial floating wind projects announced in Europe

An important measure of how close new concepts are from being commercialized is given by TRL. For values higher than 8, the technology is deemed ready for operations [14]. Figure 1.7 presents the TRL evolution for the main different types of floating substructures. It demonstrates the fast pace at which the models are becoming mature.
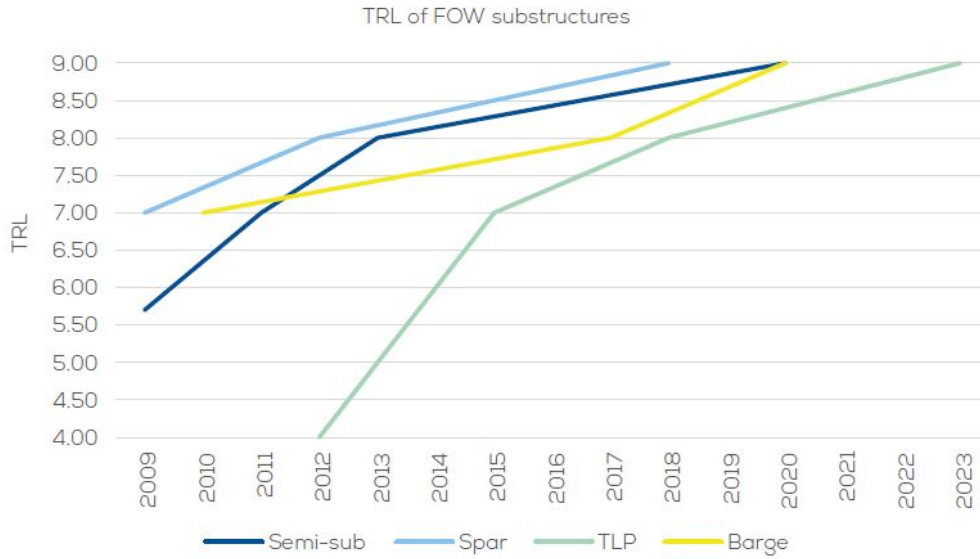
Figure 1.7: TRL evolution, with projection, for the main floating wind substructures concepts, in [14]

Although the costs of floating wind turbines are still not enough appealing for investors, there's a cost downward trajectory expected. In fact, the same trend that was experienced by onshore and bottom-fixed wind should be experienced by floating. Until 2050, floating costs are expected to decrease up to 38% [14], with even greater reductions possible. The economy of scale factor is to play a big role in this path towards cheaper floating units, as patent in figure 1.8.

(a) Capex Evolution

(b) Opex Evolution
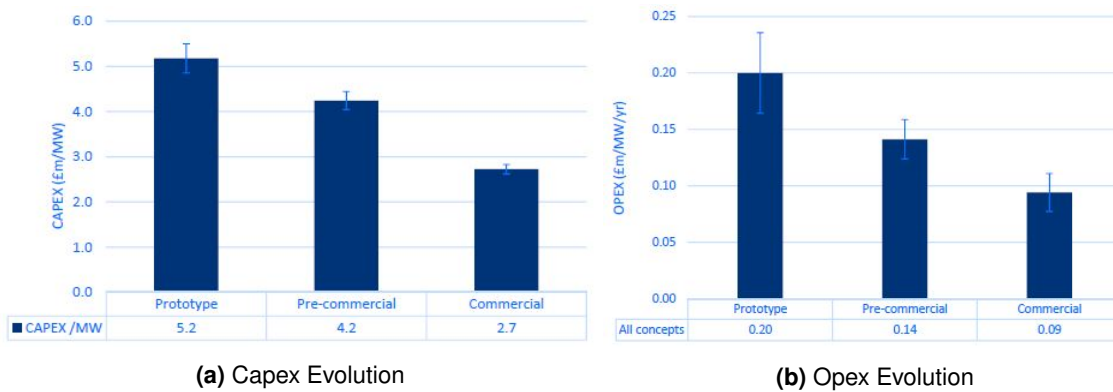
Figure 1.8: Expected cost reduction with increased production scales, in [24]

In figure 1.9, the way the LCOE of onshore wind has evolved throughout the years might cast some light on how drastic the reduction of costs can be. This is a strong argument supporting the optimistic atmosphere surrounding the industry growth. What is more, it strengths governments, R&D groups and companies quest and decision to transform FOW into a feasible and luring reality.
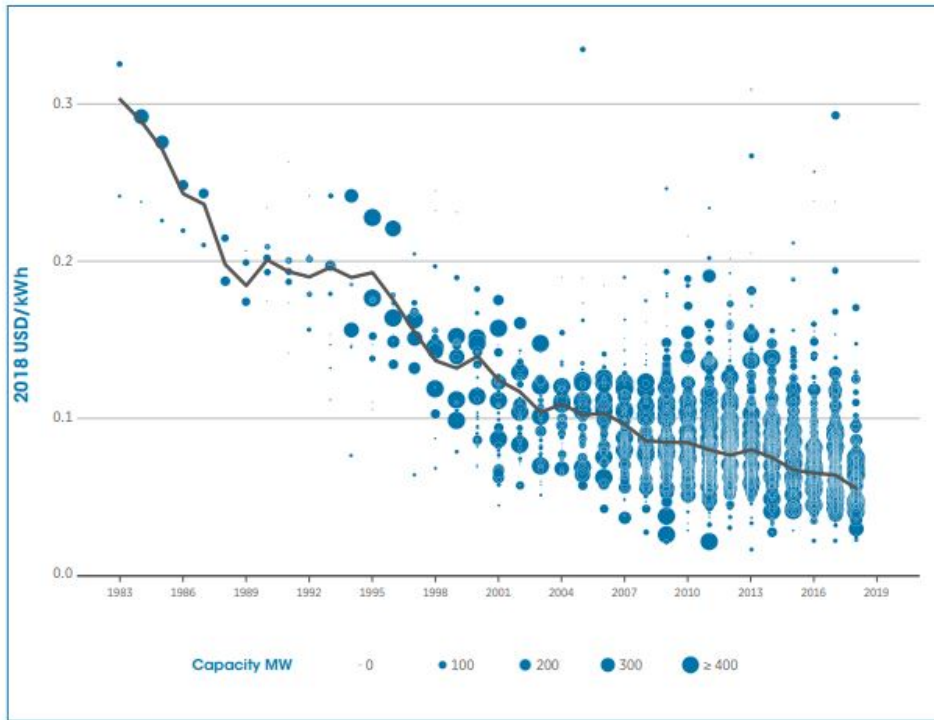
Figure 1.9: The global weighted average levelised cost of electricity of onshore wind, 1983-2017, in [19]

Furthermore, what happened some years ago with the oil and gas industry, can also be repeated with offshore wind. After going from fixed-platforms to floating-platforms, to obtain access to greater oil reserves, the industry was able to reduce its costs per barrel produced. By going into floating platforms, stronger and more reliable wind resources are available, what can possibly bring the LCOE down. This trend is depicted in figure 1.10.

Figure 1.10: Improvement in cost competitiveness in North Sea oil production, in [24]

10

1.3 Objectives

- Assess the relevance and explore the advantages of a simulation-based method (present approach) to estimate the AEP of a FOWT. To calculate the difference between the conventional (wind turbine power curve integrated in a wind distribution) and present approaches.

- To understand which are the main mechanism affecting power production in a floating situation.

- Perform a sensitivity analysis of the LCOE of a FOWT and evaluate the relevance of the first objective, as well as of other key cost drivers.

1.4 OC4 semisubersible model

In the present work, simulations and assessment of technical and economic aspects of the semisubmersible floating system designed for OC4 project, phase 2 are performed. A brief description of the model, its details and characteristics, as well as the tools used for attaining the above-mentioned goals constitute the focus of this section.

OC4 was a project with the objective of comparing simulations tools in order to validate and verify their correctness in grasping reality. In phase 1 tests were performed at 1/50th scale in a wave basin under combined wind/wave loading for three different floating concepts (one of them corresponding to the model used in phase 2), representing the design space of FOWT. Phase 2 comprised the simulation of a semisubmersible concept designed for the DeepCWind project. The turbine used was the offshore 5-MW baseline wind turbine from NREL [25]. The option utilized in this work is precisely such model: NREL's baseline wind turbine, described in figure 1.11, attached to the DeepCWind floating substructure, represented in figure 1.12 .

Rating	5 MW
Rotor Orientation, Configuration	Upwind, 3 Blades
Control	Variable Speed, Collective Pitch
Drivetrain	High Speed, Multiple-Stage Gearbox
Rotor, Hub Diameter	126 m, 3 m
Hub Height	90 m
Cut-In, Rated, Cut-Out Wind Speed	3 m/s, 11.4 m/s, 25 m/s
Cut-In, Rated Rotor Speed	6.9 rpm, 12.1 rpm
Rated Tip Speed	80 m/s
Overhang, Shaft Tilt, Precone	5 m, 5°, 2.5°
Rotor Mass	110,000 kg
Nacelle Mass	240,000 kg
Tower Mass	347,460 kg
Coordinate Location of Overall CM	(-0.2 m, 0.0 m, 64.0 m)

Figure 1.11: Resumed NREL's 5MW baseline properties

In regard to the floating substructure, the three outer columns are ballast filled. The amount of water utilized can vary, in order to face the specific dynamic needs of each operational conditions.

(a) DeepCWind semisubersible and NREL's 5MW baseline turbine design

(b) DeepCWind semisubersible detailed design

Figure 1.12: DeepCWind floating substructure

Number of Mooring Lines	3
Angle Between Adjacent Lines	120º
Depth to Anchors Below SWL	200 m
Depth to Fairleads Below SWL	14 m
Radius to Anchors from Platform Centerline	837.6 m
Radius to Fairleads from Platform Centerline	40.868 m
Unstretched Mooring Line Length	835.5 m
Mooring Line Diameter	0.0766 m
Equivalent Mooring Line Mass Density	113.35 kg/m
Equivalent Mooring Line Mass in Water	108.63 kg/m
Equivalent Mooring Line Extensional Stiffness	753.6 MN
Hydrodynamic Drag Coefficient for Mooring Lines	1.1
Hydrodynamic Added-Mass Coefficient for Mooring Lines	1.0
Seabed Drag Coefficient For Mooring Lines	1.0
Structural Damping of Mooring Lines	2.0%

(a) Main mooring system characteristics
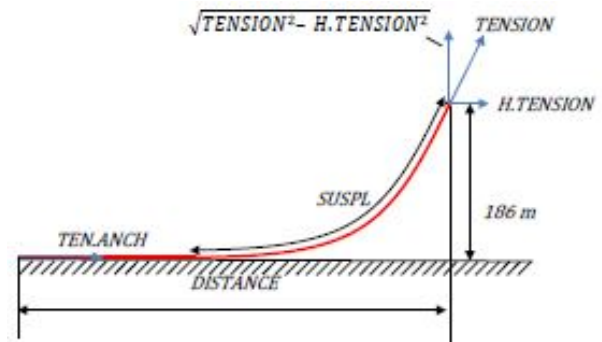
(b) Individual mooring line scheme

Figure 1.13: Mooring system implemented in the model utilized

Each mooring line is attached to one of the main columns in an underwater fairlead. A description of the mooring system characteristics is patent in figure 1.13.

More detailed information regarding the model, its characteristics and properties, as well as control and moorings issues, can be found in [25] and [26].

Chapter 2

Model mathematical formulation

This chapter presents an introduction to the code used in this thesis. More specifically, an overview of the physical and mathematical formulation, with its details, principles, limitations and validity of the OpenFAST (which stands for Fatigue, Aerodynamics, Structure,Turbulence)code and its coupled modules is done. OpenFAST code is the outcome of several improvements and modifications of an older code, called simply FAST, developed at NREL. It's constituted by different modules, that can be coupled to each other to enable simulations of HAWT's and its analysis, providing aero-hydro-servo-elastic solutions. To better express the interconnection of the different modules and the basic principles of OpenFAST, figure 2.1 provides the code's interdependencies and organization. The different modules can be seen written in blue. Although the image refers to the FAST v8 organizational layout (last version before the creation of OpenFAST), it still represents OpenFAST's, as the differences between them are not at this level. From now on, FAST and OpenFAST will be used indiscriminatingly to refer the code used in the present work. In case any important difference arises, it will be properly made noticeable.
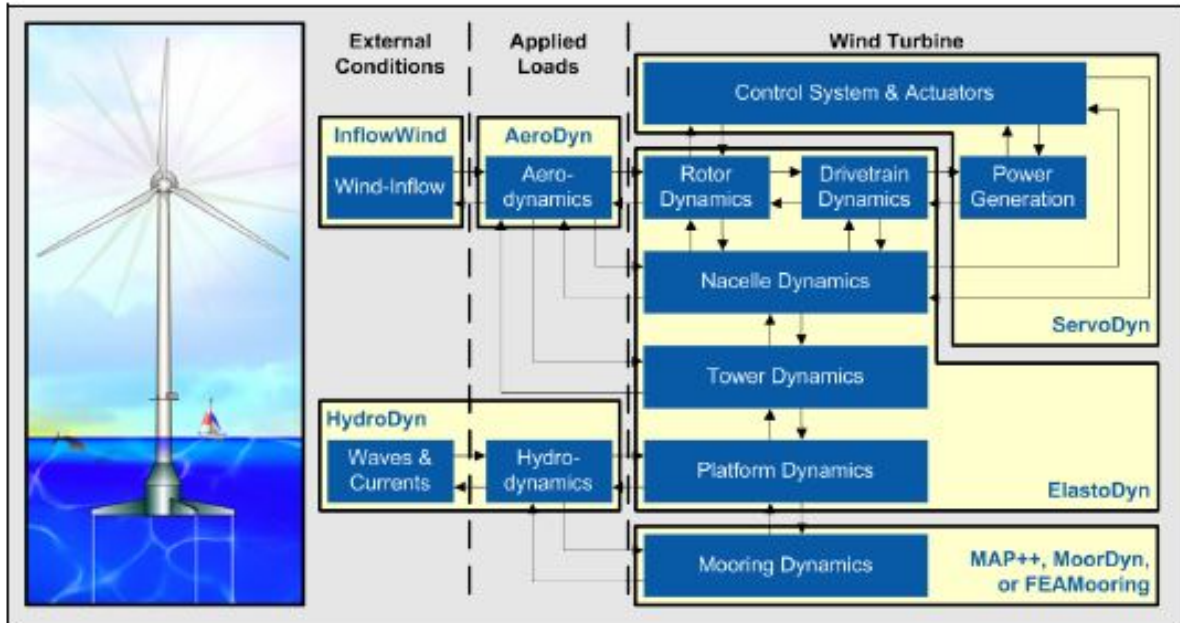
Figure 2.1: FAST v8 and OpenFAST modularization scheme from [27]

The most important modules are identified:

- AeroDyn

- HydroDyn

- ServoDyn

- ElastoDyn

- MoorDyn (chosen among the three displayed options)

- InflowWind

2.1 AeroDyn v15

A brief description of Aerodyn v15 module follows.

AeroDyn v15 is a time-domain wind turbine aerodynamics module that has been coupled into the FAST code from version 8 onwards (thus including OpenFAST). It's a multi-physics engineering tool to enable aero-elastic simulation of horizontal-axis wind turbines.

Aerodyn can assume a one, two or three bladed rotor, always atop a single tubular tower. When AeroDyn is coupled to OpenFAST, AeroDyn receives the instantaneous (possibly displaced/deflected) structural position, orientation, and velocities of analysis nodes in the tower, hub, and blades. It receives also the freestream wind velocities at those same nodes.

Aerodyn is divided into four sub-modules:

- blade airfoil aerodynamics

- blade rotor wake/induction

- tower influence on the wind close to the blade nodes

- tower drag

All other effects are not yet taken into account: nacelle, hub, and tail-vane wind influence and loading, aeroacoustics, and wake and array effects between multiple turbines in a wind plant.

As far as aerodynamic loads are concerned, calculations are based on the principle of actuator lines which approximate 3D flow around a body with a set of 2D flows at cross sections. The distributed pressure and shear stresses are approximated by lift forces, drag forces, and pitching moments lumped at a node in a 2D cross section. Then, analysis nodes are distributed along the length of each blade and tower, the 2D forces and moment at each node are computed as distributed loads per unit length, and the total 3D aerodynamic loads are found by integrating the 2D distributed loads along the length. The drawback of this approach is that it is only trustful when applied to slender bodies. Furthermore, the model cannot capture 3D behaviour. Then, it is either neglected or taken into account separately, through corrections inherent in the model (e.g., tip-loss, hub-loss, or skewed-wake corrections) or in the input data (e.g., rotational augmentation corrections applied to airfoil data). More information on actuator line theory can be found in [28] and [29].

As far as the grasping of the wake effect is concerned, Aerodyn uses a methodology based on the Blade Element/Momentum theory via induction factors. This model is similar to Rankine-Froude "actuator disk". Though, it has an improvement that consists in that it takes into account the angular momentum of the rotor. For the sake of this momentum conservation, it's necessary that a tangential component of wind downstream of the turbine arises, thus making the model more realistic. It also has some empirical corrections for cases where the model is not suitable per si. Moreover, drag is taken into account in the calculations.

The influence of the tower on the wind local to the blade is based on a potential-flow (for upwind rotors)and a tower shadow model (for downwind rotors). The potential-flow model is the analytical potential-flow solution for flow around a cylinder to model the tower effect on upwind rotors.

The wind load on the tower is based directly on the tower diameter and drag coefficient and the local relative wind velocity between the freestream (undisturbed) wind and structure at each tower analysis node (including the effects of local shear, turbulence, and structural motion, depending on features enabled). The tower drag load calculation is quasi-steady and independent from the tower influence on wind models.

Most of the information in this section comes from [30], which describes the technical aspects of the implementation, operationalization, mathematical and physical assumptions and constraints behind Aerodyn module. More details on previous version of it can be found in [31]. For more detailed insights,

these two documents are recommended.

2.2 HydroDyn v2.03

A special attention is dedicated to this module as it is responsible for the main object of study of the present work: wave dynamics and loadings. Such relevance is also justifiable due to the more complex nature of the physics behind this topic which demanded an increased effort and time allocation in its study and comprehension. This section naturally draws much of its content from the HydroDyn user guide and manual [32], though many other resources have been used.

HydroDyn is a time-domain hydrodynamics module that has been coupled into the FAST (progressively adapted to its new versions, including OpenFAST) wind turbine CAE tool to enable aero-hydro-servo-elastic simulation of offshore wind turbines. It applies to both bottomed-fixed and floating substructures.

The primary HydroDyn input file defines the substructure geometry, hydrodynamic coefficients, incident wave kinematics and current, potential-flow solution options, flooding/ballasting and marine growth, and other auxiliary parameters.

When HydroDyn is coupled to FAST, HydroDyn receives the position, orientation, velocities, and accelerations of the substructure at each coupling time step and then computes the hydrodynamic loads and returns them back to FAST. At this time, ElastoDyn assumes for a floating platform that the substructure is a six DOF rigid body. Moordyn also receives the information provided by Hydrodyn and returns its own output, thus contributing for the overall dynamic.

2.2.1 Floating platform kinematics

Firstly, the model used for the platform and its kinematic is explained. In Hydrodyn, the floating structure is considered to be a rigid body with 6 DOF's. It's such a rigid body, when compared with turbine's blades and tower, that it makes unnecessary to account for hydro-elastic dynamics. The turbine is assumed to be fixed to the floating structure and both the CM and COB are assumed to lie in the centerline of the undeflected tower. External loads on the platform are applied on the platform reference point, which is defined by the axes (x,y,z), defined in figure 2.2 (they coincide with the inertial reference frame axes, defined by (X,Y,Z), when the platform is undisplaced. X-axis is the nominal wind direction (wind direction of zero).Y-axis is lateral to the left when looking downwind. Z-axis is directed upwards being zero-valued at SWL. The tower is assumed to be rigidly cantilevered to the support platform.
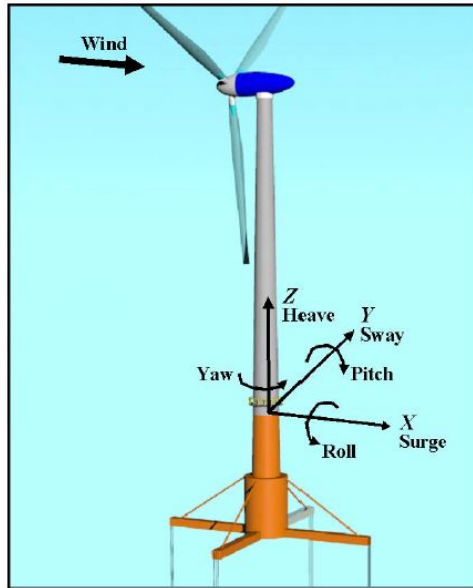
Figure 2.2: Floating platform DOF's, from [31]

2.2.2 Loads and hydrodynamic modeling

The basic equation describing the forces acting on the floating platform is:

$$F_{platf} = F_{hydro} + F_{moorings} + F_{aero} \tag{2.1}$$

Computer simulation programs incorporate a combination of wave kinematics and hydrodynamic loading models. In reality, hydrodynamic loads arise from the pressure integration over the wetted surface of a body. Such loads can be divided into the following categories:

- Linearized radiation, arising from added mass and wave damping coefficients.

- Linearized excitation force obtained from Froude-Krylov (due to unsteady pressure field generated by undisturbed waves.) and diffraction forces (accounts for the body effect on the incoming waves)

- Linearized hydrostatic restoring due to the balance between buoyancy and weight

- Non-linear viscous drag

For the present work, choices were made in the scope of Hydrodyn modelling possibilities, which results in the approximations used here. Thus, a brief overview on what is behind the Hydrodyn model used in this thesis (some features available, as were not used, are not described).

The so called "true linear hydrodynamics model" or potential flow theory, to which is added a non-linear viscous drag corrective term enhancing the model capability to capture the influence of incident-wave kinematics, sea currents and platform motions.

The potential-flow solution is applicable to bodies that are large relative to a typical wave wavelength. The hydrodynamic coefficients required by Hydrodyn are frequency dependent and must be provided before-hand. For this purpose, a frequency-domain panel code must be used (e.g., WAMIT, which was

the one used in this work). The potential-flow theory linearises the hydrodynamic problem by splitting it into three non-correlated different problems [33]:

- Linearized radiation

  This problem deals with the loads originated by the motion of the floating structure in its 6 DOF's in the absence of any incoming waves. The loads result from the radiated waves by the structure motion. This includes a damping component corresponding to wave radiation that extracts energy from the oscillating body and another component related to the added-mass (which introduces more inertia due to the water moved as a consequence of the body displacement).

  The equation describing the instantaneous radiation forces acting on the platform is:

  $$F_{rad} = -A_{\infty}(w)\ddot{q}(t) - F_{RD} \tag{2.2}$$

  Where A is the hydrodynamic added-mass matrix, F_{RD} is the radiation memory-effect force and $q(t)$ denotes the complex displacement vector. The second term on the right hand side of the equation, is obtained from a convolution integral in time in order to capture the displacement memory effects. The integrand includes a matrix called wave-radiation-retardation kernel, $K_{i,j}(t)$ that accounts for the hydrodynamic force in i direction, resulting from a unit impulse in j direction, at a time t. It is also dependent on the displacement velocity of the body, $\dot{q}$. The kernel is obtained through the cosine transform of the 6x6 frequency-dependent hydrodynamic damping and added mass matrix from the radiation problem and decays to zero after a short time. Here's the integral form:

  $$F_{RD} = \int_0^t K(t - \tau)\dot{q}(\tau)d\tau \tag{2.3}$$

  Where τ is a dummy variable with the same units as the time variable t.

  The convolution integral implies an assumption of linearity. In fact, superimposition of the radiation problem means that a complex and varied impulse situation is equal to the sum of each of the individual impulse that constitute it.

- Linearized excitation

  This problem is connected with the loads arising from an incident wave and its scattering, considering that the floating body is fixed at its mean position. In other words, excitation force is the sum of Froude-Krylov (due to unsteady pressure field generated by undisturbed waves.) and diffraction forces (accounts for the body effect on the incoming waves). The underlying equation for a single Airy linear wave (single amplitude, frequency and wavelength) is:

  $$F_{exc} = A_{wave}e^{iwt} * \hat{f}_{exc}(w, \beta) \tag{2.4}$$

  Being A_{wave} the wave amplitude, w the wave frequency and $\hat{f}_{diffraction}$ is the complex wave excitation force per unit wave amplitude, obtained from WAMIT. This approach implies that the

excitation force is linearly proportional to the wave amplitude and that the wave-excitation force from multiple superimposed waves is the same as the sum of the wave-excitation forces produced by each individual wave component. It also uses waves modeled with Airy wave theory in which waves are assumed sinusoidal, what is progressively less accurate as waves become higher. Moreover, the equation also implies that the forces are independent of the platform motions, underlying its decoupling from the radiation problem. As a consequence, it brings a small displacement condition for the substructure, if the results are to be taken as accurate.

- Linearized hydrostatic

Related with the floating platform volume immersed, as describe by Archimedes principle, it is simpler than the two phenomena already described, but hydrostatic force is nevertheless at the core of a floating structure concept. Naturally, this is dependent on the platform displacement, as it changes both the volume submerged as well as the COB. On the other hand, neither outgoing nor incoming waves have influence on hydrostatic loads. This is mathematically described as:

$$F_{hydros} = \rho g V_0 - C_{hydros} q \tag{2.5}$$

Where V_0 is the displaced volume of water at the platform undisplaced position and C_{hydros} is the linear hydrostatic-restoring matrix from the effects of water-plane area and the COB. It is responsible for the change in hydrostatic force and moment due to the platform displacement from its at-rest position. The generic formulation of the matrix is as follows:

$$C_{hydros} = \begin{bmatrix} 0 & 0 & 0 & 0 & 0 & 0 \\ 0 & 0 & 0 & 0 & 0 & 0 \\ 0 & 0 & \rho g A_0 & 0 & -\rho g \int_{A_0} x dA & 0 \\ 0 & 0 & 0 & \rho g \int_{A_0} y^2 dA + \rho g V_0 z_{COB} & 0 & 0 \\ 0 & 0 & -\rho g \int_{A_0} x dA & 0 & \rho g \int_{A_0} x^2 dA + \rho g V_0 z_{COB} & 0 \\ 0 & 0 & 0 & 0 & 0 & 0 \end{bmatrix} \tag{2.6}$$

Where z_{COB} is the body-fixed vertical location of the center of buoyancy of the support platform.

- Non-linear viscous drag

Regarding the nonlinear viscous-drag term mentioned previously, a corrective term from Morrison's equation has been added into Hydrodyn. Morrison equation has several handicaps and limitation to handle alone a floating platform hydrodynamic problem. It assumes a cylindric-shaped platform (many platform concepts do not comply with such assumption), which affects the accurateness of the added-mass matrix. It also has a long-wavelength approximation, in order to ignore the diffraction problem with which it cannot deal. It assumes very small vertical displacements, as the wave-radiation drag term is ignored. For practical purposes, Morrison equation must be integrated

along the floater draft, what requires the use of the strip theory. It further includes more limitations, as the flow for each strip is considered independent from the others.

Nevertheless, the nonlinear viscous drag term has been included (by assigning an effective platform diameter, D) due to the importance of this source of drag in the general platform dynamics and damping. The equation, for a given instant t, depth z and DOF direction i is:

$$dF_i^{viscous} = \frac{1}{2}C_D \rho D dz[v_i - \dot{q}_i]|v_i - \dot{q}_i|$$ (2.7)

where C_D is the normalized viscous drag coefficient, v is the undisturbed fluid velocity. This is valid for Surge, Sway, Pitch and Roll. As a cylinder is axisymmetric the Yaw moment is zero and as Morison equation doesn't apply to vertical movement, the heave force is also zero. For the complete nonlinear viscous force, it's necessary to integrate the equation through its entire draft.

Although the Hydrodyn version used in this work can model second-order wake kinematics to be used with strip theory, and second-order diffraction loads for the potential flow theory, they were not used. For the scope of this work, the approach based on the linearised potential flow with the nonlinear viscous drag term was found sufficient.

As a final note, Hydrodyn can still be "manually" hydrodynamically adjusted or tuned. It is done in the "Platform Additional Stiffness and Damping" matrix, that allows the user to include extra damping, stiffness and pre-loads. An example is given in the Hydrodyn file attached.

2.2.3 Wave Kinematics

Regarding wave kinematics, Hydrodyn can model regular (periodic) or irregular (stochastic) and short-crested (wave energy is spread across a range of directions) or long-crested (unidirectional) waves. Waves were treated using first-order (linear Airy). In the case of regular waves, the free-surface elevation is given by:

$$\eta(x,t) = A cos(kx - wt)$$ (2.8)

Where A is the wave amplitude, ω is the wave angular frequency, g is the gravitational constant and k is the angular wave number given by:

$$k = \frac{2\pi}{\lambda}$$ (2.9)

This theory can describes how the undisturbed fluid-particle velocities and accelerations decay exponentially with depth. In the case of irregular or random waves, linear Airy theory is also used but a myriad of wave heights and frequencies are superposed, as determined by a given wave spectrum. The water depth is assumed the same throughout all simulation, with a value of 200m, to ensure a valid deep water assumption:

$$\frac{d}{\lambda} > 0,5$$ (2.10)

Where d stands for water depth and λ for wavelength. The dispersion relation is patent in equation 2.11, that permits to calculate a wave wavelength, given its period.

$$\omega^2 = gktanh(kd) \tag{2.11}$$

If within the deep water regime, equation 2.11 reduces to:

$$\omega^2 = gk \tag{2.12}$$

The chosen depth (200m) also safeguards the linear wave theory that imposes a limit on wave height regarding the water depth, as patent in figure 2.3.
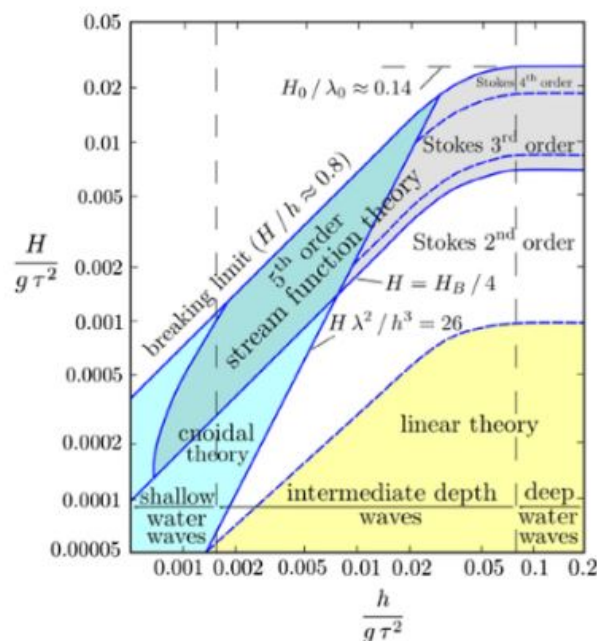
Figure 2.3: Range of applicability of linear wave theory, in [34]

Figure 2.3 is important as it provides the criteria that guarantees that the wave parameters used in the simulations are within the limits of the Airy wave theory assumptions.

Although Hydrodyn is able to integrate current and its effects, this capability was not used in the present work.

2.2.4   WAMIT

Although WAMIT has not been directly used in this work, this program was of the utmost importance for the successful realization of the simulations. In fact, it has provide the linearised hydrodynamic and hydrostatic coefficients, which Hydrodyn uses as inputs in order to solve the linearised hydrodynamic problem. It is for this reason that a resume of this software is presented.

Much of the information present in this chapter is based on the WAMIT 7.3 User's Manual [35]

WAMIT is a radiation/diffraction program developed for the analysis of the interaction of surface waves with offshore structures being based on a three-dimensional panel method.

A panel method is a numerical scheme that solves the Laplace equation for linear, inviscid and irrotacional flows. The underlying base is the principle of superimposing surface distributions of singularities (that are solutions to the above-mentioned equation) over small discretized portions of the surface being studied. This singularities include sources, sinks, doublets and vortices. In order to shape the solution to a desired body geometry, boundary conditions are imposed at points of the panels [36]. They are called control points, while the points defining the panel shape/limit are the panel joints. There is an option in WAMIT to choose either a low-order panel method or a more sophisticated higher-order panel method. Regardless of the differences implemented, their basic operating principle is the same. LOM represents the body surface as a set of flat quadrilateral panels and the solutions for the overall velocity potencial and sources strength are approximated by constant values on each panel. On the other hand, HOM uses more complex and approximated strategies to define the body geometry, namely B-spline approximations and explicit analytical formulae, among others. The velocity potential is represented continuously throughout the body. As a result, the solution becomes more accurate and with less unknowns although the linear system of equations is not so well-conditioned. For a deeper comparison between both methods, see [35].
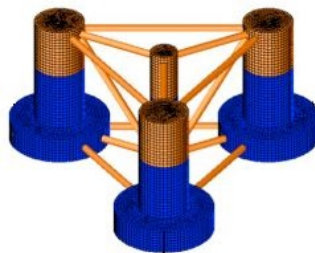
Figure 2.4: The semisubmersible platform discretized with a panel method

WAMIT assumes the flow to be potential, free of separation or lifting effects. A harmonic time dependence is adopted. Also, The free-surface condition and body-boundary conditions are linearized (what allows the decomposition of the velocity potential into the radiation and diffraction problem). This first-order analysis is what has been used for this work.

Mathematically, the problem description becomes:

Laplace equation:

$$\nabla^2 \Phi = 0 \tag{2.13}$$

Kinematic bottom boundary condition:

$$\frac{\partial \Phi}{\partial z} = 0 \qquad at \quad z = -d \tag{2.14}$$

Kinematic free-surface boundary condition:

$$\frac{\partial \Phi}{\partial z} = \frac{\partial \eta}{\partial z} \qquad at \quad z = \eta(x,t) \tag{2.15}$$

Dynamic free surface boundary condition:

$$\frac{\partial \Phi}{\partial t} + g\eta = 0 \qquad at \quad z = \eta(x,t) \tag{2.16}$$

For the present work, the complex potential is:

$$\Phi = \Phi_R + \Phi_E \tag{2.17}$$

where Φ_R is the radiation velocity potential and Φ_E is the excitation velocity potential.

$$\Phi_R = iw \sum_{j=1}^{6} \xi_j \varphi_j \tag{2.18}$$

where ξ_j represents the complex amplitude of the body oscillatory motion and Φ_j stands for the unit-amplitude radiation potentials

$$\Phi_E = \Phi_I + \Phi_D \tag{2.19}$$

where Φ_I is the complex potential of the incoming wave and Φ_D is the complex potential from the diffracted wave.

When the potential functions are known, the first order hydrodynamic pressure distribution can be calculated. Then, the fluid forces are computed by integrating the pressure over the wetted surface of the body. For calculating the hydrostatic restoring matrix, the matrix patent in equation 2.6 is used.

These internal calculations and steps are merely a way of reaching the final goal of WAMIT. Its role is to output files containing the information required by Hydrodyn to solve the set of linearized equations described in section 2.2.2:

- the hydrostatic restoring matrix

- the frequency-dependent hydrodynamic added mass matrix and damping matrix for all modes

- the frequency- and direction-dependent wave excitation force vector per unit wave amplitude

2.2.5 Assumptions

A short resume of the main assumptions and limitations of the Hydrodyn model is given.

- Apart from the corrective nonlinear drag term, the fluid is assumed to be inviscid, incompressible and irrotacional

- linearisation of the wave kinematics implies that the waves amplitudes must be much smaller than their wavelengths and the water depth. The velocity potential must satisfy Laplace equation. As a consequence, steep and breaking waves are out of scope of the model.

- linearisation of the hydrodynamic problem demands small platform translational displacements compared to its size. Regarding rotational motion, angles exceeding 20° lead to loss of accurateness.

- superposition of irregular sea states permits random seas to be treated as a sum of linear Airy waves. Considering stochastic waves as long-crested, simplifies the diffraction problem.

- no second order forces and wave kinematics were included and neither potential loadings arising from VIV nor current effects on the radiation and diffraction problems were considered as well.

2.3   Elastodyn v1.03

Elastodyn is a structural-dynamic model for HAWT. It has structural modules for the tower, platform, nacelle, drivetrain and rotor. Rotor blades can be imported using Beamdyn, for a more complex model than Elastodyn, but this option has not been used in this work. Following the new modularization framework adopted with FAST v8, it is a callable module, independent from the FAST driver code. The inputs ans outputs are presented in figure 2.5.
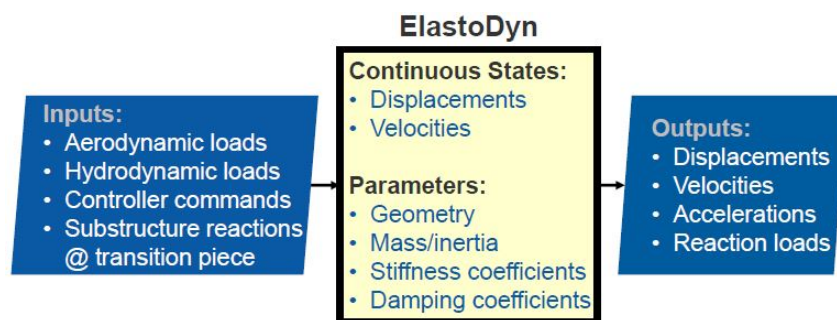
Figure 2.5: Elastodyn's inputs and outputs, from [37]

Regarding the Elastodyn model, it comprises a total of 16 DOF's plus the 6 DOF's associated with the platform displacements and rotations. See figure 2.6.

The main Elastodyn's assumptions and limitations, are:

- Bernoulli-Euler beam theory is applied for the rotor blades, which implies there's no shear deformation as well as axial or torsional deformation.

- Beams are considered to be made of isotropic material and without mass or elastic offset

- Small tower and beam deflections areassumed. Other DOF's have no relevant limitations, as full nonlinearity is included.
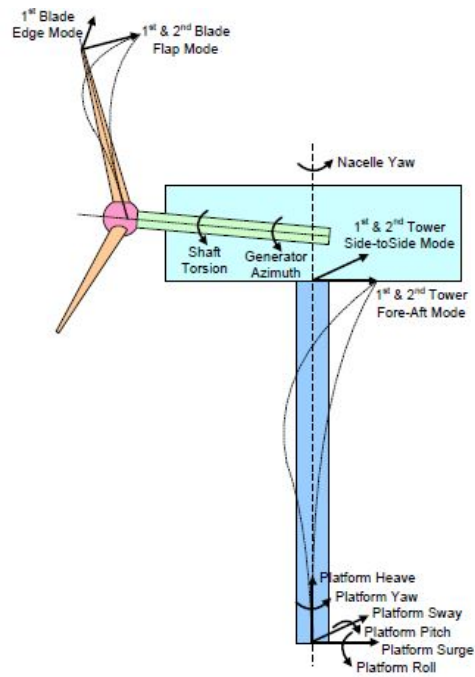
Figure 2.6: Elastodyn's DOF's, from [37]

- Platform DOF's are subject to the constraints already described in Hydrodyn's section, i.e., small-angle assumption for rotational components.

2.4 Moordyn

Moordyn is an open source lumped-mass mooring line discretized model. In this work, it has been coupled within OpenFast's framework.

Moordyn can incorporate:

- line interconnections

- clump weight and floaters

- different line properties

Regarding the internal physical model, it accounts for:

- internal axial stiffness and damping forces

- weight and buoyancy forces

- hydrodynamic forces from Morison's equation

- vertical spring-damper forces from contact with the seabed

- wake kinematics (from Hydrodyn) interactions with the mooring lines

25
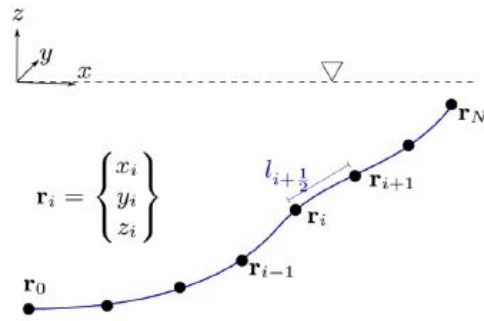
Figure 2.7: Moordyn's discretized model structure, from [38]

Each line has a set of defined properties. These include: length; diameter; density; Young modulus.

In order to model the ends of each line there are two options: fixed connection, which is used to the anchor point and vessel connection, which is used as the fairlead. As the names indicate, one is fixed and the other moves accordingly to a given outside program.

Regarding the load-displacement relation, the model used is non-linear. In fact, this feature is very important. In the case the displacements of the substructures increase away from the undisplaced position, important non-linearities arise and a non-linear model is needed to capture them and accurately simulate the behaviour of the structure. The extent to which this happens and the relations between restoring forces and moments and the platform displacement is made clear in figure 2.8

(a) Schematic drawing of a single mooring line

(b) Loads and mooring line displacement relation
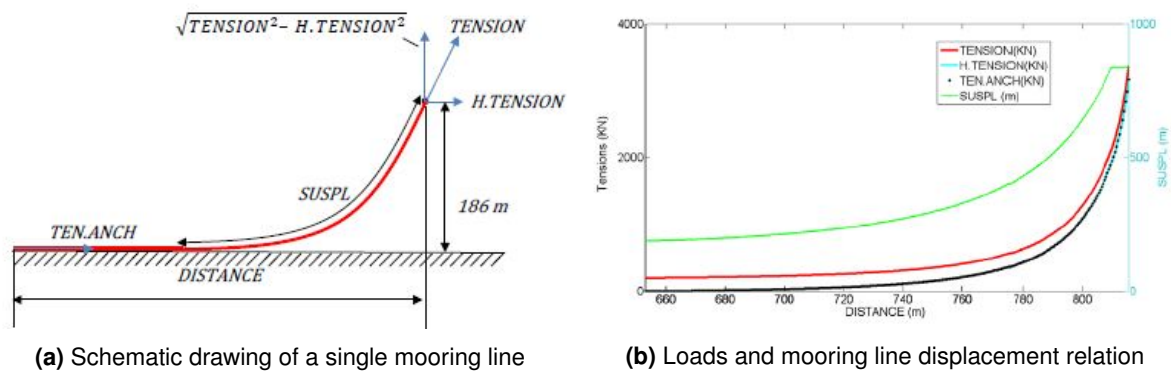
Figure 2.8: Overview of the geometric and kinematic implementation of one mooring line for the OC4 semisubersible platform, from [25]

2.5 ServoDyn v1.05

A conventional variable-speed, variable blade-pitch-to-feather control configuration has been adopted in this module. For such choice, two basic control systems are applied: a generator-torque controller for the under-rated wind speed regime and a blade-pitch controller for the over-rated wind speed range.

In figure 2.9, the black, optimal line is for the optimized TSR value. There are five different areas in the figure above. Each one is defined for a specific objective. Region 1 is where turbine extracts energy from the wind to accelerate the rotor before producing any power. In region 2, the control strategy aims at optimize the power production, by keeping an optimal TSR, for a given wind condition. For region 3, the
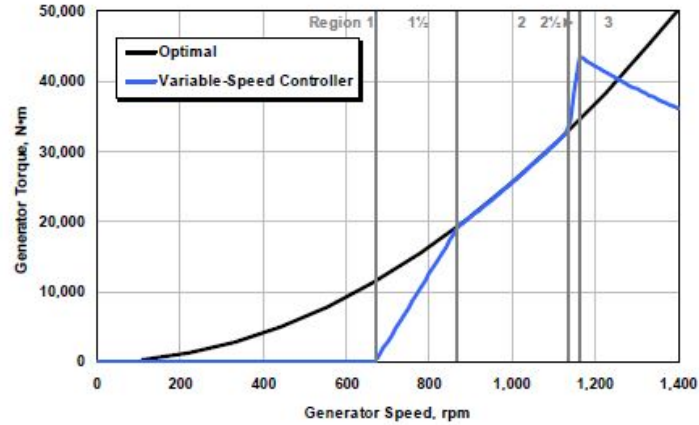
Figure 2.9: Torque-versus-speed response of the variable-speed controller, from [31]

goal is to extract the turbine rated power (in this case, 5MW) by holding the generator torque inversely to the generator speed, as becomes evident from the equation:

$$P_{ext} = T_{gen} w_{gen} \tag{2.20}$$

For calculating the exact extracted power, it is necessary to introduce efficiency parameters and other sources of loss. Still, the approximate relation is valid for the scope of this brief discussion.

Then, there are the two intermediary regions, that simply serve as transitional areas between the main regions. The first intermediary region sets the lower limit from which the turbine starts to extract power. The second intermediary region has the characteristic slope from an induction machine.

Wind Speed (m/s)	Rotor Speed (rpm)	Pitch Angle (°)	$\partial P / \partial \theta$ (watt/rad)
11.4 - Rated	12.1	0.00	-28.24E+6
12.0	12.1	3.83	-43.73E+6
13.0	12.1	6.60	-51.66E+6
14.0	12.1	8.70	-58.44E+6
15.0	12.1	10.45	-64.44E+6
16.0	12.1	12.06	-70.46E+6
17.0	12.1	13.54	-76.53E+6
18.0	12.1	14.92	-83.94E+6
19.0	12.1	16.23	-90.67E+6
20.0	12.1	17.47	-94.71E+6
21.0	12.1	18.70	-99.04E+6
22.0	12.1	19.94	-105.90E+6
23.0	12.1	21.18	-114.30E+6
24.0	12.1	22.35	-120.20E+6
25.0	12.1	23.47	-125.30E+6

Figure 2.10: Sensitivity of aerodynamic power to blade pitch in region 3, from [31]

From the onset of region 3, the second control strategy comes into effect. Indeed, the blade-pitch angle command are calculated through a proportional-integral control on the difference between the rated generator speed (1174 RPM) and the filtered actual generator speed. Figure 2.10 shows the effect and sensitivity of the blade-pitch role on controlling the aerodynamic power and keeping the rotor rated speed for varying wind speeds.

From the analysis of figure 2.11, it is very clear how the two control principles act in the different regions. Region 3 start is very clear as this is marked with the beginning of the blade pitch rotation.

In region 2 it is also possible to confirm generator-torque controller presence, as TSR is kept constant at an optimized value. Altough region 1 is not represented, it can be inferred, as no power production arises before wind speed reach the 3m/s lower limit, while at that value the shaft is already rotating at a considerable rotational speed. The power curve also shows a typical behaviour, with 5MW as its rated capacity. Such power is produced when wind velocity reaches about 11.4m/s and ends when it overtakes 25m/s which are, respectively the turbine's rated and cut-out speed.

(a) Power curve and other parameters

(b) TSR, blade-pitch and other parameters
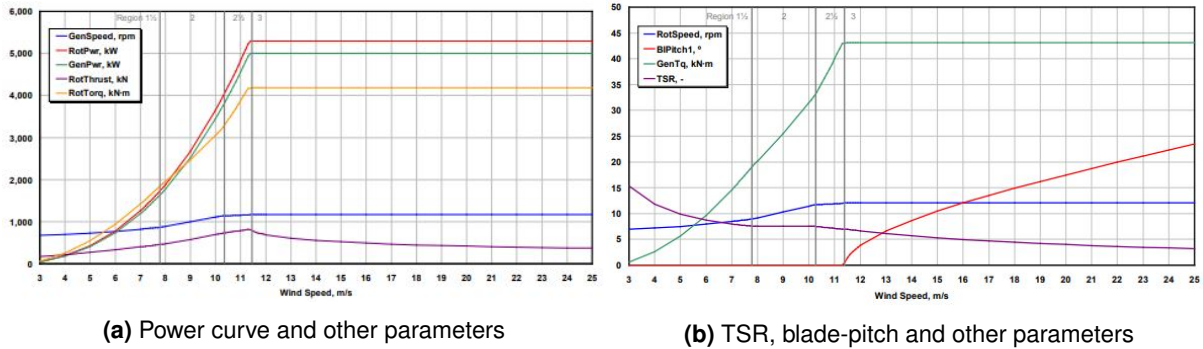
Figure 2.11: Steady-state responses as a function of wind speed, from [26]

All in all, the practical result agree pretty much with what was expected from the model implemented. Nevertheless, there's a drawback regarding this model: it cannot account for blade-pitch actuator dynamic effects, when the control of the turbine is done through that approach.

2.6 InflowWind

InflowWind is the module used for processing wind-inflow that has been coupled into the FAST version 8 and is used in this work. It is the module that specifies all characteristics of the wind flow with which the turbine will interact. In other words, depending on the selected wind type, it details the wind speed, direction, wind profile shape, turbulence parameters, among other.
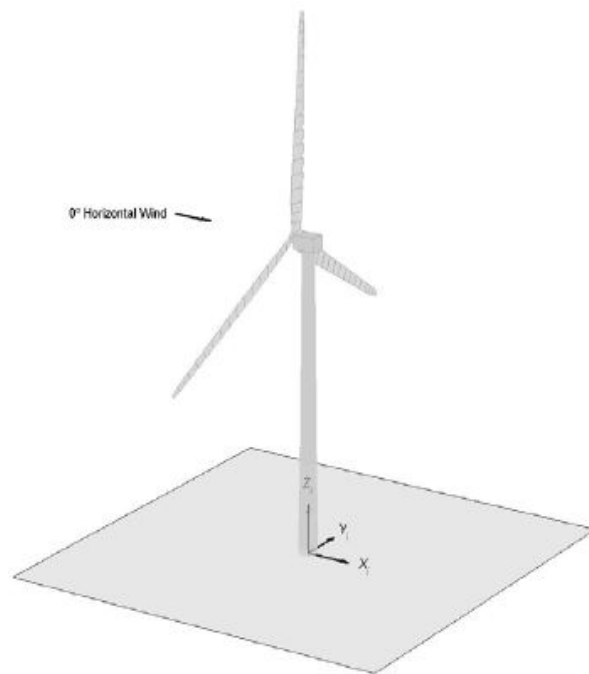
Figure 2.12: The global coordinate system used in InflowWind, from [39]

Chapter 3

Validation and consistency tests

In this chapter, the main goal is to better understand and validate the behaviour of the simulated floating wind turbine through a series of simulations that focus on key aspects of the structure dynamics. Thus, it has both an academic and learning interest as well as a more practical objective. In practice, a series of simple tests of increasing complexity are performed. This enables a checking procedure to detect where eventual errors or unexpected behaviours occur. In other words, if this part was skipped, final simulations were run, and problems arose, it would be very difficult to track them. Thus, such methodology provides more trust regarding the validity of the final results.

The path is loosely based on the methodology followed on [40]. However, not all tests were performed as only a few of them have been found relevant for the scope of this analysis. Moreover, a few load cases outside of the scope of the above mentioned task were run.

Regardless of that, a image with the full list of the load cases run in OC4 Phase II is displayed:

Table 3: Load cases run in OC4 Phase II

Load Case	Description	Enabled DOFs	Wind Condition	Wave Condition
1.1	Eigenanalysis	All	No air	Still water
1.2	Static equilibrium	All	No air	Still water
1.3a	Free decay, surge	Platform and moorings	No air	Still water
1.3b	Free decay, heave	Platform and moorings	No air	Still water
1.3c	Free decay, pitch	Platform and moorings	No air	Still water
1.3d	Free decay, yaw	Platform and moorings	No air	Still water
2.1	Regular waves	Support structure	No air	Regular airy: H = 6 m, T = 10 s
2.2	Irregular waves	Support structure	No air	Irregular airy: H_s = 6 m, T_p = 10 s, γ=2.87, JONSWAP spectrum
2.3	Current only	Support structure	No air	Surface = 0.5 m/s, 1/7th power law decrease with depth
2.4	Current and regular waves	Support structure	No air	Regular airy: H = 6 m, T = 10 s; current at surface = 0.5 m/s, 1/7th power law
2.5	50-year extreme wave	Support structure	No air	Irregular airy: H_s = 15.0 m, T_p = 19.2 s, γ=1.05, JONSWAP spectrum
2.6	RAO estimation, no wind	Support structure	No air	Banded white noise, PSD =1 m²/Hz for 0.05-0.25 Hz
3.1	Deterministic, below rated	All	Steady, uniform, no shear: V_{hub} = 8 m/s	Regular airy: H = 6 m, T = 10 s
3.2	Stochastic, at rated	All	Turbulent (Mann model): V_{hub} = V_r (11.4 m/s)	Irregular airy: H_s = 6 m, T_p = 10 s, γ=2.87, JONSWAP spectrum
3.3	Stochastic, above rated	All	Turbulent (Mann model): V_{hub} = 18 m/s	Irregular airy: H_s = 6 m, T_p = 10 s, γ=2.87, JONSWAP spectrum
3.4	Wind/wave/current	All	Steady, uniform, no shear: V_{hub} = 8 m/s	Regular airy: H = 6 m, T = 10 s; current at surface = 0.5 m/s, 1/7th power law
3.5	50-year extreme wind/wave	All	Turbulent (Mann model): V_{hub} = 47.5 m/s	Irregular airy: H_s = 15.0 m, T_p = 19.2 s, γ=1.05, JONSWAP spectrum
3.6	Wind/wave misalignment	All	Steady, uniform, no shear: V_{hub} = 8 m/s	Regular airy: H = 6 m, T = 10 s, direction = 30°
3.7	RAO estimation, with wind	All	Steady, uniform, no shear: V_{hub} = 8 m/s	Banded white noise, PSD =1 m²/Hz for 0.05-0.25 Hz
3.8	Mooring line loss	All	Steady, uniform, no shear: V_{hub} = 18 m/s	Regular airy: H = 6 m, T = 10 s
3.9	Flooded column	All	Turbulent (Mann model): V_{hub} = 8 m/s	Irregular airy: H_s = 6 m, T_p = 10 s, γ=2.87, JONSWAP spectrum
RAO = response amplitude operator			V_{hub} = hub-height wind speed, V_r = rated wind speed, PSD = power-spectral density	H = wave height, H_s = significant wave height, T = wave period, T_p = peak-spectral wave period, γ = peak enhancement factor

Figure 3.1: OC4 Load Cases Full List in [40]

3.1 Static Equilibrium

This is the first and simplest load case run. It is characterized for not having neither wind, waves nor current. It was run and everything was as expected: no relevant translational or rotational movements were detected. Basically, the platform stands floating. No images of the simulations are shown due to very simple and static nature of them.

3.2 Dynamic Tests

3.2.1 Decay Tests

Next, decay tests have been run for the 6 DOF's of the rigid floating structure ,i.e.: Surge, Sway, Heave, Roll, Pitch and Yaw. For Surge, Sway and Yaw two different offsets are tested.

All of these tests were undertaken with only the platform and moorings DOF's enabled, accordingly with the OC4 load cases specifications. This means that all of the floating substructure DOF's were turned on (Surge, Sway, Heave, Roll, Pitch, Yaw) but all the others were not. For Surge and Sway two different simulations are considered: one with a 50m offset and other with a 5m offset, as patent in figures 3.2a and 3.2b.

The first checking procedure is to see whether the results obtained in this free-decay test match those that arose from the OC4 project . To do so, an analysis of the mean motion frequencies of the 6 rigid
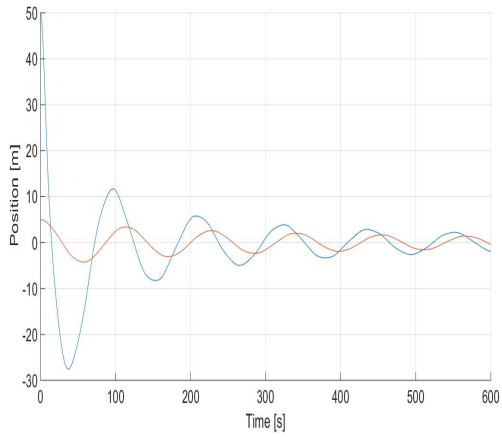
(a) Surge. Blue line: 50m; red line: 5m
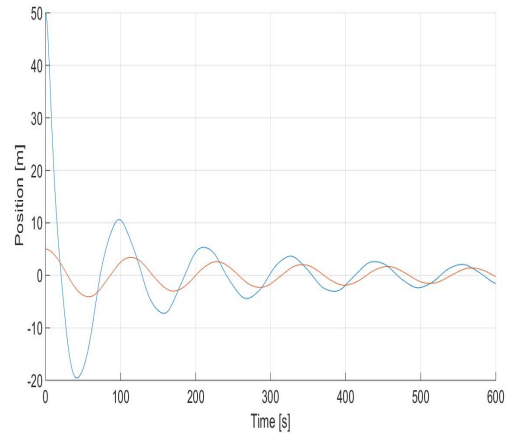
(b) Sway. Blue line: 50m; red line: 5m
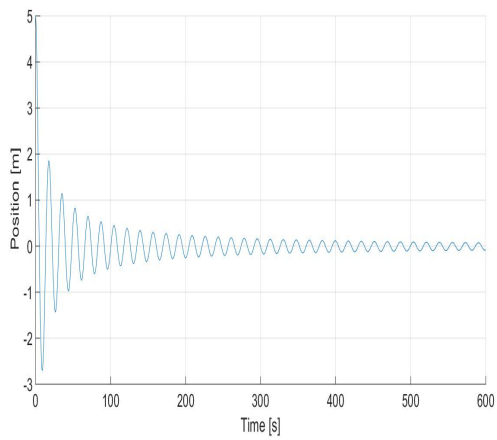
(c) Heave
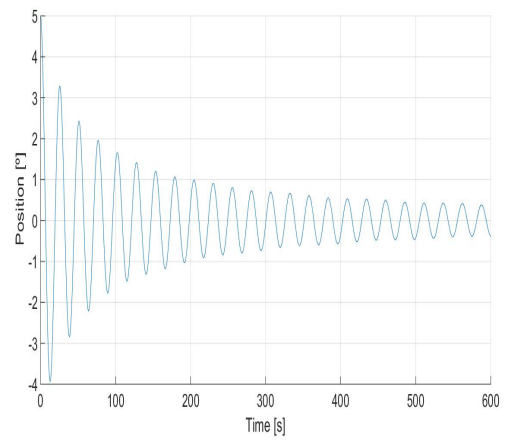
(d) Roll
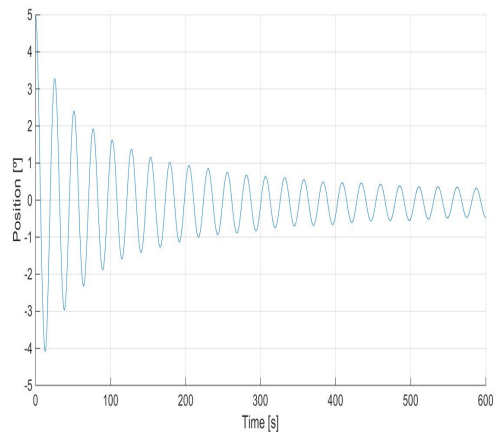
(e) Pitch
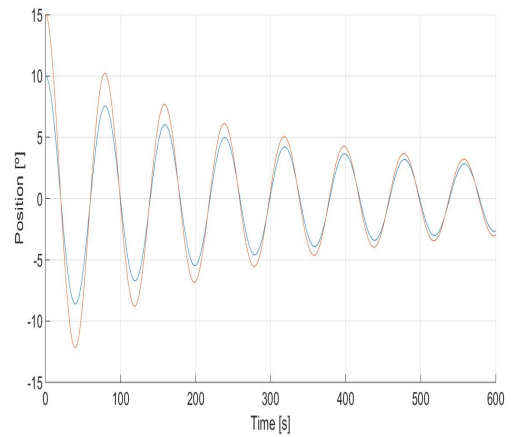
(f) Yaw

Figure 3.2: Set of decay tests for each platform DOF

body DOF's being studied, has been performed, through an average calculation. Results are presented in table 3.1.

DOF's	Surge (5m)	Surge (50m)	Sway (5m)	Sway (50m)	Heave	Roll	Pitch	Yaw
Freq. [Hz]	0.0088	0.0090	0.0088	0.0090	0.0577	0.0391	0.0391	0.0125

Table 3.1: Platform responses' natural frequencies, as calculated in this work

In figure 3.3, the natural frequency data regarding the rigid platform DOF's is presented (each column refers to a specific code). In this task, many codes were used to validate each other. As can be stated, although there are some minor oscillations, they all have a high level of concordance:
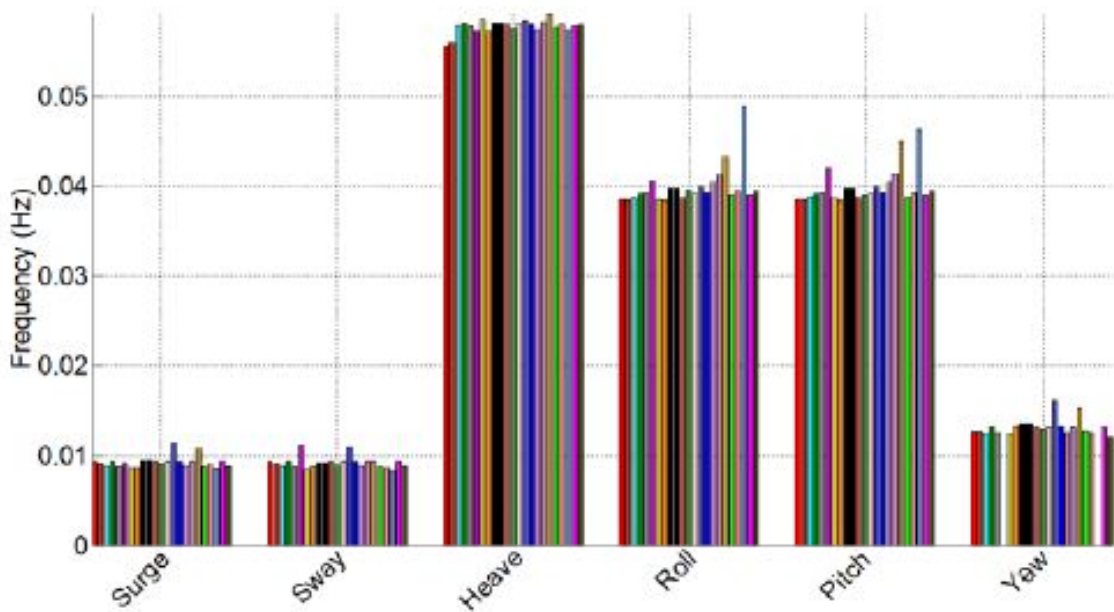
Figure 3.3: Rigid Body Natural Frequencies in [40]

The following table presents the values from one of the codes used in the study, "Wavec2Wire", which is a good representative of the mean value. The exact frequency values might be found here [41]

DOF's	Surge	Sway	Heave	Roll	Pitch	Yaw
Freq. [Hz]	0.0088	0.0088	0.0580	0.0395	0.0395	0.0120

Table 3.2: Platform responses' natural frequencies, as calculated per "Wavec2Wire" in the OC4 task

The conclusion is that the results obtained in the scope of this thesis match pretty much the ones provided in the report. Again, this reinforces the solidity of this preliminary tests. There is, nevertheless, small differences in frequency regarding Surge and Sway, when subject to different offsets.

Two cases were run for Surge as well as for Sway: one with a initial displacement of 5m and the other of 50m. The ideia is to check the differences and evaluate the evolution of both cases. The reason why two different offsets were chosen is connected to the different nature of the restitution force. In fact, Surge, Sway and Yaw are the only DOF's where there is not any restoring force except from the moorings. All of the stiffness of the "restoring spring" comes from the mooring lines, when in the others it's a combination

of both mooring lines and hydrodynamics. This applies too for the damping: in the three cases mentioned, there is only viscous drag while for the others wave radiation also plays a role. So, by running these two cases it is possible to confirm what has been previously stated in section 2.4, i.e. the nonlinear nature of the mooring line restitution relation. In this case, the difference arises due to the first complete oscillation, which has a higher frequency than the average. In fact, if the first oscillation was not taken into account, the average frequency would be the same both in the 5m case as in the 50m case (as the following oscillations are already considered to be small). This behaviour is due to the nature of the mooring lines force-displacement relation which is not linear, as described previously. In fact, as the moorings used are catenary, their behaviour is more complex than that of a simple cable stretching and unstretching. Still, to some extent, it has a qualitatively similar behaviour to the simple cable. This means that for big displacements, a second order trend becomes important and thus the system overall "stiffness" is no longer independent of the displacement, increasing faster when compared with a linearized model. This affects the system's frequency as stated in the following equation:

$$\omega_n = \sqrt{\frac{k}{m}} \tag{3.1}$$

$$\omega_d = \sqrt{1 - \xi^2}\omega_n \tag{3.2}$$

The reasoning is the same as for the simple pendulum case which requires a small oscillation condition for vibrating at a constant frequency [42]. So, these two different offsets in the Pitch and Roll decay tests show how the results are matching what was expected according to the mooring line model.

Another important conclusion to be drawn from this tests regards the viscous-drag force component of the model. In fact, in the Surge and Sway decay tests the nonlinear nature of the drag force is evident. In fact drag force is, per the definition:

$$D = \frac{C_{drag}U^2 A\rho}{2} \tag{3.3}$$

By checking the plot of the platform velocity in the x direction (Surge), it is clear how the initial speed in the 50m case is much larger than in the 5m's and how fast it slows down until both cases display the same average speed. Indeed, drag force is proportional to square of the platform speed, which explains the large decrease in its modulus. Of course, such energy dissipation also affects the amplitude of Surge (the mechanism regarding Sway is analogous), thus explaining its initial large damping, followed by an almost damping-free oscillation. So, thanks to these decay-tests, it is possible to confirm a correct utilization of the viscous-drag term from Morison equation.
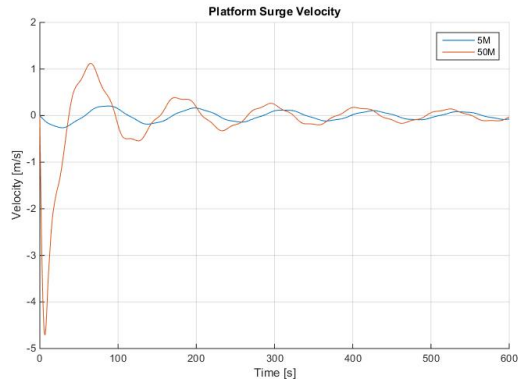
Figure 3.4: Surge velocity for the 5m and 50m cases

3.2.2 Coupling analysis

Regarding the interconnection of the platform DOF's a coupling analysis has been performed, using data from the decay tests of the section 3.2.1 (the 50m offset case was chosen for Surge and Sway, while for the other DOF's the normal 5m offset case was chosen). The most important cases are shown. The major dependencies were found to be the dependence of Pitch with Surge; Roll with Sway and of Sway on Surge (unilaterally). Both Heave and Yaw couplings are absent from figure 3.5 as both are negligibly small.
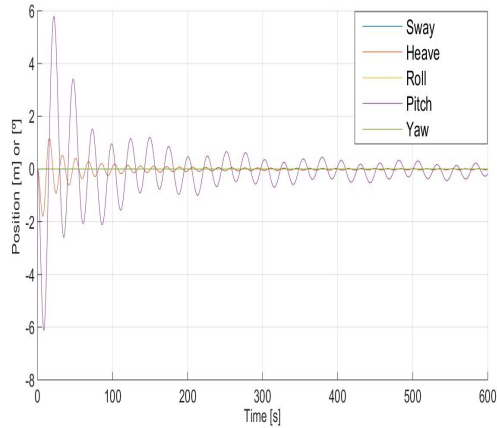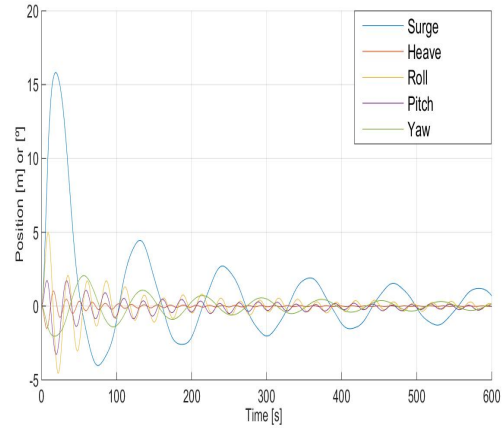
(a) Surge **(b)** Sway
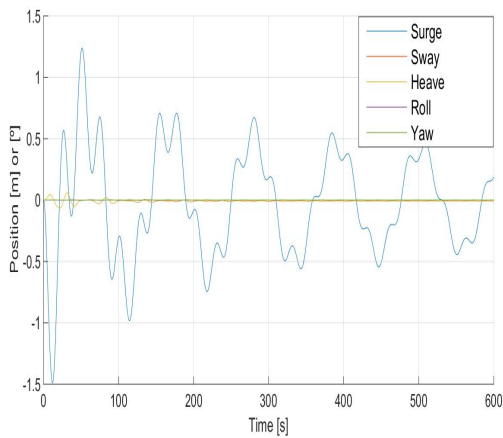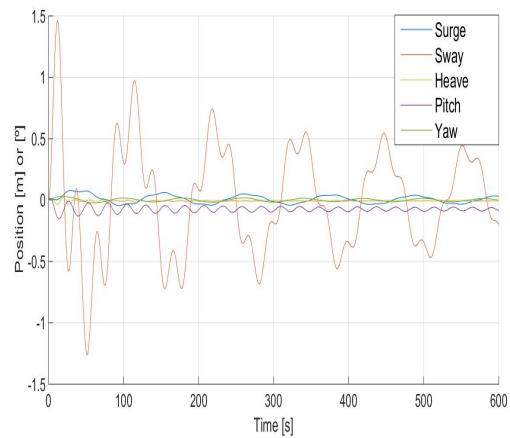
(c) Pitch **(d)** Roll

Figure 3.5: group of DOF's coupling to a set of individual DOF's

Almost all of the phenomena observed in figure 3.5 can be explained in regard to the excitation and radiation hydrodynamic coefficient matrices. First of all, it's patent how some entries of the matrices are null. Moreover, each DOF is only coupled to two other DOF's. In figure 3.5a, only Pitch and Heave are coupled to Surge. In figure 3.5c,only Surge and Heave are coupled to Pitch. If it was not for the unexpected Surge movement in figure 3.5b, the same would happen there, as well as in figure 3.5d, but with a different set of DOF's. So, another conclusion is that there are two groups of coupled DOF's. Group A constituted by DOF's 1, 3 and 5. Group B constituted by DOF's 2, 4 and 6. Each group is not influenced by the other. By observing figure 3.5 again, it is noticeable as the effect 1 has on 5 is exactly the symmetric of the effect 2 has on 4. Another remark is that among each group the coupled intensity between different DOF's varies. For example correlation between 1 and 5 or 5 and 1 (they are the same) is always larger than any correlation with 3. The same happens for the other group: 2 and 4 or 4 and 2 is always greater than any correlation involving 6. It's explained why both Heave and Yaw coupling graphs are not significant. The most interesting is that all these differences arise directly from the hydrodynamic matrices. A sample of those matrices is available in the appendixes.

Arguably the less expected coupling is Surge oscillation in figure 3.5b. This is so because the norm is to have a mutual influence between two DOF's. In this case, that does not happen, as Sway's response

in Surge free-decay test is null. The reason behind this uncorresponded relation is the asymmetry about the yy axis of the floating platform as already shown. So for Surge, as the xx axis is symmetric, there's no Sway coupled to Surge. On the other hand, as the set up and arrangement of the mooring line is asymmetric regarding yy, a Surge displacement takes place in the Sway free-decay test. As members from the two mentioned groups are excited, than all DOF's are coupled, leading to the two more chaotic characteristics of figures 3.5b and 3.5d.

All in all, this analysis permitted to identify two sources of DOF's interconnection. One arising from the model hydrodynamic coupling characteristics, very well defined in the matrices. A second one, whose cause is the asymmetry in the mooring lines layout.

3.2.3 High and low frequency tests

In this subsection, a series of tests involving two different kinds of waves are presented. Neither current nor wind are enabled. Also, in this load cases, the enabled DOF's were increased (with respect to the decay tests). Now, the support structure DOF's were enabled. This means that the tower is flexible, being able to bend in two directions (fore-aft and side-side) and with two modes. By using these simple wave cases and enabling all possible DOF's, the present simulations are increasingly closer to the final ones.

Two simulations are carried out: with a low-frequency and with a high-frequency regular waves. The objective of these load cases is to assess if it platform behaves as expected in such conditions. This means, accompanying the wave elevation in the low frequency case (0.02 Hz) and remaining still when subject to a high frequency wave (0,5 Hz). The waves kinematic were modelled using airy wave theory, to describe regular waves with a wave amplitude of 3m.

(a) High frequency = 0,5 Hz

(b) Low frequency = 0,02 Hz
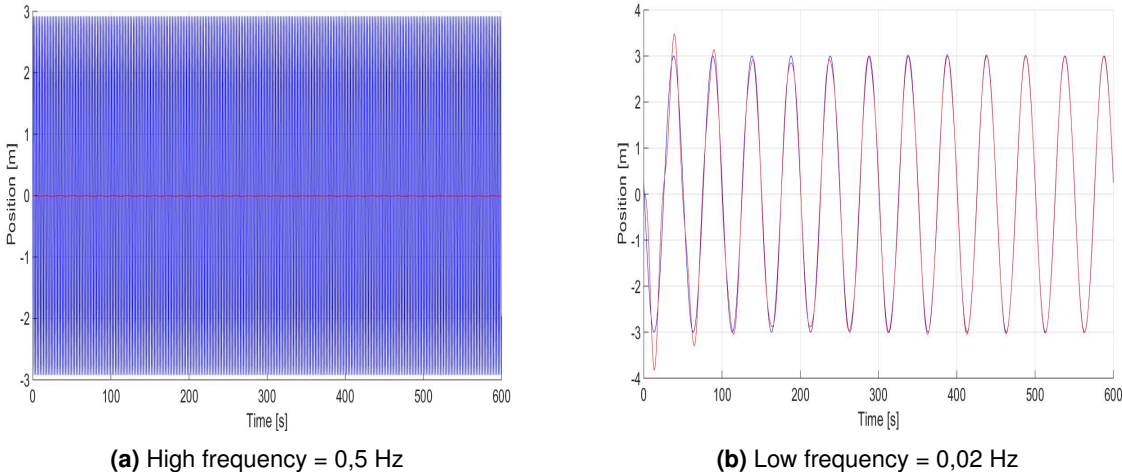
Figure 3.6: Wave elevation (blue line) and Heave response (red line)

The results presented in figure 3.6 confirm the expectations, what further strengthen the confidence in the model. In fact, regarding the Heave response, in case (a) the platform stands vertically quiet, while in (b) it follows exactly the wave elevation (except for the transition initial phase).

3.2.4 JONSWAP spectrum tests

In this subsection the simulations carried out involve the use of the two different JONSWAP spectrum. The test is relevant as can be compared with load case 2.2 and 3.2 from [40]. LC 2.2 has been modelled exactly as prescribed in [40]. LC 3.2 is almost similar but for the fact that the inflow wind is taken to be steady instead of turbulent. Still, as the results present in figure 3.7 and 3.8 show, the responses assessed are pretty much the same (between OC4 LC 3.2 and what is modelled in this work). So, LC 3.2 will be dealt indiscriminately, not taking into account the small difference in the wind modelling. The responses presented in figure 3.7 correspond to the more relevant ones. The other responses (Sway, Roll and Yaw) were not strongly influenced by these LC's, so were left out. The fore-aft tower displacement response is included due to its influence in the generated power. By its turn, it is displayed to capture the raw difference between the power generated by a floating and a fixed turbine. For the sake of comparison, the average value of Surge and Pitch are represented in the graphs as a straight line. Moreover, a "fixed turbine" case (all platform DOF's are disabled) has been introduced for allowing a better comprehension of the effect of the JONSWAP spectrum and the wind-induced loads in relation with the more common case of a fixed wind turbine, for a given wind condition (in this case, the rated wind speed $U_{rated} = 11, 4m/s$). This is done as a preliminary approach as this topic will be addressed more carefully afterwards. In figure 3.7e, the fixed turbine case as well as the fixed turbine and rigid turbine (tower DOF's are disabled) cases have the same mean value. That is why there is no need to represent two different mean values lines in the figure. Heave is also compared for discussing the effect that different JONSWAP have in its response.
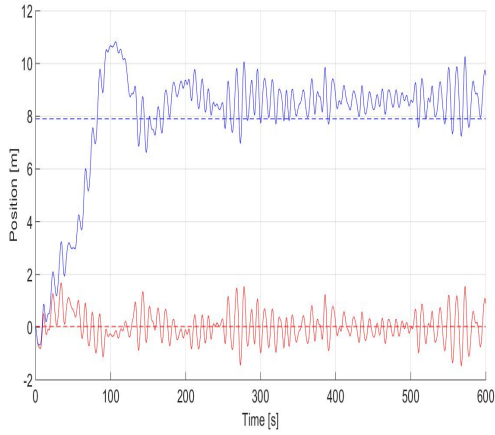
(a) Surge.Red line for: LC 2.2; blue line: LC 3.2; dashed lines: mean values: 0,03m and 7,90m respectively
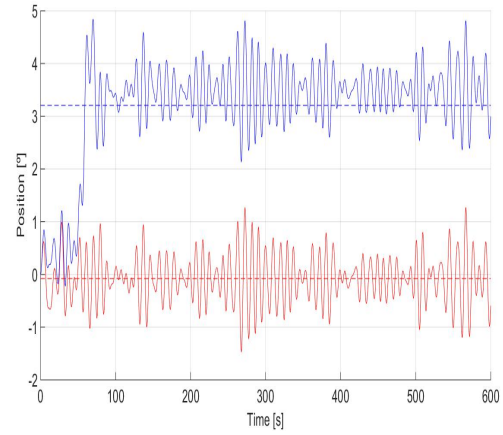
(b) Pitch.Red line for: LC 2.2; blue line: LC 3.2; dashed lines: mean values: -0,08º and 3,21º respectively
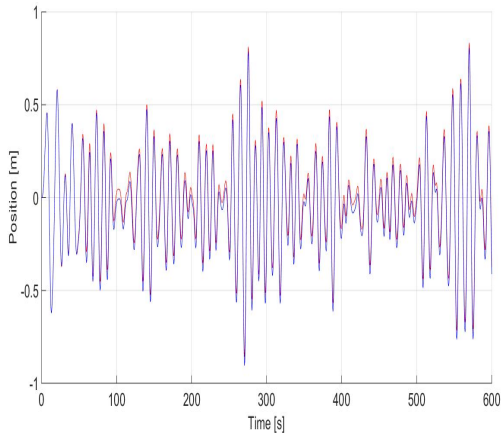
(c) Heave. Red line for: LC 2.2; blue line: LC 3.2
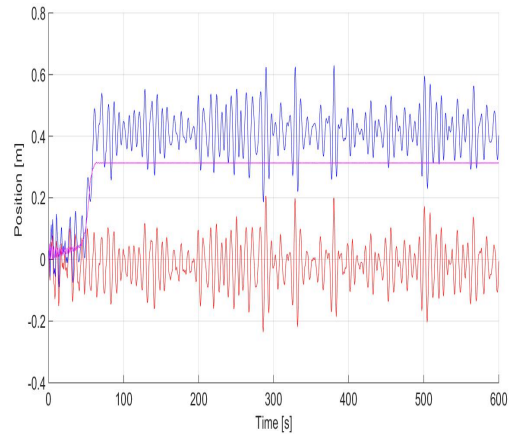
(d) Fore-aft Tower Displacement. Red line for: LC 2.2; blue line: LC 3.2; magenta line: fixed turbine
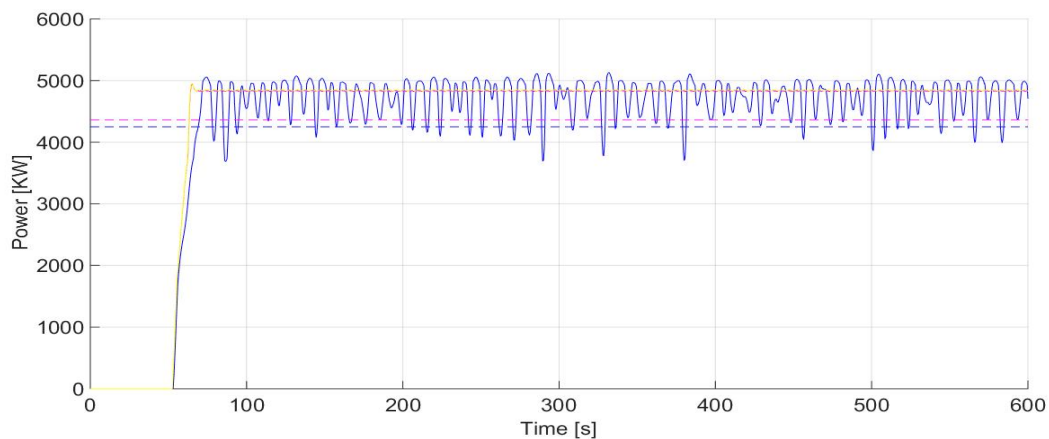
(e) Generated Power. Blue line: LC 3.2; magenta line: fixed turbine; yellow line: fixed and rigid turbine; dashed lines: mean values: 4249 KW and 4363 KW, respectively

Figure 3.7: Model behaviour when subject to different load cases

The first conclusion is that the mean values for Surge and Pitch for both LC 2.2 and LC 3.2 match the values found for the same LC's in the scope of OC4 task as patent in figure 3.8. The most uncertain

one is related with Surge in LC 2.2 as the results significantly vary due to different modelling options (inclusion of non-linear terms or not,...) For instance, LC 3.2's Surge is much more constant as the wind loads mask the drift force. Again, this validates the model implemented in this work.

(a) Surge in LC 2.2   (b) Surge in LC 3.2   (c) Pitch in LC 2.2   (d) Pitch in LC 3.2
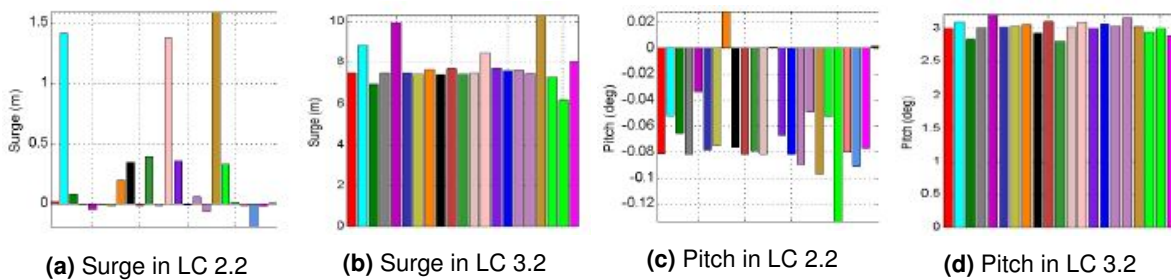
Figure 3.8: Mean value of the responses available in [40]

Heave response, patent in figure 3.7c is interesting as it states how the wind presence barely influences vertical displacement of the platform.

Relevant issues arise from an analysis of the influence both Pitch, figure 3.7a and fore-aft tower top displacement, figure 3.7d have on power production, figure 3.7e. Is the Pitch oscillation responsible for the diminished power generated, or is the its mean value? While the largest peaks in the fore-aft tower displacement coincide with the largest decreases in generated power, is this enough to establish a correlation between the amplitude of the oscillation and the effect on power generated? Indeed, the comparison of the yellow and red curves in figure 3.7e seems to establish a different conclusion: that the fore-aft tower displacement has no direct influence in the power generation. Indeed, the generated power curve of the fixed turbine and of the fixed turbine with rigid tower are exactly the same while one has a small amplitude tower oscillation, and the other is still, due to its infinite stiffness. Of course, the ultimate effect of the fore-aft tower displacement is more complex since its dynamic influences other responses. Some of this questions are more deeply explored in the next chapter.

In the end, these results underline the evidence of the patent inter-dependency of all the variables involved in the power production problem. From the platform responses to the external loads from wind and waves. For instance, fore-aft tower displacement is influenced by both Surge and Pitch oscillations which are, by their turn, a consequence of the wind but mainly of wave loads. These remarks highlight the importance of integrating the different dynamics present in a floating wind turbine for a more accurate analysis of its overall performance.

Chapter 4

AEP Calculation, Comparison and Analysis

4.0.1 Methodology

Two approaches to calculate the AEP of the proposed wind turbine are compared. The conventional one, is to integrate the turbine power curve along the discretized wind's Weibull distribution. This one will be identified as "conventional approach". The other is to perform simulation with FAST using the same wind condition, incorporating the sea kinematics. This one will be identified as "present approach". The difference lies in consideration of the sea-effect in the floating system dynamics, which is expected to jeopardize the turbine's energetic output efficiency. Both results will be extrapolated for a one year period, with the same hypothesis. No transient transitory dynamics between different wind speeds are considered

4.0.2 Assumptions regarding the simulations

- The same JONSWAP spectrum will be used for different wind conditions simulations. This means that wind-generated seas are not taken into consideration but swell waves are. There are a set of reasons for this choice: Firstly, because the more energetic-relevant waves are swell waves which JONSWAP spectrum describes well, and not those originated by local winds, as presented in figure 4.1. As can be seen in the following equation, the average energy flux per unit wave crest length, $\overline{P}_{wave}$, is proportional to the square of significant wave height, which is an indicator of the energy waves carry.

$$\overline{P}_{wave} = 0,49H_s^2 T_e \tag{4.1}$$

Moreover, swell (as well as the JONSWAP spectrum waves) have lower frequencies, when compared to local waves, much closer to the platform natural frequencies, presented in table 3.1, which is a key factor regarding resonance and consequently has a stronger potential for decreasing energy

production. Both remarks are evident from:
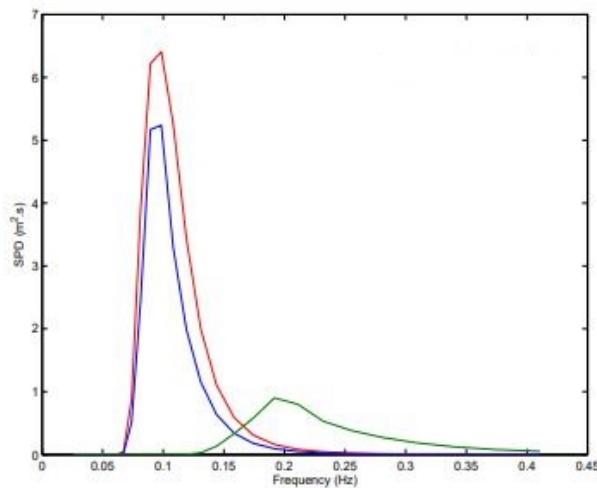
Figure 4.1: Swell system: blue line, wind sea: green line and fitted JONSWAP spectrum:red line. Results for an analysis in the Bay of Biscay [43]

Thus, by using the same sea state throughout all simulations the most potentially impacting cases are dealt with. Such assumption might lead to an overestimation of waves impact on power production. Nevertheless, such hypothesis is not completely irrealistic, as there isn't any connection between the local wind blowing and the swell. In other words, it's reasonable to find the same sea state with different wind conditions.

- The wind and wave directions are aligned and no combinations thereof are considered.

- The wind model is InflowWind's simple type which is defined by an exponential profile characterized by a hub-height wind reference value and a power law exponent. Neither turbulence nor wind-shear effects are taken into account.

- The wind distribution is discretized into nine classes. Again, the goal is to compare the present AEP evaluation method with the conventional approach. So, the discretization is not critic as both approaches are under the same conditions.

- The turbine efficiency is assumed to be 100%. Although some absolute energy values will vary due to this hypothesis, it still doesn't really affect the main objective of this work, which is a comparison between both approaches.

4.1 Wind Resource

The wind distribution is obtained from data available in [44] for a specific location. In this work the coordinates chosen are approximately 40°N,10°E, which is roughly 150km off the coast of northern Portugal, which is in the range of the most interesting regions of the country regarding offshore wind power potential. It is shown in figure 4.2.
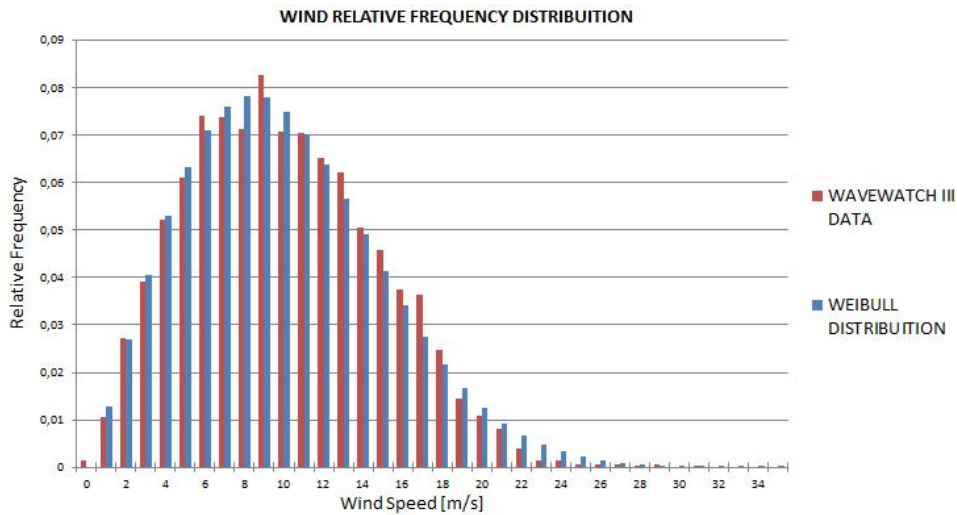
Figure 4.2: Relative frequency distribution from the WAVEWATCH III data and fitted Weibull distribution

The fitted Weibull wind distribution has a shape parameter of 2,1 and a scale parameter of 11,3. The average wind speed from the model data is 10,0 m/s and from the Weibull distribution is also 10,0 m/s.

Accordingly, this location's wind resource is found suitable and in accordance with modern offshore projects, for a 5MW turbine, which is clear from data regarding most recent offshore projects, shown in figure 4.3:

Year of commissioning	Country	Project name	Project capacity (MW)	Individual turbine rating (MW)	Average water depth (m)	Average distance from port (km)	Average wind speed (m/s)
2014	DE	Borkum West II phase 1 (Trianel)	200	5	30	65.6	9.9
2014	DE	Butendiek	288	3.6	19	34	10.0
2014	DE	Dan Tysk	288	3.6	27	70	10.0
2014	DE	Global Tech 1 1	200	5	32	77	10.0
2014	DE	Global Tech 1 2	200	5	40	77	10.0
2014	DE	Nordsee Ost	295.2	6.15	23.5	38	9.8
2014	UK	West of Duddon Sands	388.8	3.6	18.5	28	10.0
2015	DE	Amrumbank West	288	3.6	23	40	9.8
2015	DE	Baltic 2a (previously Kriegers Flak 1)	140.4	3.6	30	32	8.8
2015	DE	Borkum Riffgrund 1	312	4	26	34	9.9
2015	UK	Humber Gateway	219	3	14.5	42	9.5
2015	UK	Westermost Rough	210	6	20	36	9.5

Figure 4.3: Inventory of some recent operating wind farms [45]

The WAVEWATCH III model uses wind speeds that are 10m above the sea level[46]. As the standard wind speed height reference is at hub height (in the present case, 90m) for better dealing and analysing the data and results, it is necessary to extrapolate the initial results. As far as the simulations are concerned, this is not a problem as the wind model used in InflowWind has a power-law profile. So, it would always be possible to provide a wind speed at some given height that the model would calculate the wind speed at the desired hub height. The power-law is defined as:

$$U_z = U_H \left(\frac{z}{H} \right)^\alpha \tag{4.2}$$

Where z and H are two different heights and α is the power-law exponent which depends on the

terrain roughness. For open sea with wave conditions, a value of $\alpha = 0,12$ is assumed[**POWERLAW**].

4.2   Analysis of power reducing factors

The influence that the platform and tower responses have on power production, is now considered in more detail.

4.2.1   Pitch

Three simulations have been run and plotted together in figure 4.4. One represents the LC 3.2 (blue line). Another represents the LC 3.2 with Rigid Tower, which has exactly the same set of conditions than LC 3.2 but for the tower displacement DOF's which are disabled, thus modelling a infinite-stiffness, rigid tower (red line). The other case, represents a fixed turbine, meaning there are no platform dynamics as found in a regular on-shore turbine, but with an assigned constant pitch value of $3,4°$ and a rigid tower (magenta line). The Pitch value has been chosen to match the mean Pitch value of the LC 3.2 case, considered from the onset of power production (approximately at time 100s).
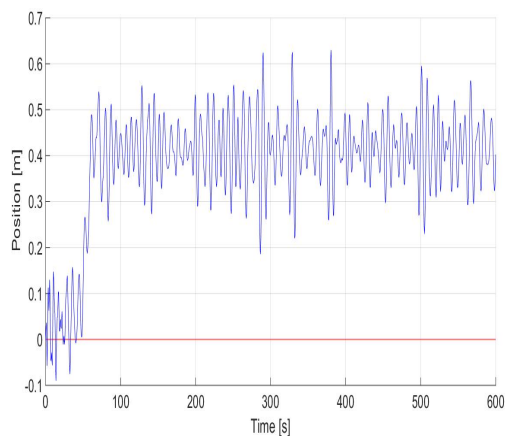
(a) TowerTop Fore-Aft Movement
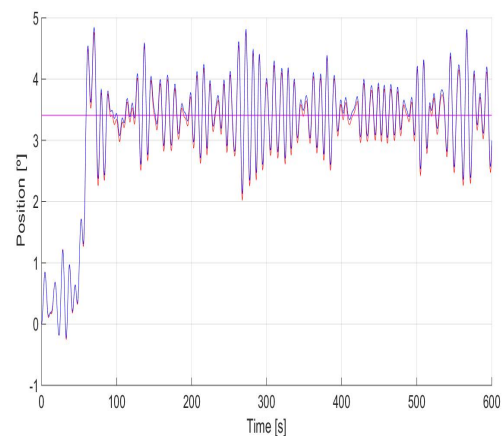
(b) Pitch
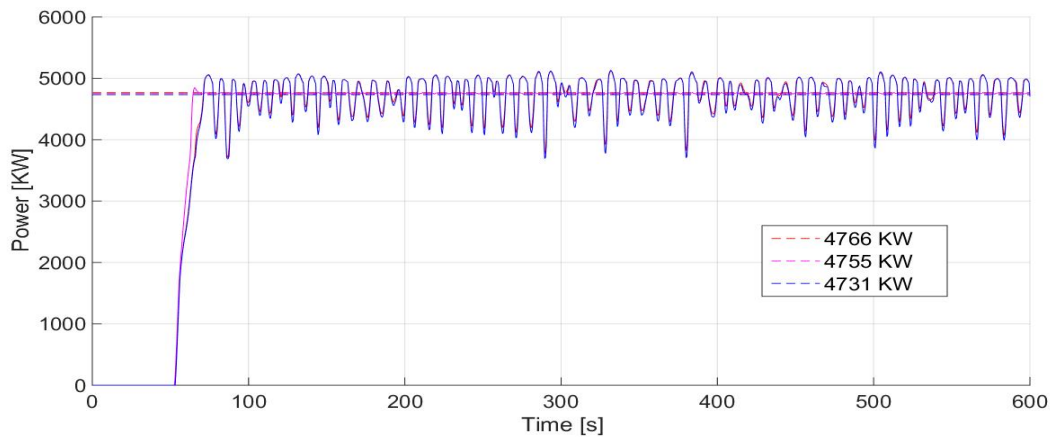
(c) Generated Power

Figure 4.4: Analysis of power production variation with fore-aft tower movement and pitch, for rated conditions.

Regarding the mean generated power, there is almost no difference between the dashed red and blue lines, i.e., around $0,2\%$. Between the dashed red and magenta lines the difference is larger but still very small, around $0,7\%$. The more relevant conclusion to be drawn from figure 4.4, 3.7e and the percentages calculated, are:

- The most relevant factor affecting the power production is the mean offset value of Pitch and not its oscillation. In fact, the difference between the red and magenta lines is almost negligible (the differences are most likely due to the differences in the two models,i.e., Heave, Surge responses,...). This shows that, as far as averaged power production is concerned (not considering quality and constancy in the power output) the Pitch oscillation seem not to be directly relevant for the amount of energy produced in these conditions.

- The effect of for-aft tower displacement is very reduced. In fact, even the influence it has arises indirectly from the influence it has on Pitch. By looking at figure 5.3 b), it's possible to check how the mean Pitch value is slightly smaller in the fixed tower case. Unfortunately, FAST code doesn't allow for setting a constant fore-aft tower displacement case. Such simulation would allow the comparison of the fore-aft vibrations effect with the mean fore-aft displacement effect, and possibly differentiate both.

- The higher the deviation from the horizontal turbine axis position , the more jeopardized the power production is.

- These results are to be taken carefully, as they might depend on wind conditions (in other words, on the turbine power curve region), on the control system itself and naturally on the complex, interconnected overall structure dynamics. A broader and more extensive verification of the dependence of this trend with these variables is out of the present work scope, but might constitute an interesting subject for future work. Anyway, such conclusions show a path towards optimizing

floating offshore wind power production: the first priority being to diminish the mean Pitch offset. The second, being clearly less relevant, to reduce the fore-aft tower top oscillations.

The following natural question is then: how does mean Pitch angle affects power production? To answer this question a series of simulation were run in conditions of similarity, except for the constant Pitch angle, which is varying. The platform is fixed and the wind is at rated conditions:
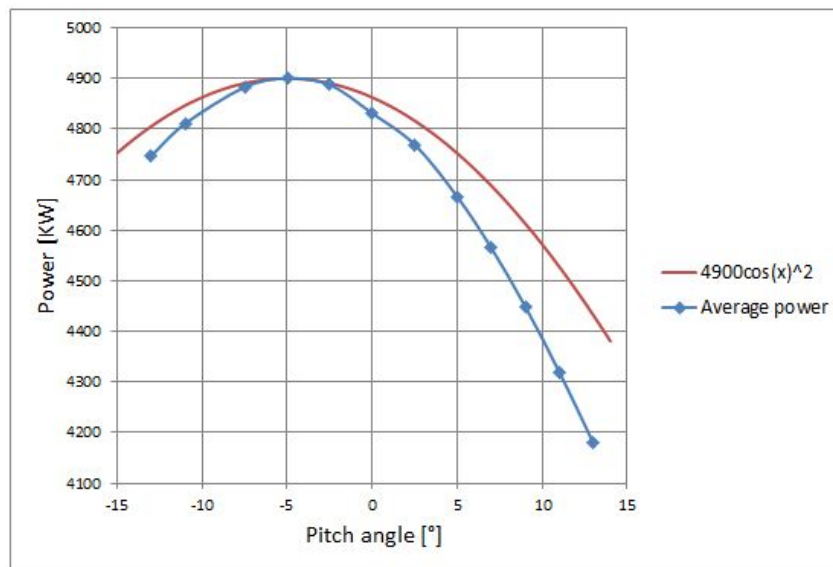
Figure 4.5: Power production sensitiveness to pitch angle, at rated condition

The reason why the squared cosine function is displayed is because the power depends on the area perpendicular to the wind direction, which by its turn, depends on the square of the rotor diameter, either aligned or not. Mathematically, the general law for wind power :

$$P = \frac{1}{2}\rho A_{perpendicular} U^3 \tag{4.3}$$

This equation states the dependence of power with the projected rotor area. The following is the simple circular area equation.

$$A_{perpendicular} = \frac{\pi}{4} D^2_{pependicular} \tag{4.4}$$

where the "perpendicular" diameter to the wind is given by:

$$D_{perpendicular} = Dcos(\alpha) \tag{4.5}$$

where α is the angle between the blades orientation and the vertical. So, in the end, the power could be expected to be proportional to the squared cosine. Naturally there are other factors to consider which justify the differences between both curves. The bending of blades due to their own weight; the precone angle; the change in aerodynamic coefficients due to the angle between the wind and the blades; the different turbine dynamics due to different loadings in each pitch case, as evident in figure 4.6:
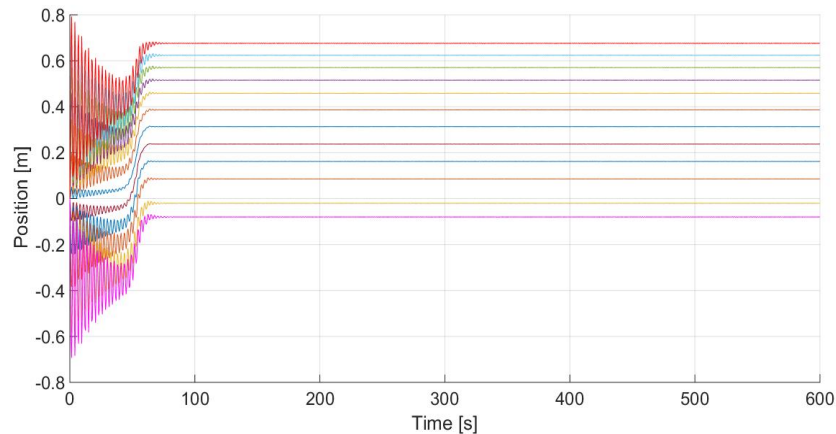
Figure 4.6: Different fore-aft tower top displacements, for different pitch angles

This figure is based on the same condition than figure 4.5 where the red line represents the highest positive pitch case, 13° and the magenta line the highest negative pitch case, -13°. It is possible to see that the incremental differences between all cases, reach a total of 0,8m between the two opposed extremes. This dynamic behaviour plays a role in the power production, as stated above.

Another interesting finding is how the maximum power is achieved for a Pitch angle of -5°. The reason is due to the shaft tilt angle, as seen in figure 1.11, meaning that the blades (not counting with the precone) are actually aligned vertically for a Pitch angle of -5°. In this region, for a range of about -5°, the two curves present a very good correlation as that is the region where the modelling conditions approach more accurately the hypothesis of equation 4.3 and 4.5.

4.2.2 JONSWAP severity

The results for the sensitiveness of power production to the sea state conditions are presented in figure 4.7 (always in the frame of the JONSWAP spectrum). 4 different cases have been studied with the same platform modelling conditions and wind resource (rated) but different wave kinematic model specifications. The most extreme case is similar to LC 3.5, except for the wind velocity, that is taken to be 11,4 m/s instead of the prescribed 47,5 m/s and is represented in red. Such case will be designed as "extreme". Next, comes LC 3.2, represented in blue. The third case wave spectrum characteristics are: half of the wave height of LC 3.2, 3m; a peak spectral period of 8 s and the same peak shape parameter as LC 3.2: 2,87, and is represented in magenta. Such case will be designated as "weak". The last case is one in which there are no waves, so the sea is perfectly calm, and is represented in green. This last case will be designated as "flat".

The analysis of figure 4.7 allows for a set of important and unexpected conclusions.

- Firstly, the extremely low dependence of the mean responses displayed with the severity of the sea state. In fact, there's almost no variation of the parameters considered ranging from flat sea condition to LC 3.2. For the 50-year extreme condition (as the name indicates, a very rare situation), the relative difference is still very low, around 6%.
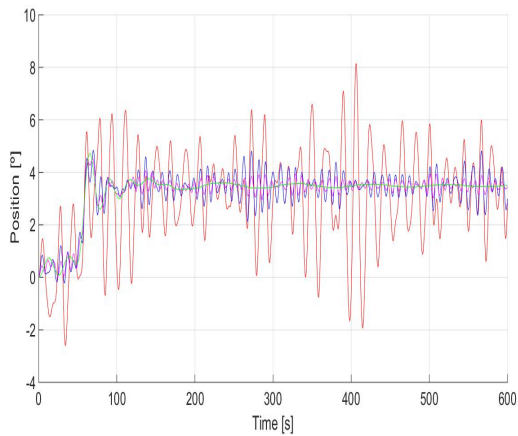
(a) Pitch
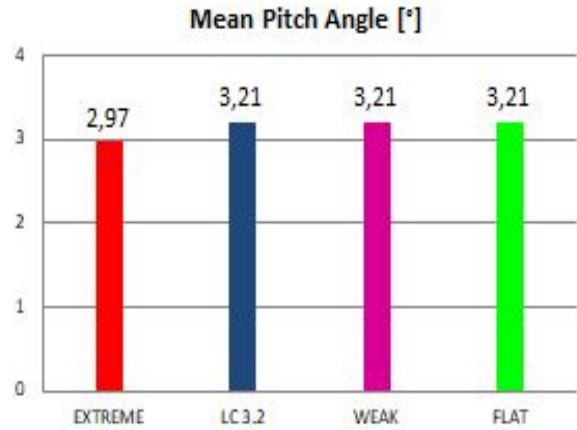
(b) Mean Pitch values
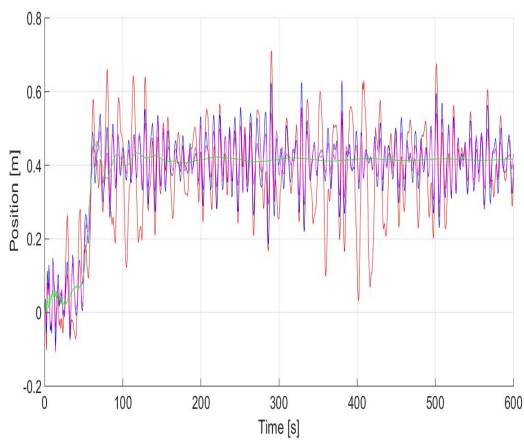
(c) Fore-aft tower displacement
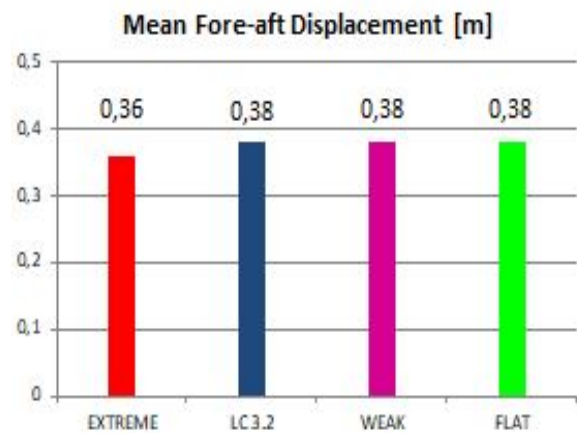
(d) Fore-aft tower displacement mean values
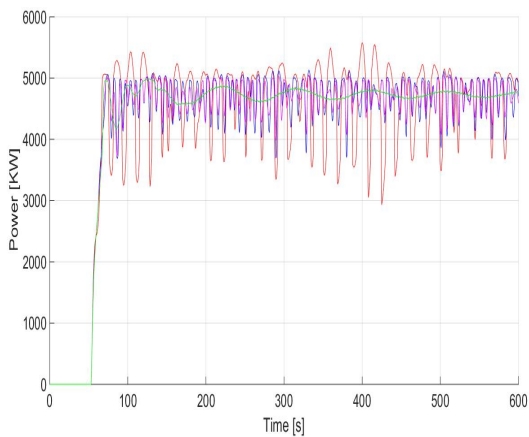
(e) Generated power
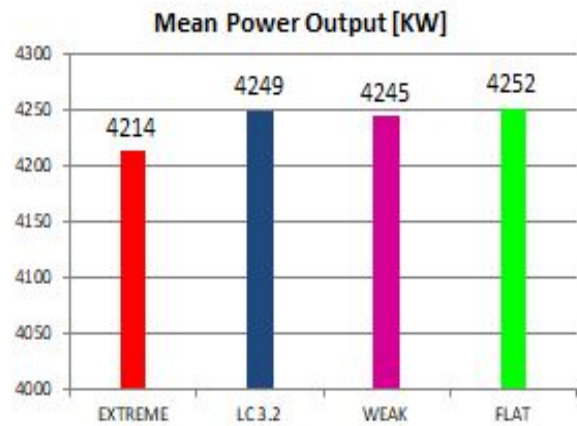
(f) Mean generated power values

Figure 4.7: Response analysis of four different JONSWAP intensity cases

- Although the mean values are very close to each other, the same does not happen with the oscillations amplitude. In fact, the extreme case Pitch oscillation amplitude might be about 5 times larger than LC 3.2 and even larger if the weak case is considered. The oscillations, as will be concluded below, can have a relevant effect on mean power production for some operational situations. Moreover, they are surely critical regarding structural and fatigue constraints.

48

- Probably the most interesting insight figure 4.7 provide is connected with the apparent contradiction with what has been stated in the previous sub-section 4.2.1. In fact, the extreme case mean power output is smaller than the other cases, while both mean Pitch angle and mean fore-aft tower displacement have also lower values! What explains this unexpected results? A careful look into figure4.7f provides the answer. The Pitch and fore-aft oscillations clearly continuously bring down and up the power output. They do so as these movements affects the apparent wind the rotor experiences, increasing when the tower rotates/vibrates into the wind and diminishing when rotating/vibrating downwind. This change in apparent wind forces the control system to constantly adapt the operational region of the power curve, providing more or less power, respectively. As long as the lower peaks are counterbalanced with the higher peaks, the mean power output remains roughly independent of such perturbations. This happens due to a combination of two factors: oscillations amplitude and proximity to the rated power output (5000KW). In this analysis, the inflow wind velocity is kept constant, so the second factor is not changing. As the oscillations amplitude increase in the extreme case the lower peaks are no longer balanced with the higher ones due to the control system. Indeed, there is no limit for the low power peaks. On the other hand, the high power peaks are constrained by the control mechanisms that work towards avoiding an over rated power output. This balance of unconstrained low power peaks with a maximum (5000KW or a bit more, when the control system does not actuate fast enough) power peak condition results in a reduction of the mean power production, even if the mean Pitch angle is smaller when compared with other cases. Relying on this reasoning, a reasonable forecast is that the turbine behaviour is more critically affected by wave conditions in the vicinity of rated conditions (being the range of "vicinity" dependent on the oscillations amplitude). Figure 4.8 depicts this dynamics through a scheme and by providing the tower top speed for the four cases being dealt with in this sub-section.
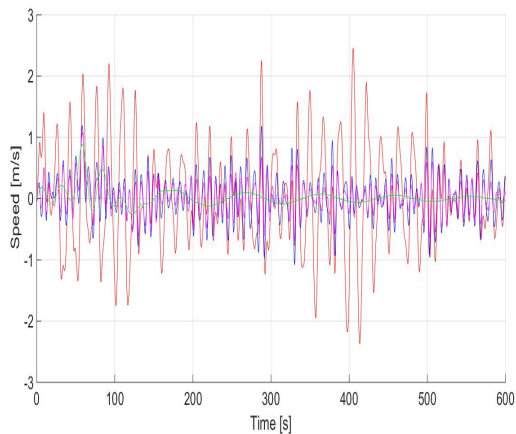
(a) Total tower top speed in the xx direction
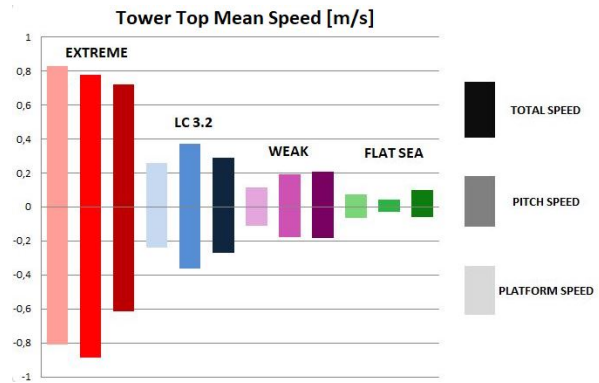
(b) Total, pitch and platform speed, for the four cases analysed, in the xx direction
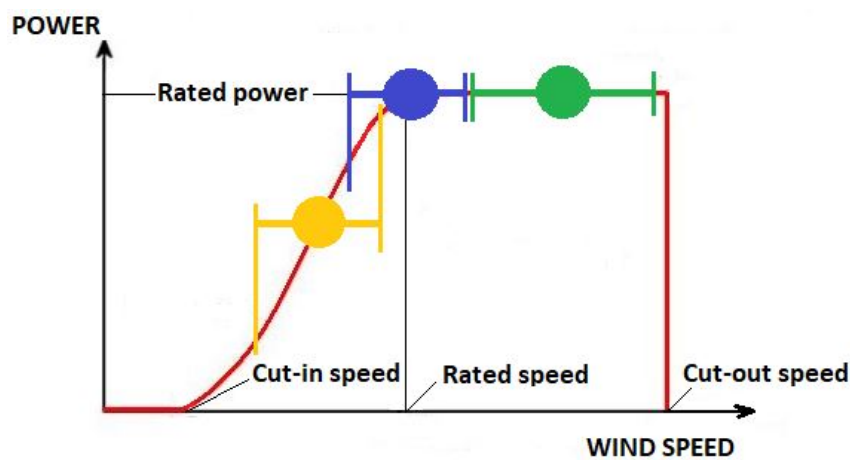
(c) Schematic different turbine operational regions

Figure 4.8: Possible effect of speed oscillations for different sea states in the xx direction

In figure 4.8b the total speed stands for total tower top mean speed; Pitch speed for the Pitch rotational speed multiplied by the tower top height; platform speed for the translational platform speed in the xx direction (Surge). The total speed mean amplitudes were calculated by averaging the summation of the platform Surge speed with platform Pitch speed, multiplied by the tower height. Each case has the "low amplitude" and "high amplitude", meaning they have been calculated averaging the negative and positive data from figure 4.8a. For the sake of succinctness the temporal curves of the Pitch and platform speeds are not presented, though they've been used.

In figure 4.8c, if the the turbine is working at the yellow point (defined by the inflow wind speed) and it experiences perturbations (turbulence or changing apparent wind due to the rotor movement) of a given amplitude, the left low power peak is compensated by the right high power peak, so that in average the power production remains around the yellow circle (the exact balancing depends on the nature of the power curve in that region, i.e. if it a straight line, curved,...). It happens the same for the green circle with a minor difference which is that it has a higher capability of facing larger perturbation amplitudes, due to the different operational point in the power curve. As far as the blue circle is concerned, it's evident that the balancing is no longer possible. For the left range

50

extreme implies a low power peak, but the right range extreme doesn't provide any extra power to compensate for it. By looking at figure 4.8a and 4.8b it is possible to check how the more severe sea conditions have a major role determining the tower top speed.

- Other interesting conclusion is on the role Pitch and Surge play on the total tower top speed. However, note that fore-aft tower displacement has been excluded from this analysis. Although it theoretically also influences the tower top speed, FAST doesn't provide any output regarding its speed, making it impossible to evaluate its detailed role. To check the accuracy of such claim, an analysis of the fore-aft tower displacement figure (not presented in this work) has been done. By analysing the oscillations amplitude and the frequency, it's possible to estimate the mean speed. The conclusion is that the apparent wind arising from this specific movement is very much negligible (around 0,025m/s of amplitude for the extreme case and 0m/s for the flat sea case). Returning to the initial point, Pitch-induced and Surge-induced mean speed are very much equivalent regarding its amplitude. Due to the oscillatory nature of both, the mean total speed, is not simply summed and surprisingly ends up being either slightly superior or inferior to its components. This raises an interesting issue regarding the different floating concepts. For instance, can the Surge speed act as an "active damper" of the Pitch-induced velocities for strong seas, reducing the total speed? If so, by increasing the platform stability, this could constitute a potentially important contribution towards the evolution and definition of future FOW concepts. In other words, this observation might provide renewed insights into platform development strategies and engineering approaches. Of course, to be useful, such results would need to be more strongly confirmed, by testing different platforms, operational conditions, modelling options... However, such extensive research is, again, out of the scope of the present work.

- So, in the end, the conjunction of the two above mentioned factors (speed oscillations amplitude and operational region of the power curve) adds another conclusion regarding power production: it is not only dependent on the mean Pitch angle (as concluded on the previous subsection 4.2.1) but also on the Pitch and Surge oscillations mean speed.

4.3   AEP Calculation and Comparison

Firstly the Weibull wind distribution is discretized into nine classes, as shown in figure 4.9.

CLASS	SPEED RANGE [m/s]	MEAN SPEED [m/s]	PROBABILITY
1	3 ----> 5,5	4,3	13,7%
2	5,5 ----> 8,5	7,0	22,6%
3	8,5 ----> 10,5	9,5	15,3%
4	10,5 ----> 12,5	11,5	13,4%
5	12,5 ----> 14,5	13,5	10,6%
6	14,5 ----> 17,5	15,9	10,3%
7	17,5 ----> 20,5	18,8	5,1%
8	20,5 ----> 23,5	21,8	2,1%
9	23,5 ----> 25	24,3	0,4%

		TOTAL	93,4%

Figure 4.9: Discretization of the wind distribution with respect to nine wind classes

With the Weibull wind curve discretized and the wind classes defined, the calculation of the respective power and energy outputs can be calculated for both approaches. As far as the conventional approach is concerned, the power output for the selected mean wind speeds have been obtained through a careful analysis of the turbine's power curve with a dedicated data digitizer software. For the above rated speeds, such methodology is not necessary as the turbine rated output value is assumed, 5000KW. The results of the present approach, are displayed in figure 4.10.
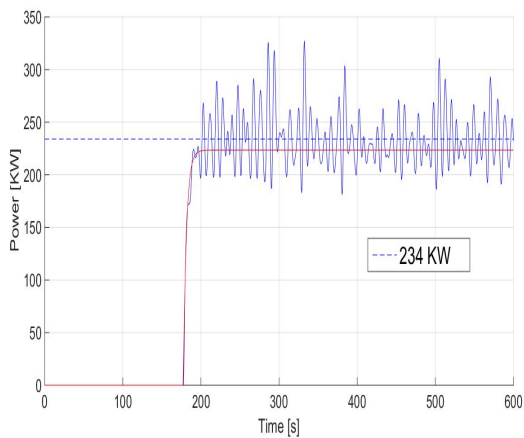
(a) Class 1
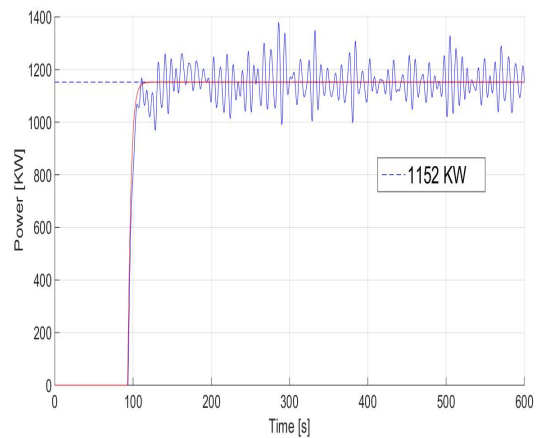
(b) Class 2

(c) Class 3

(d) Class 4

52
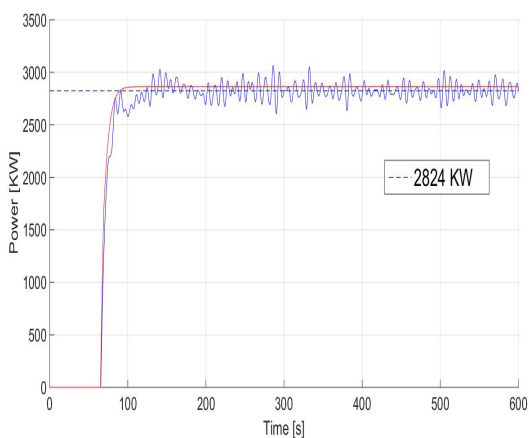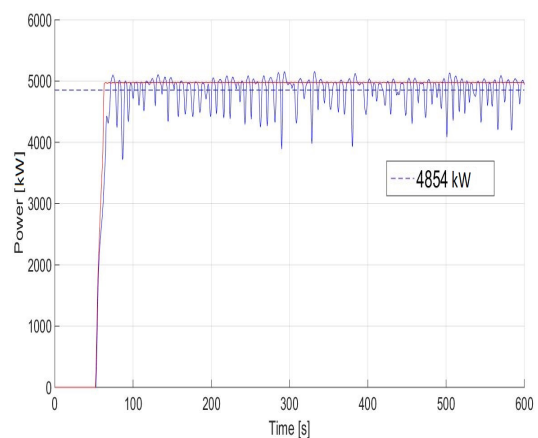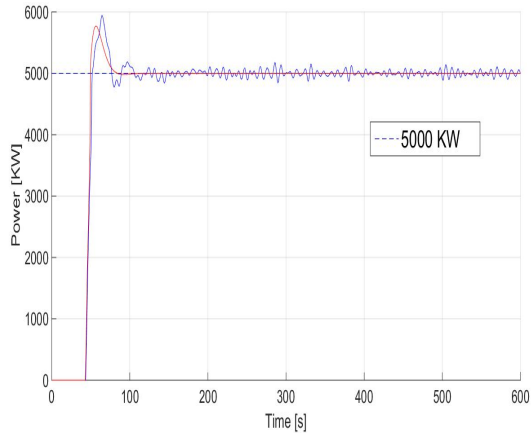
(e) Class 5
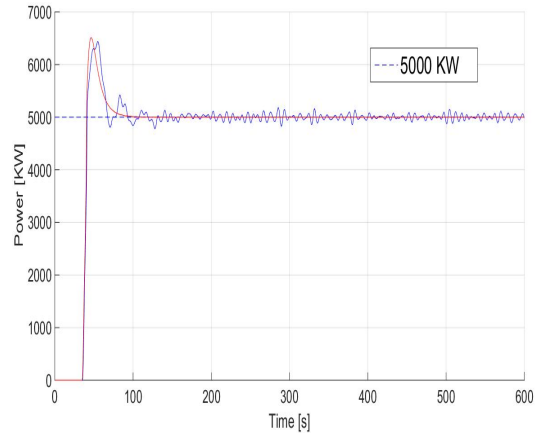
(f) Class 6
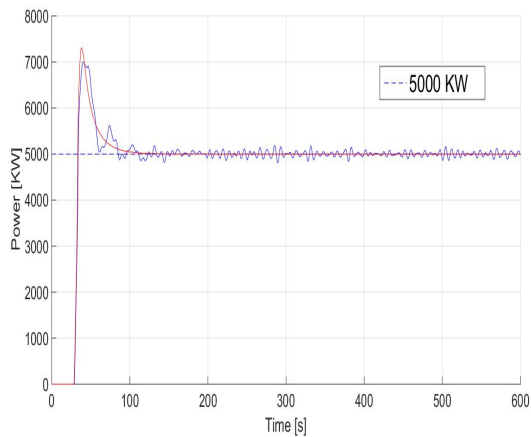
(g) Class 7
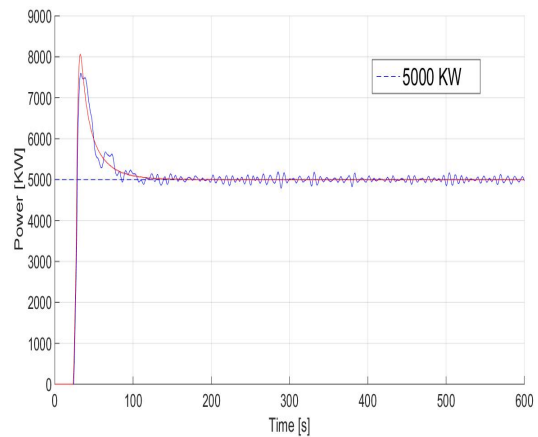
(h) Class 8
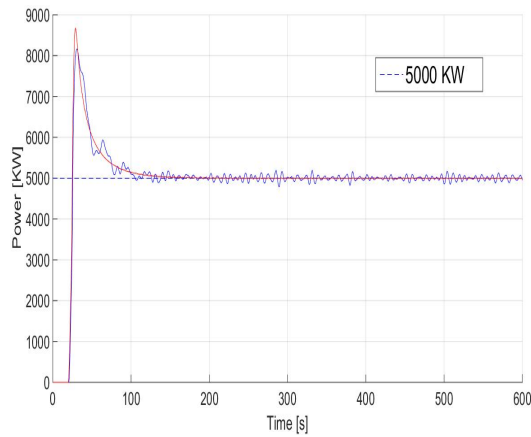
(i) Class 9

Figure 4.10: Temporal output power for each wind class.

Figure 4.10, shows the blue line representing the output power from each wind class coupled with JONSWAP spectrum sea conditions (present approach). The dashed blue line represents the average output power from the filled blue line from the onset of the transient-non-influenced part of the line. The red line represents a fixed and rigid tower. It is presented to visually enhance the difference between

assessing a turbine's power output with and without considering wave loads and dynamics.

A series of conclusions regarding the nine power production simulations are presentd below:

- The effect mean amplitude of wind speed oscillations has on power production, as previously described, is clearly patent and confirmed in this set of figures. Class 4, the closest to rated speed conditions, is the only one in which the oscillations are not evenly distributed by the upper and lower side of the mean power. In fact, class 4 represents the yellow case in figure 4.8c. It's very clear how it presents power drops of more than 1000KW while the highest power peaks over the red curve do not go much above 100 KW, what represents a difference of over 10 fold. This happens only for this specific class. An exception is class 3 case. Although the power output is much more similar to all other cases it still presents a considerable lower mean power output when compared with the fixed, rigid turbine. The reason is due to the final part of the turbine power curve before rated conditions which is slightly rounded. So, even if the power output increases for increased apparent wind, it does so but in a less accentuated way. At least when compared with the power reductions when the apparent wind goes down. All the others cases present equilibrated oscillations around the red line. This provides a conclusion for what has been previously foreseen. That the sea loads affect power production mainly on the rated speed operational region. Again, the extent of this effect along the power curve depends on the tower oscillations amplitude which are by their turn dependent on the sea state severity.

- Class 1 case also displays an interesting feature as it casts light on the opposite effect of class 3. In fact, this is the only case in which the sea-induced apparent wind oscillations carry a benefit! Instead of diminishing the power production, it increases in relation to the fixed, rigid turbine! This happens due to the shape of the turbine power curve. For above operational point the curve is more vertically tilted than below the operational point. This mean that for a symmetric speed oscillation the variation in power is not equilibrated, but has a positive output result. Basically, the opposite effect of class 3 case.

- An important remark concerns the wind speed class band width. As the platform dynamics matters mostly for the rated speed region, it is necessary to be careful when discretizing the wind distribution. In fact, by attributing a higher probability to a class whose speed is close to the rated, the power reducing effect might be exaggerated. The extreme case would be to consider only one wind class (in this case it would be attributed a mean speed value of 10m/s). If so, the overall power reduction factor would be between 3% and 5% (as attributed to classes 4 and 3, respectively, see figure 4.10) when its known that the difference is about 2% or less. So, while it's not needed to perform an infinitesimal discretization to safeguard an erroneous analysis, it must be done considering the specificity of the region affected and the wind classes speed range.

- Note the fact that from class 5 upwards the control system shows a typical overshoot of increasing amplitude, reaching almost the double of the rated power for the strongest wind conditions (class 9). The stronger the wind conditions, the slower the system reaches rated conditions. Although

transitory effects are out of the scope of the present work, they nevertheless constitute an important matter regarding power integration, fatigue, components reliability and structural-related topics.

A summary of the data obtained for both approaches is presented in figure 4.11. A simple data analysis is performed in order to compare the differences arising from the two different methodologies.

	CLASS	1	2	3	4	5	6	7	8	9
POWER OUTPUT [KW]	CONVENTIONAL APPROACH	260	1195	2960	5000	5000	5000	5000	5000	5000
	PRESENT APPROACH	234	1152	2824	4854	5000	5000	5000	5000	5000
	ABSOLUTE DIFFERENCE [KW]	26	43	136	146	0	0	0	0	0
	RELATIVE DIFFERENCE	11%	4%	5%	3%	0%	0%	0%	0%	0%

Figure 4.11: Power output for each wind class

The final annual energy production results are presented in figure 4.12. The absolute values are not exactly what the turbine produces for the network as an overall efficiency factor must be taken into account. Still, the more interesting result is the overall energy estimated reduction that the present approach provides in comparison to the conventional approach. Such value is not affected by efficiency.

	CLASS	1	2	3	4	5	6	7	8	9	TOTAL
AEP [MWh/year]	CONVENTIONAL APPROACH	312,03	2365,8	3967,2	5869,2	4642,8	4511,4	2233,8	919,8	175,2	24997
	PRESENT APPROACH	280,83	2280,7	3785	5697,8	4642,8	4511,4	2233,8	919,8	175,2	24527
	ABSOLUTE DIFFERENCE [MWh/year]	31,203	85,13	182,28	171,38	0	0	0	0	0	470
								RELATIVE DIFFERENCE			2%

Figure 4.12: Annual energy production for each wind class and total value

Chapter 5

Costs and LCOE Analysis

5.1 Introduction

The present chapter aims at an analysis of the main costs involved in setting up an offshore wind farm, namely the CAPEX, OPEX and DECEX. CAPEX is associated with project development and consenting; production and material acquisition; and the infrastructures installation and consenting. OPEX deals with the necessary maintenance and all kind of operation necessary to ensure the longevity and quality of the wind farms operations. Finally, the DECEX is about the decommissioning of the project and all of its intrinsic activities.

Figure 5.1: Breakdown of a wind farm costs in respect to its different phases in [47]

By using the costs and energy produced, the LCOE is also estimated according to the formula:

$$LCOE = \frac{\sum_{t=1}^{n} \frac{CAPEX_0 + OPEX_t + DECEX_{n+1}}{(1+r)^t}}{\sum_{t=1}^{n} \frac{E_t}{(1+r)^t}} \tag{5.1}$$

As patent in equation 5.1 the LCOE accounts for both the discounted costs and the discounted annually produced energy, according to the year in which they are generated, depending on r, the discount rate or WACC. So, it is noticeable how both the discount rate and the project lifetime play decisive roles in the LCOE calculation. It is one of the most used indicators regarding energetic investments evaluation and can be seen as the minimum price at which the energy must be sold in order to break-even at the end of the project lifetime.

The goal of the present chapter is to understand how relevant each kind of cost is in the final budget and to evaluate how strongly can the parameters variation affect the LCOE. This aspect is actually the most important. Indeed, there is not much exact data available regarding floating offshore wind projects, thus making the sensitiveness analysis more important than the exact costs breakdown. Even if there was, it would not be a very relevant information. In fact, as an industry still in an early stage, many of its associated costs are not optimized, leading to probable future costs oscillation or, in other words, to an uncertainty regarding their upcoming values. Naturally, if the industry thrives, becoming commercially luring, costs are expected to diminish, as mentioned in the first chapter. All in all, these remarks make the study of the LCOE's components variation the most adequate set of insights regarding the discussion and analysis of the industry future.

A techno-economic model from WavEc is used. It receives a set of inputs such as the different project costs types, AEP, financial parameters, project life time, among other possible options and calculates the LCOE.

5.2 Sensitiveness analysis

5.2.1 Data and chosen parameters discussion

In order to perform the proposed analysis, data from [47] is used. It will be designated as standard data, in opposition to data obtained from its variation. The WindFloat concept [48] is used as the base model for estimating the costs. It follows that the data is not random, but still it is necessary to estimate many costs. Indeed, even with a supporting model, the unknowns are manifold. The reason why the WindFloat concept is selected as the basis is connected to its similarity with the concept studied throughout this work. In fact, they are both structures of the semi-submersible kind, presenting the same operating principles. Moreover, one of the main cost drivers is steel price and the amount of steel utilized in the construction. Semi-submersible concepts rely heavily on a large steel utilization, making their LCOE potentially higher than other concepts and comparison with those other concepts not very accurate. A summary of the costs is presented in figure 5.2. CAPEX and DECEX values are in thousand Euro per MW, while OPEX values are in thousand Euro per MW per year of operation.

CAPEX	
Development and Consenting	208
Turbine (excl. Tower)	1 281
Mooring Costs (incl. Installation)	170
Grid (incl. Installation)	1097
Production (incl. Tower)	1 640
Construction Phase Insurance	50
Installation of Wind Turbine	129

OPEX	
Annual Operation & Maintenance	113
Annual Operation Insurance	18

DECEX	
Decommissioning	195
Scrap Revenue	424

Figure 5.2: Cost data assumed in [47]

It is important to clarify that the assumptions and factors leading to such expenditures are obtained assuming a 100 5MW turbine wind farm, occupying a 9km*9km square, 200km from the land grid connecting point. Water depth is assumed to be 200m. The project life-time is taken as 20 years and the discount rate as 10,7%. There is also an important note regarding the DECEX. In its breakdown, a scrap revenue is considered. In fact, the massive steel structures can potentially be sold after their decommissioning, given the high market value of steel. This would transform the DECEX from an expenditure into a positive cash flow to be considered in the LCOE. In spite of this hypothesis, a more conventional model (linked to bottom-fixed evaluation) is considered. For instance, in [49] it is assumed that the DECEX is around 60% to 70% of the installation costs. In the present work a value of 400 thousand euros per MW is assumed as described in [50]. On the one hand, it is important to keep in mind the high level of uncertainty regarding this aspect, as the industry has very limited experience and errors in DECEX estimation are very common [50]. On the other hand, DECEX is expected not to be very crucial, as its costs are expected to correspond to less than 1% of the LCOE [51] , making its analysis not a major concern.

The main issue concerning the direct utilization of this information in the present work arises from the project size differences. In fact, the bigger a wind farm is, the more reduced the costs per MW will be due to an economy of scale. While this effect is true for the three different types of costs, it is specially relevant for OPEX, in which operational optimization is key. Again, this points to the interest in studying the effect of possible scale economies factors on the LCOE.

Project life-time and discount rate have already been introduced as determining factors regarding LCOE evaluation. Although they do not exactly represent costs or energy production outputs, they are very much determining factors in regard to the LCOE. At the same time, and this is specially keen for the discount rate, it is a highly changeable parameter. The latter mirrors investors trust and confidence, project risk, expected return from other projects, taxation, inflation and a balance between the market value of debt and equity. Thus, it is expected that as the industry grows and is increasingly proven, the discount rate is expected to decrease. The former depends, among other, on the technology used, site condition, maintenance plan...

Naturally, energy output is also a determining factor influencing the LCOE. In fact, a more accurate estimation of its value is the goal of the previous chapter. Than, it is evidently interesting to undertake an

analysis of the overall effect of the AEP variation. For the same reasoning as the other factors but also as a complement of the previous chapter, by allowing an economic perspective on the relevance of the proposed method (so far, only a techno-energetic perspective had been made clear).

5.2.2 Results discussion

Some factors have been discussed in the previous subsection. Now, a more extensive analysis is performed, with the data available. The sensitiveness analysis results are presented in figure 5.5. The estimated LCOE value is 130€/MWh. This value fits in the estimations provided in [52] and [47] bringing confidence to the validity of the results. Nonetheless, as already mentioned, the objective of the present chapter is to discuss its sensitiveness and not its exact value.

The sensitiveness analysis is undertaken by changing all cost parameters by 10%, both for the increased as well as for the decreased scenario. An exception is on the turbine output power (same meaning as AEP), for which two analysis are studied: one with a 2% variation, reflecting the difference obtained in the previous chapter. Other with the same 10% variation, in order to be compared with all other parameters. The standard values on which the percentages are based are the ones presented in figure 5.2. For each parameter variation, all the others are kept constant.

A discussion on the different parameters follows:

- CAPEX

  The three main cost drivers are all linked to costs that tend to depend directly with farm size and its number of turbines. So, CAPEX is not expected to be strongly dependent on scale economy factors, but on other factors to be readily explored.

  Turbine costs are specially prone for change. In fact, in the past 5 years a decrease of more than 50% has taken place.
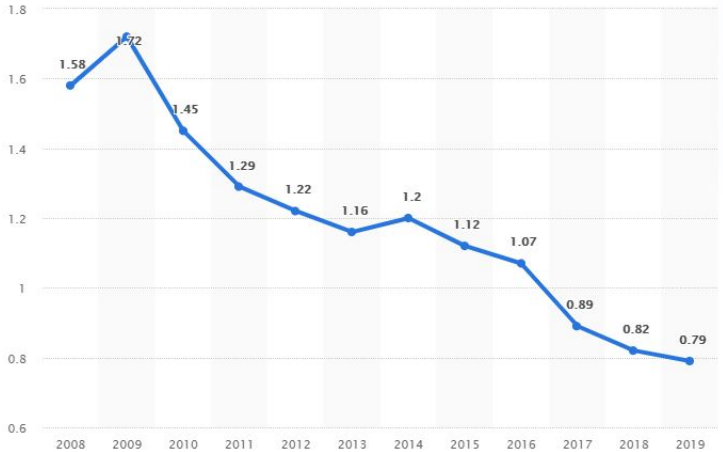
Figure 5.3: Wind turbine cost evolution in the U.S, in million U.S. dollars per MW in [53]

As far as production costs (including tower) are concerned, they are heavily dependent on steel prices. In fact, for the floating structure production, almost 40% of the costs come directly from

59

material consumption (basically steel), while tower construction cost breakdown attributes about 30% of its total value to steel consumption [47]. This is to say that steel price alone is a major driver of the LCOE. As can be seen in figure 5.4 the unstable nature of steel price makes it an extremely crucial parameter to be accessed, regarding its influence on LCOE. Other factors such as labour are also important, though more complex to evaluate.

Figure 5.4: Iron and steel producer price index evolution in the U.S.A [54]

Grid and its installation costs are also expected to vary but due to a broader range of factors. The main drivers are OHVS and offshore export cable [55]. As such, wind farm distance to shore is a major unknown regarding overall grid costs. Other important factors include cost of materials (copper, among others); wind farm layout; vessel costs (dependant on supply and demand; fuel prices;..), among others.

• OPEX

Annual maintenance operations is an important cost that is expected to be heavily dependent (over 70%) on vessel utilization [47]. Such hypothesis makes this field highly prone to be optimized with increasing wind farm sizes. Thus, variations that it can induce in LCOE are likely to be felt as the industry grows. Also, insurance costs are naturally expected to diminish as more reliable and proven projects are set (but its influence is much smaller)

• Energy

This parameter allows a conclusion on the relevance of the main proposed goal: the estimation of the AEP through the present thesis methodology. In fact, it is patent how a change of 2% in the AEP or turbine energy output can produce a greater or similar effect on LCOE as a 10% change in the majority of the other factors analysed. This strengthens the relevance and usefulness of committing more deeply to a more accurate estimation of the AEP, in order to better estimate an offshore wind project LCOE. Although an increased energy output is unlikely, many factors play a role in bringing it down. Sea dynamics; unpredictable stops; energy losses; among others... So, in this case, the red part of the graph is also the most interesting to be studied.

• Finance

The base values of this analysis are assumed to be a 25-year project life time and a discount rate of 10%. As offshore wind investments have typically values ranging between 8% and 12% [52], it means that the discount rate range is broader than what has been analysed here, potentially leading to big increases in the estimated LCOE. Indeed, this is clearly the most important parameter regarding LCOE value, with 10% variations leading to changes of around 5%. This is a parameter in which positive changes are expectable as the industry becomes more trustful, among other parameters already discussed
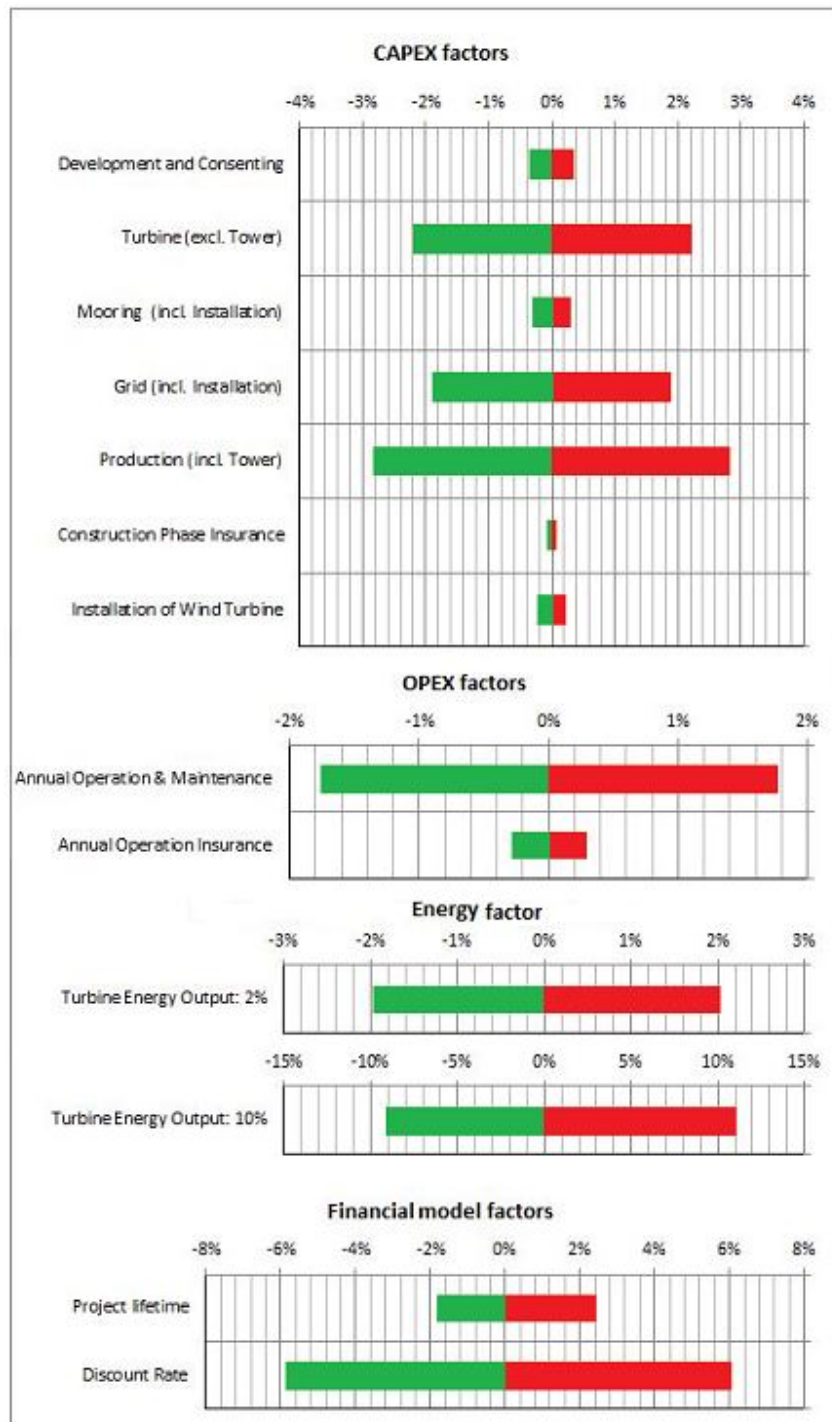
Figure 5.5: Impact analysis of different costs on LCOE

Chapter 6

Conclusions

Throughout the research and work committed in developing this thesis, several important insights have been obtained. They concern mostly the different factors driving a floating offshore turbine power production. They are presented below:

- The platform mean Pitch value importance towards power production. Fore-aft tower displacement also plays a role but is considerably less relevant. Its effect has been quantified and the main reason for its influence is strongly connected with the change in the rotor area perpendicular to the wind flow. Other factors contribute to intensify this trend, though. The optimal case has been found for the horizontal rotor axis position.

- On the one hand, the low dependence of the Pitch and fore-aft tower displacement mean values with the severity of the sea state has been observed. Mean values are more influenced by wind conditions. On the other hand, an important dependence regarding the mean oscillations amplitude is connected to the sea state.

- The tower top speed oscillations influence the turbine power output. The most critical operational area along the power curve corresponds to the rated conditions. Below that point, power production is also influenced due to the non-linear nature of the curve, though to a diminished degree. Above that point, and it's important to define "how above", the speed oscillations do not play a role at all. Indeed, the onset of this no-effect region depends on the intensity of the speed oscillations. For higher speeds, the further away in the power curve the power output is affected. This implies that the strategy of numerically calculating the average power production is tendentiously pointless for higher wind speeds, but important for less intense regimes.

- The analysis of the factors driving the total tower top speed brought out the mutual effect and leading role of Surge and Pitch responses. They present similar values in a quite restricted range, meaning they are equally relevant responses to tackle in order to prevent production losses. Statistically, their oscillation speed is not summed up. On the contrary, their combined association might even decrease the total value. If this was not the case, the annual energy calculation between both approaches studied in this work could be much larger.

- An overall difference of 2% between the conventional and present approaches regarding annual energy production estimations. This is the main result from this thesis. Care must be taken due to the approximations assumed in its calculation (specially regarding the wind distribution discretization), as the real difference might become lower.

- The leading role discount rate has on LCOE. Among all other parameters studied, the discount rate was found to be the most relevant driver of total costs. Moreover, the complete range of plausible values has not been fully analysed meaning that even larger increases/decreases on LCOE can occur in normal conditions. Other important sources of cost are the turbine, platform and tower production. Increased wind farms life time can also lead to significant reductions in LCOE.

- A decreasing cost trend is clearly patent both on the expectancies explored in the first chapter as well as in the more detailed analysis presented in chapter 5. All major cost vectors are expected to lower their toll on LCOE within the frame of a industry growing scenario. This includes turbine production whose cost has been steadily decreasing for the last decade; annual operations and maintenance which is looked upon as a very likely parameter to increase its efficiency with bigger wind farms. Even tower and platform production which are heavily dependent on steel prices are expected to possibly lower their costs by introducing new and more efficient means of production, necessary to keep up with an eventual increasing demand. But, most of all, a decrease in the discount rate as a result of the industry growth and maturing might definitely bring a luring light into floating offshore wind.

- To a less extent, some costs can also be expected to increase. Deeper and further away from the coast projects will necessarily bring with them new challenges. Costs involving the grid and moorings set up are likely to increase in such situation. Even maintenance related-issues can present a contrary trend to what is expected in these scenarios. Other renewable technologies steady development and advantages might jeopardize investors' will to finance offshore wind projects, thus making them very hard to become attractive.

Chapter 7

Future Work

Recommended future work arising from this thesis include:

- Validation of the results presented through simulations with other codes and scaled model tank tests. Investigate the possible advantages of incorporating second-order forces, non linearities, wind turbulence and wind-shear as well as other complex modelling option not taken into account in this work.

- Also, extending the range of conditions from which the conclusion have been drawn. This includes combinations of different wind and wave direction; wave spectrum and wave type variations.

- Improve the wind discretization (more and narrower wind classes) to obtain more accurate results.

- Study other platforms designs and analyse the conclusions for checking if they are general or concept dependent.

- Study other platforms designs and analyse the conclusions. To see if they are general or concept dependent.

- Finally, deepen and strengthen the economic analysis, taking advantage of more consistent information that becomes available as more projects and studies are developed.

Bibliography

[1] "Regulation (EU) 2018/1999 of the European Parliament and of the Council of 11 December 2018 on the Governance of the Energy Union and Climate Action." In: *Official Journal of the European Union* 61 (Dec. 21, 2018). URL: `https://eur-lex.europa.eu/legal-content/EN/TXT/PDF/?uri=OJ:L:2018:328:FULLfrom=EN` (visited on 2019-09-13).

[2] eia. *Wind explained: History of wind power*. URL: `https://www.eia.gov/energyexplained/wind/history-of-wind-power.php` (visited on 2019-09-12).

[3] G. B. Ivan Komusanac Daniel Fraile. *Wind energy in Europe in 2018: Trends and statistics*. Wind Europe, 2019.

[4] I. 2018. *RENEWABLE CAPACITY STATISTICS 2018*. International Renewable Energy Agency (IRENA), 2018.

[5] *Trends in renewable energy*. URL: `https://www.irena.org/Statistics/View-Data-by-Topic/Capacity-and-Generation/Statistics-Time-Series`.

[6] O. W. I. G. task force. *Deep Water: The next step for offshore wind energy*. European Wind Energy Association, 2013.

[7] G. B. Florian Selot Daniel Fraile. *Offshore Wind in Europe:Key trends and statistics 2018*. Wind Europe, 2019.

[8] B. Helen, B. Kate, and T. Paul. "Assessing Environmental Impacts of Offshore Wind Farms: Lessons Learned and Recommendations for the Future". In: *Aquatic biosystems* 10 (Sept. 2014), p. 8. DOI: `10.1186/2046-9063-10-8`.

[9] M. VESTAS. "MHI Vestas Launches the First 10 MW Wind Turbine in History". In: *http://www.mhivestasoffshore.com* (Sept. 25, 2018). URL: `http://www.mhivestasoffshore.com/mhi-vestas-launches-the-first-10-mw-wind-turbine-in-history/` (visited on 2019-09-12).

[10] P. Fairley. *Two-Bladed Wind Turbines Make a Comeback*. 2014. URL: `https://www.technologyreview.com/s/528581/two-bladed-wind-turbines-make-a-comeback/` (visited on 2019-09-13).

[11] D. W. I. Association. *Wind Turbines: Upwind or Downwind Machines*. 2003. URL: `http://xn--drmstrre-64ad.dk/wp-content/wind/miller/windpower%20web/en/tour/design/updown.htm` (visited on 2019-09-13).

[12] X. Wind. URL: `https://www.x1wind.com/` (visited on 2019-09-13).

[13] N. Windpower. URL: `https://www.nauticawindpower.com` (visited on 2019-09-13).

[14] W. Europe. *Floating Offshore Wind Energy A Policy Blueprint For Europe*. Wind Europe, 2017. URL: `https://windeurope.org/wp-content/uploads/files/policy/position-papers/Floating-offshore-wind-energy-a-policy-blueprint-for-Europe.pdf`.

[15] AGI. *What are the advantages and disadvantages of offshore wind farms?* URL: `https://www.americangeosciences.org/critical-issues/faq/what-are-advantages-and-disadvantages-offshore-wind-farms` (visited on 2019-10-21).

[16] *The Danish Offshore Wind Farm Demonstration Project: Horns Rev and Nysted Offshore Wind Farms Environmental impact assessment and monitoring*. DONG Energy, 2006. URL: `https://tethys.pnnl.gov/sites/default/files/publications/Horns-Rev-Nysted-2006.pdf`.

[17] S. B. Laura Small and O. Gutin. *Fact Sheet - Offshore Wind: Can the United States Catch up with Europe?* 2016. URL: `https://www.eesi.org/papers/view/factsheet-offshore-wind-2016#targetText=Offshore%20wind%20is%20also%20stronger,the%20cube%20of%20wind%20speed.` (visited on 2019-09-15).

[18] L. HARTMAN. *Top 10 Things You Didn?t Know About Offshore Wind Energy*. Aug. 12, 2019. URL: `https://www.energy.gov/eere/wind/articles/top-10-things-you-didn-t-know-about-offshore-wind-energy#targetText=Offshore%20Wind%20is%20Right%20on,2.` (visited on 2019-09-15).

[19] I. 2018. *Renewable Power Generation Costs in 2018*. International Renewable Energy Agency (IRENA), 2019.

[20] *Report says offshore wind could beat onshore wind on cost*. URL: `https://www.renewableenergyworld.com/2019/01/29/report-says-offshore-wind-could-beat-onshore-wind-on-cost/#gref` (visited on 2019-09-15).

[21] N. Nixon. *Timeline: The history of wind power*. URL: `https://www.theguardian.com/environment/2008/oct/17/wind-power-renewable-energy` (visited on 2019-09-15).

[22] M. Lempriere. *Full circle: decommissioning the first ever offshore windfarm*. Nov. 21, 2017. URL: `https://www.power-technology.com/features/full-circle-decommissioning-first-ever-offshore-windfarm/` (visited on 2019-09-15).

[23] T. Ackermann. *Wind Power in Power Systems*. WILEY, 2012. ISBN: 9780470974162.

[24] M. C. R. Rhodri James. *Floating Offshore Wind: Market and Technology Review*. Carbon Trust, 2015.

[25] A. R. et al. *Definition of the Semisubmersible Floating System for Phase II of OC4*. NREL, 2014.

[26] J. J. S. B. W. Musial; and G. Scott. *Definition of a 5-MW Reference Wind Turbine for Offshore System Development*. National Renewable Energy Center. 2009.

[27] B. Jonkman and J. Jonkman. *README FAST8*. NREL, 2016.

[28] J. N. Sørensen and W. Z. Shen. "Numerical Modeling of Wind Turbine Wakes". In: *Journal of Fluids Engineering* 124 (2002).

[29] S. Schmitz and P. Jha. "Modeling the Wakes of Wind Turbines and Rotorcraft Using the Actuator-Line Method in an OpenFOAM -LES Solver". In: 69th AHS Forum. Phoenix, AZ, May 2013.

[30] J. J. G. H. B. J. R. Damiani. *AeroDyn v15 User?s Guide and Theory Manual*. NREL.

[31] J. Jonkman. *Dynamics Modeling and Loads Analysis of an Offshore Floating Wind Turbine4*. NREL, 2007.

[32] J. J. G. H. A. Robertson. *HydroDyn User?s Guide and Theory Manual*. NREL.

[33] 0. M. Faltinsen. *Sea Loads on Ships and Offshore Structures*. Cambridge University Press, 1990. ISBN: 0521458706.

[34] *CFD modelling of a tidal stream turbine subjected to profiled flow and surface gravity waves*. International Journal of Marine Energy, 2016.

[35] *WAMIT User Manual Version 7.3*. WAMIT, Inc. 2019.

[36] L. L. Erickson. "Panel Methods - An introduction". In: *NASA technical reports* (1991).

[37] J. Jonkman. "Overview of the ElastoDyn Structural-Dynamics Module". In: EWEA Offshore. Frankfurt, Germany, Nov. 2013.

[38] M. Hall. *MoorDyn Users Guide*. University of Prince Edward Island. 2017.

[39] B. J. Andy Platt and J. Jonkman. *InflowWind Users Guide*. National Wind Technology Center. 2016.

[40] A. R. J. J. et al. "Offshore Code Comparison Collaboration Continuation Within IEA Wind Task 30: Phase II Results Regarding a Floating Semisubmersible Wind System". In: 33rd International Conference on Ocean, Offshore and Arctic Engineering. San Francisco, California, June 2014.

[41] *Task 30 OC4*. URL: https://drive.google.com/drive/folders/1HCniNYy9h5fkBTxJANqcKb73PUVBJ6ZX.

[42] *Mooring Dynamics*. URL: https://ocw.mit.edu/courses/mechanical-engineering/2-019-design-of-ocean-systems-spring-2011/lecture-notes/MIT2_019S11_MD3.pdf.

[43] M.-A. K. P. C. M. A. A.Babarit. "Influence of Sea-States Description on Wave Energy Production Assessment". In: ().

[44] *sowfia data management platform*. URL: http://sowfia.hidromod.com.

[45] *INNOVATION OUTLOOK OFFSHORE WIND*. IRENA, 2016. URL: https://www.irena.org/DocumentDownloads/Publications/IRENA_Innovation_Outlook_Offshore_Wind_2016.pdf.

[46] D. S. Arun Chawla and H. Tolman. *WAVEWATCH III R Hindcasts with Re-analysis winds. Initial report on model setup*. NOAA, 2011. URL: https://polar.ncep.noaa.gov/mmab/papers/tn291/MMAB_291.pdf.

[47] C. B. A. Âgotnes. *Levelized cost of energy for offshore floating wind turbines concepts*. Norwegian University of Life Sciences, 2013.

[48] URL: http://www.principlepowerinc.com/en/windfloat.

[49] G. S. C. G. G. Gibberd. *Logistics and Cost Reduction of Decommissioning Offshore Wind Farms*. EWEA Offshore 2015.

[50] URL: `http://analysis.newenergyupdate.com/wind-energy-update/offshore-operators-act-early-decommissioning-data-limit-costs`.

[51] URL: `https://www.windpoweroffshore.com/article/1487845/offshore-decommissioning-cost-uk-36bn`.

[52] M. L. M. D.-P.-G. M. ; Benveniste. *Sensitivity analysis on the levelized cost of energy forfloating off shore wind farms*. Elsevier, 2018.

[53] T. Wang. *U.S. price index for wind turbines 2008-2019*. URL: `https://www.statista.com/statistics/499491/us-wind-turbine-price-index/`.

[54] S. Levy. *Rising steel prices*. URL: `http://www.cbrecapitalwatch.com/?p=3540`.

[55] *Connecting Offshore Wind Farms A Comparison of Offshore Electricity Grid Development Models in Northwest Europe*. NAVIGANT.

Appendix A

FAST input files

A.0.1 Driver file

```
------- OpenFAST example INPUT FILE ---------------------------------------
FAST Certification Test #25: NREL 5.0 MW Baseline Wind Turbine with OC4-DeepCwind semi configuration, for use in offshore analysis
---------------------- SIMULATION CONTROL -----------------------------------
True            Echo            - Echo input data to <RootName>.ech (flag)
"FATAL"         AbortLevel      - Error level when simulation should abort (string) {"WARNING", "SEVERE", "FATAL"}
         600    TMax            - Total run time (s)
      0.0125    DT              - Recommended module time step (s)
           2    InterpOrder     - Interpolation order for input/output time history (-) {1=linear, 2=quadratic}
           0    NumCrctn        - Number of correction iterations (-) {0=explicit calculation, i.e., no corrections}
       99999    DT_UJac         - Time between calls to get Jacobians (s)
       1E+06    UJacSclFact     - Scaling factor used in Jacobians (-)
---------------------- FEATURE SWITCHES AND FLAGS ---------------------------
           1    CompElast       - Compute structural dynamics (switch) {1=ElastoDyn; 2=ElastoDyn + BeamDyn for blades}
           1    CompInflow      - Compute inflow wind velocities (switch) {0=still air; 1=InflowWind; 2=external from OpenFOAM}
           2    CompAero        - Compute aerodynamic loads (switch) {0=None; 1=AeroDyn v14; 2=AeroDyn v15}
           1    CompServo       - Compute control and electrical-drive dynamics (switch) {0=None; 1=ServoDyn}
           1    CompHydro       - Compute hydrodynamic loads (switch) {0=None; 1=HydroDyn}
           0    CompSub         - Compute sub-structural dynamics (switch) {0=None; 1=SubDyn; 2=External Platform MCKF}
           3    CompMooring     - Compute mooring system (switch) {0=None; 1=MAP++; 2=FEAMooring; 3=MoorDyn; 4=OrcaFlex}
           0    CompIce         - Compute ice loads (switch) {0=None; 1=IceFloe; 2=IceDyn}
---------------------- INPUT FILES ------------------------------------------
"NRELOffshrBsline5MW_OC4DeepCwindSemi_ElastoDyn.dat"    EDFile          - Name of file containing ElastoDyn input parameters (quoted string)
"../5MW_Baseline/NRELOffshrBsline5MW_BeamDyn.dat"    BDBldFile(1)    - Name of file containing BeamDyn input parameters for blade 1 (quoted string)
"../5MW_Baseline/NRELOffshrBsline5MW_BeamDyn.dat"    BDBldFile(2)    - Name of file containing BeamDyn input parameters for blade 2 (quoted string)
"../5MW_Baseline/NRELOffshrBsline5MW_BeamDyn.dat"    BDBldFile(3)    - Name of file containing BeamDyn input parameters for blade 3 (quoted string)
"../5MW_Baseline/NRELOffshrBsline5MW_InflowWind_Steady43mps.dat"    InflowFile     - Name of file containing inflow wind input parameters (quoted string)
"NRELOffshrBsline5MW_OC3Hywind_AeroDyn15.dat"    AeroFile       - Name of file containing aerodynamic input parameters (quoted string)
"NRELOffshrBsline5MW_OC4DeepCwindSemi_ServoDyn.dat"    ServoFile       - Name of file containing control and electrical-drive input parameters (quoted string)
"NRELOffshrBsline5MW_OC4DeepCwindSemi_HydroDyn.dat"    HydroFile       - Name of file containing hydrodynamic input parameters (quoted string)
"unused"        SubFile         - Name of file containing sub-structural input parameters (quoted string)
"NRELOffshrBsline5MW_OC4DeepCwindSemi_MoorDyn.dat"    MooringFile     - Name of file containing mooring system input parameters (quoted string)    NRELOffshrBsline5MW_MIT_NREL_TLP_MoorDyn.dat
NRELOffshrBsline5MW_OC4DeepCwindSemi_MoorDyn.dat
"unused"        IceFile         - Name of file containing ice input parameters (quoted string)
```

A.0.2 Hydrodyn file

```
------- HydroDyn v2.03.* Input File ------------------------------------------
NREL 5.0 MW offshore baseline floating platform HydroDyn input properties for the OC4 Semi-submersible.
False          Echo          - Echo the input file data (flag)
---------------------- ENVIRONMENTAL CONDITIONS --------------------------------
          1025  WtrDens       - Water density (kg/m^3)
           200  WtrDpth       - Water depth (meters)
             0  MSL2SWL       - Offset between still-water level and mean sea level (meters) [positive upward; unused when WaveMod = 6; must be zero if PotMod=1 or 2]
---------------------- WAVES ---------------------------------------------------
             1  WaveMod       - Incident wave kinematics model {0: none=still water, 1: regular (periodic), 1P#: regular with user-specified phase, 2: JONSWAP/Pierson-Mosko
             0  WaveStMod     - Model for stretching incident wave kinematics to instantaneous free surface {0: none=no stretching, 1: vertical stretching, 2: extrapolation
          4600  WaveTMax      - Analysis time for incident wave calculations (sec) [unused when WaveMod=0; determines WaveDOmega=2Pi/WaveTMax in the IFFT]
           0.2  WaveDT        - Time step for incident wave calculations     (sec) [unused when WaveMod=0; 0.1<=WaveDT<=1.0 recommended; determines WaveOmegaMax=Pi/WaveDT i
        6   WaveHs         - Significant wave height of incident waves (meters) [used only when WaveMod=1, 2, or 3]
        2   WaveTp         - Peak-spectral period of incident waves    (sec) [used only when WaveMod=1 or 2]
1.05       WavePkShp      - Peak-shape parameter of incident wave spectrum (-) or DEFAULT (string) [used only when WaveMod=2; use 1.0 for Pierson-Moskowitz]
      0.314159  WvLowCOff    - Low  cut-off frequency or lower frequency limit of the wave spectrum beyond which the wave spectrum is zeroed (rad/s) [unused when WaveMod=0
      1.570796  WvHiCOff     - High cut-off frequency or upper frequency limit of the wave spectrum beyond which the wave spectrum is zeroed (rad/s) [unused when WaveMod=0
             0  WaveDir       - Incident wave propagation heading direction               (degrees) [unused when WaveMod=0 or 6]
             0  WaveDirMod    - Directional spreading function {0: none, 1: COS2S}        (-)      [only used when WaveMod=2,3, or 4]
             1  WaveDirSpread - Wave direction spreading coefficient ( > 0 )              (-)      [only used when WaveMod=2,3, or 4 and WaveDirMod=1]
             1  WaveNDir      - Number of wave directions                                 (-)      [only used when WaveMod=2,3, or 4 and WaveDirMod=1; odd number
             0  WaveDirRange  - Range of wave directions (full range: WaveDir +/- 1/2*WaveDirRange) (degrees) [only used when WaveMod=2,3,or 4 and WaveDirMod=1]
     123456789  WaveSeed(1)   - First  random seed of incident waves [-2147483648 to 2147483647]   (-)      [unused when WaveMod=0, 5, or 6]
    1011121314  WaveSeed(2)   - Second random seed of incident waves [-2147483648 to 2147483647]   (-)      [unused when WaveMod=0, 5, or 6]
FALSE          WaveNDAmp     - Flag for normally distributed amplitudes                  (flag)   [only used when WaveMod=2, 3, or 4]
""             WvKinFile     - Root name of externally generated wave data file(s)      (quoted string)   [used only when WaveMod=5 or 6]
             1  NWaveElev     - Number of points where the incident wave elevations can be computed (-)       [maximum of 9 output locations]
             0  WaveElevxi    - List of xi-coordinates for points where the incident wave elevations can be output (meters) [NWaveElev points, separated by commas or white
             0  WaveElevyi    - List of yi-coordinates for points where the incident wave elevations can be output (meters) [NWaveElev points, separated by commas or white
---------------------- 2ND-ORDER WAVES ------------------------------------------ [unused with WaveMod=0 or 6]
FALSE          WvDiffQTF     - Full difference-frequency 2nd-order wave kinematics (flag)
FALSE          WvSumQTF      - Full summation-frequency  2nd-order wave kinematics (flag)
             0  WvLowCOffD    - Low  frequency cutoff used in the difference-frequencies (rad/s) [Only used with a difference-frequency method]
      1.256637  WvHiCOffD     - High frequency cutoff used in the difference-frequencies (rad/s) [Only used with a difference-frequency method]
      0.618319  WvLowCOffS    - Low  frequency cutoff used in the summation-frequencies  (rad/s) [Only used with a summation-frequency  method]
      3.141593  WvHiCOffS     - High frequency cutoff used in the summation-frequencies  (rad/s) [Only used with a summation-frequency  method]
---------------------- CURRENT -------------------------------------------------- [unused with WaveMod=6]
             0  CurrMod       - Current profile model {0: none=no current, 1: standard, 2: user-defined from routine UserCurrent} (switch)
           0.5  CurrSSV0       - Sub-surface current velocity at still water level  (m/s) [used only when CurrMod=1]
             0  CurrSSDir     - Sub-surface current heading direction (degrees) or DEFAULT (string) [used only when CurrMod=1]
            20  CurrNSRef     - Near-surface current reference depth         (meters) [used only when CurrMod=1]
             0  CurrNSV0      - Near-surface current velocity at still water level (m/s) [used only when CurrMod=1]
             0  CurrNSDir     - Near-surface current heading direction       (degrees) [used only when CurrMod=1]
             0  CurrDIV       - Depth-independent current velocity            (m/s) [used only when CurrMod=1]
             0  CurrDIDir     - Depth-independent current heading direction  (degrees) [used only when CurrMod=1]
```

```
---------------------- FLOATING PLATFORM ------------------------------------------------------- [unused with WaveMod=6]
             1   PotMod          - Potential-flow model {0: none=no potential flow, 1: frequency-to-time-domain transforms based on WAMIT output, 2: fluid-impulse theory (FIT)} (switch)
"../5MW_Baseline/HydroData/marin_semi"    PotFile        - Root name of potential-flow model data; WAMIT output files containing the linear, nondimensionalized, hydrostatic restoring ma
             1   WAMITULEN       - Characteristic body length scale used to redimensionalize WAMIT output (meters) [only used when PotMod=1]
         13917   PtfmVol0        - Displaced volume of water when the platform is in its undisplaced position (m^3) [only used when PotMod=1; USE THE SAME VALUE COMPUTED BY WAMIT AS OUTP
             0   PtfmCOBxt       - The xt offset of the center of buoyancy (COB) from the platform reference point (meters)  [only used when PotMod=1]
             0   PtfmCOByt       - The yt offset of the center of buoyancy (COB) from the platform reference point (meters)  [only used when PotMod=1]
             1   RdtnMod         - Radiation memory-effect model {0: no memory-effect calculation, 1: convolution, 2: state-space} (switch) [only used when PotMod=1; STATE-SPACE REQUIRES
            60   RdtnTMax        - Analysis time for wave radiation kernel calculations (sec) [only used when PotMod=1; determines RdtnDOmega=Pi/RdtnTMax in the cosine transform; MAKE SU
        0.0125   RdtnDT          - Time step for wave radiation kernel calculations (sec) [only used when PotMod=1; DT<=RdtnDT<=0.1 recommended; determines RdtnOmegaMax=Pi/RdtnDT in the
---------------------- 2ND-ORDER FLOATING PLATFORM FORCES ---------------------- [unused with WaveMod=0 or 6, or PotMod=0 or 2]
             0   MnDrift         - Mean-drift 2nd-order forces computed                         {0: None; [7, 8, 9, 10, 11, or 12]: WAMIT file to use} [Only one of MnDrift,
             0   NewmanApp       - Mean- and slow-drift 2nd-order forces computed with Newman's approximation {0: None; [7, 8, 9, 10, 11, or 12]: WAMIT file to use} [Only one of MnDrift,
             0   DiffQTF         - Full difference-frequency 2nd-order forces computed with full QTF          {0: None; [10, 11, or 12]: WAMIT file to use}        [Only one of MnDrift,
             0   SumQTF          - Full summation -frequency 2nd-order forces computed with full QTF          {0: None; [10, 11, or 12]: WAMIT file to use}
---------------------- FLOATING PLATFORM FORCE FLAGS  -------------------------- [unused with WaveMod=6]
True             PtfmSgF         - Platform horizontal surge translation force (flag) or DEFAULT
True             PtfmSwF         - Platform horizontal sway translation force (flag) or DEFAULT
True             PtfmHvF         - Platform vertical heave translation force (flag) or DEFAULT
True             PtfmRF          - Platform roll tilt rotation force (flag) or DEFAULT
True             PtfmPF          - Platform pitch tilt rotation force (flag) or DEFAULT
True             PtfmYF          - Platform yaw rotation force (flag) or DEFAULT
---------------------- PLATFORM ADDITIONAL STIFFNESS AND DAMPING  --------------
             0              0              0              0              0              0   AddF0   - Additional preload (N, N-m)
             0              0              0              0              0              0   AddCLin - Additional linear stiffness (N/m, N/rad, N-m/m, N-m/rad)
             0              0              0              0              0              0
             0              0              0     1451298897              0              0
             0              0              0              0     1451298897              0
             0              0              0              0              0              0
             0              0              0              0              0              0   AddBLin  - Additional linear damping(N/(m/s), N/(rad/s), N-m/(m/s), N-m/(rad/s))
             0              0              0              0              0              0
             0              0              0              0              0              0
             0              0              0              0              0              0
             0              0              0              0              0              0
             0              0              0              0              0              0
             0              0              0              0              0              0   AddBQuad - Additional quadratic drag(N/(m/s)^2, N/(rad/s)^2, N-m(m/s)^2, N-m/(rad/s)^2)
             0              0              0              0              0              0
             0              0              0              0              0              0
             0              0              0              0              0              0
             0              0              0              0              0              0
             0              0              0              0              0              0
---------------------- AXIAL COEFFICIENTS --------------------------------------
             2   NAxCoef         - Number of axial coefficients (-)
AxCoefID  AxCd     AxCa     AxCp
   (-)    (-)      (-)      (-)
     1    0.00     0.00     1.00
     2    9.60     0.00     1.00
```

```
---------------------- MEMBER JOINTS ----------------------------------------------
          44   NJoints         - Number of joints (-)   [must be exactly 0 or at least 2]
JointID   Jointxi     Jointyi     Jointzi  JointAxID   JointOvrlp   [JointOvrlp= 0: do nothing at joint, 1: eliminate overlaps by calculating super member]
  (-)       (m)         (m)         (m)       (-)       (switch)
    1      0.00000     0.00000   -20.00000      1           0
    2      0.00000     0.00000    10.00000      1           0
    3     14.43376    25.00000   -14.00000      1           0
    4     14.43376    25.00000    12.00000      1           0
    5    -28.86751     0.00000   -14.00000      1           0
    6    -28.86751     0.00000    12.00000      1           0
    7     14.43376   -25.00000   -14.00000      1           0
    8     14.43376   -25.00000    12.00000      1           0
    9     14.43375    25.00000   -20.00000      2           0
   10    -28.86750     0.00000   -20.00000      2           0
   11     14.43375   -25.00000   -20.00000      2           0
   12      9.23760    22.00000    10.00000      1           0
   13    -23.67130     3.00000    10.00000      1           0
   14    -23.67130    -3.00000    10.00000      1           0
   15      9.23760   -22.00000    10.00000      1           0
   16     14.43375   -19.00000    10.00000      1           0
   17     14.43375    19.00000    10.00000      1           0
   18      4.04145    19.00000   -17.00000      1           0
   19    -18.47520     6.00000   -17.00000      1           0
   20    -18.47520    -6.00000   -17.00000      1           0
   21      4.04145   -19.00000   -17.00000      1           0
   22     14.43375   -13.00000   -17.00000      1           0
   23     14.43375    13.00000   -17.00000      1           0
   24      1.62500     2.81500    10.00000      1           0
   25     11.43376    19.80385    10.00000      1           0
   26     -3.25000     0.00000    10.00000      1           0
   27    -22.87000     0.00000    10.00000      1           0
   28      1.62500    -2.81500    10.00000      1           0
   29     11.43376   -19.80385    10.00000      1           0
   30      1.62500     2.81500   -17.00000      1           0
   31      8.43376    14.60770   -17.00000      1           0
   32     -3.25000     0.00000   -17.00000      1           0
   33    -16.87000     0.00000   -17.00000      1           0
   34      1.62500    -2.81500   -17.00000      1           0
   35      8.43376   -14.60770   -17.00000      1           0
   36      1.62500     2.81500   -16.20000      1           0
   37     11.43376    19.80385     9.13000      1           0
   38     -3.25000     0.00000   -16.20000      1           0
   39    -22.87000     0.00000     9.13000      1           0
   40      1.62500    -2.81500   -16.20000      1           0
   41     11.43376   -19.80385     9.13000      1           0
   42     14.43376    25.00000   -19.94000      1           0
   43    -28.86751     0.00000   -19.94000      1           0
   44     14.43376   -25.00000   -19.94000      1           0
```

```
---------------------- MEMBER CROSS-SECTION PROPERTIES -------------------------
          4   NPropSets     - Number of member property sets (-)
PropSetID   PropD       PropThck
  (-)        (m)          (m)
   1        6.50000      0.03000        ! Main Column
   2       12.00000      0.06000        ! Upper Columns
   3       24.00000      0.06000        ! Base Columns
   4        1.60000      0.01750        ! Pontoons
-------------------- SIMPLE HYDRODYNAMIC COEFFICIENTS (model 1) --------------
    SimplCd    SimplCdMG    SimplCa    SimplCaMG    SimplCp    SimplCpMG    SimplAxCa    SimplAxCaMG    SimplAxCp    SimplAxCpMG
    (-)        (-)          (-)        (-)          (-)        (-)          (-)          (-)            (-)          (-)
    0.00       0.00         0.00       0.00         1.00       1.00         0.00         0.00           1.00         1.00
-------------------- DEPTH-BASED HYDRODYNAMIC COEFFICIENTS (model 2) ---------
          0   NCoefDpth     - Number of depth-dependent coefficients (-)
Dpth   DpthCd   DpthCdMG   DpthCa   DpthCaMG     DpthCp   DpthCpMG   DpthAxCa   DpthAxCaMG     DpthAxCp   DpthAxCpMG
(m)    (-)      (-)        (-)      (-)          (-)      (-)        (-)        (-)            (-)        (-)
-------------------- MEMBER-BASED HYDRODYNAMIC COEFFICIENTS (model 3) --------
         25   NCoefMembers     - Number of member-based coefficients (-)
MemberID   MemberCd1   MemberCd2   MemberCdMG1   MemberCdMG2   MemberCa1   MemberCa2   MemberCaMG1   MemberCaMG2   MemberCp1   MemberCp2   MemberCpMG1   MemberCpMG2
  (-)       (-)         (-)         (-)           (-)           (-)         (-)         (-)           (-)           (-)         (-)         (-)           (-)
   1        0.56        0.56        0.00          0.00          0.00        0.00        0.00          0.00          0.00        0.00        0.00          0.00
   2        0.61        0.61        0.00          0.00          0.00        0.00        0.00          0.00          0.00        0.00        0.00          0.00
   3        0.61        0.61        0.00          0.00          0.00        0.00        0.00          0.00          0.00        0.00        0.00          0.00
   4        0.61        0.61        0.00          0.00          0.00        0.00        0.00          0.00          0.00        0.00        0.00          0.00
   5        0.68        0.68        0.00          0.00          0.00        0.00        0.00          0.00          0.00        0.00        0.00          0.00
   6        0.68        0.68        0.00          0.00          0.00        0.00        0.00          0.00          0.00        0.00        0.00          0.00
   7        0.68        0.68        0.00          0.00          0.00        0.00        0.00          0.00          0.00        0.00        0.00          0.00
  23        0.68        0.68        0.00          0.00          0.00        0.00        0.00          0.00          0.00        0.00        0.00          0.00
  24        0.68        0.68        0.00          0.00          0.00        0.00        0.00          0.00          0.00        0.00        0.00          0.00
  25        0.68        0.68        0.00          0.00          0.00        0.00        0.00          0.00          0.00        0.00        0.00          0.00
   8        0.63        0.63        0.00          0.00          0.00        0.00        0.00          0.00          0.00        0.00        0.00          0.00
   9        0.63        0.63        0.00          0.00          0.00        0.00        0.00          0.00          0.00        0.00        0.00          0.00
  10        0.63        0.63        0.00          0.00          0.00        0.00        0.00          0.00          0.00        0.00        0.00          0.00
  11        0.63        0.63        0.00          0.00          0.00        0.00        0.00          0.00          0.00        0.00        0.00          0.00
  12        0.63        0.63        0.00          0.00          0.00        0.00        0.00          0.00          0.00        0.00        0.00          0.00
  13        0.63        0.63        0.00          0.00          0.00        0.00        0.00          0.00          0.00        0.00        0.00          0.00
  14        0.63        0.63        0.00          0.00          0.00        0.00        0.00          0.00          0.00        0.00        0.00          0.00
  15        0.63        0.63        0.00          0.00          0.00        0.00        0.00          0.00          0.00        0.00        0.00          0.00
  16        0.63        0.63        0.00          0.00          0.00        0.00        0.00          0.00          0.00        0.00        0.00          0.00
  17        0.63        0.63        0.00          0.00          0.00        0.00        0.00          0.00          0.00        0.00        0.00          0.00
  18        0.63        0.63        0.00          0.00          0.00        0.00        0.00          0.00          0.00        0.00        0.00          0.00
  19        0.63        0.63        0.00          0.00          0.00        0.00        0.00          0.00          0.00        0.00        0.00          0.00
  20        0.63        0.63        0.00          0.00          0.00        0.00        0.00          0.00          0.00        0.00        0.00          0.00
  21        0.63        0.63        0.00          0.00          0.00        0.00        0.00          0.00          0.00        0.00        0.00          0.00
  22        0.63        0.63        0.00          0.00          0.00        0.00        0.00          0.00          0.00        0.00        0.00          0.00
```

```
            25   NMembers      - Number of members (-)
MemberID  MJointID1  MJointID2  MPropSetID1  MPropSetID2  MDivSize  MCoefMod  PropPot   [MCoefMod=1: use simple coeff table, 2: use depth-based coeff table, 3: use member-based coeff table]
  (-)       (-)        (-)         (-)          (-)          (m)     (switch)   (flag)
   1         1          2           1            1          1.0000      3       TRUE     ! Main Column
   2         3          4           2            2          1.0000      3       TRUE     ! Upper Column 1
   3         5          6           2            2          1.0000      3       TRUE     ! Upper Column 2
   4         7          8           2            2          1.0000      3       TRUE     ! Upper Column 3
   5        42          3           3            3          1.0000      3       TRUE     ! Base Column 1
   6        43          5           3            3          1.0000      3       TRUE     ! Base Column 2
   7        44          7           3            3          1.0000      3       TRUE     ! Base Column 3
  23         9         42           3            3          1.0000      3       TRUE     ! Base column cap 1
  24        10         43           3            3          1.0000      3       TRUE     ! Base column cap 2
  25        11         44           3            3          1.0000      3       TRUE     ! Base column cap 3
   8        12         13           4            4          1.0000      3       TRUE     ! Delta Pontoon, Upper 1
   9        14         15           4            4          1.0000      3       TRUE     ! Delta Pontoon, Upper 2
  10        16         17           4            4          1.0000      3       TRUE     ! Delta Pontoon, Upper 3
  11        18         19           4            4          1.0000      3       TRUE     ! Delta Pontoon, Lower 1
  12        20         21           4            4          1.0000      3       TRUE     ! Delta Pontoon, Lower 2
  13        22         23           4            4          1.0000      3       TRUE     ! Delta Pontoon, Lower 3
  14        24         25           4            4          1.0000      3       TRUE     ! Y Pontoon, Upper 1
  15        26         27           4            4          1.0000      3       TRUE     ! Y Pontoon, Upper 2
  16        28         29           4            4          1.0000      3       TRUE     ! Y Pontoon, Upper 3
  17        30         31           4            4          1.0000      3       TRUE     ! Y Pontoon, Lower 1
  18        32         33           4            4          1.0000      3       TRUE     ! Y Pontoon, Lower 2
  19        34         35           4            4          1.0000      3       TRUE     ! Y Pontoon, Lower 3
  20        36         37           4            4          1.0000      3       TRUE     ! Cross Brace 1
  21        38         39           4            4          1.0000      3       TRUE     ! Cross Brace 2
  22        40         41           4            4          1.0000      3       TRUE     ! Cross Brace 3
-------------------- FILLED MEMBERS ---------------------------------------------
            2   NFillGroups     - Number of filled member groups (-) [If FillDens = DEFAULT, then FillDens = WtrDens; FillFSLoc is related to MSL2SWL]
FillNumM FillMList          FillFSLoc    FillDens
 (-)       (-)                 (m)        (kg/m^3)
   3   2   3   4    -6.17         1025
   3   5   6   7   -14.89         1025
```

A.0.3 Aerodyn file

```
------- AERODYN v15 for OpenFAST INPUT FILE ----------------------------------------------
NREL 5.0 MW offshore baseline aerodynamic input properties.
======  General Options  ================================================================
False          Echo           - Echo the input to "<rootname>.AD.ech"?  (flag)
"default"      DTAero         - Time interval for aerodynamic calculations {or "default"} (s)
        1      WakeMod        - Type of wake/induction model (switch) {0=none, 1=BEMT, 2=DBEMT} [WakeMod cannot be 2 when linearizing]
        2      AFAeroMod      - Type of blade airfoil aerodynamics model (switch) {1=steady model, 2=Beddoes-Leishman unsteady model} [AFAeroMod must be 1 when linearizing]
        1      TwrPotent      - Type tower influence on wind based on potential flow around the tower (switch) {0=none, 1=baseline potential flow, 2=potential flow with Bak correction}
False          TwrShadow      - Calculate tower influence on wind based on downstream tower shadow? (flag)
True           TwrAero        - Calculate tower aerodynamic loads? (flag)
False          FrozenWake     - Assume frozen wake during linearization? (flag) [used only when WakeMod=1 and when linearizing]
False          CavitCheck     - Perform cavitation check? (flag) [AFAeroMod must be 1 when CavitCheck=true]
======  Environmental Conditions  =======================================================
    1.225      AirDens        - Air density (kg/m^3)
 1.464E-05     KinVisc        - Kinematic air viscosity (m^2/s)
      335      SpdSound       - Speed of sound (m/s)
   103500      Patm           - Atmospheric pressure (Pa) [used only when CavitCheck=True]
     1700      Pvap           - Vapour pressure of fluid (Pa) [used only when CavitCheck=True]
      0.5      FluidDepth     - Water depth above mid-hub height (m) [used only when CavitCheck=True]
======  Blade-Element/Momentum Theory Options  =========================================== [unused when WakeMod=0]
        2      SkewMod        - Type of skewed-wake correction model (switch) {1=uncoupled, 2=Pitt/Peters, 3=coupled} [unused when WakeMod=0]
"default"      SkewModFactor  - Constant used in Pitt/Peters skewed wake model {or "default" is 15/32*pi} (-) [used only when SkewMod=2; unused when WakeMod=0]
True           TipLoss        - Use the Prandtl tip-loss model? (flag) [unused when WakeMod=0]
True           HubLoss        - Use the Prandtl hub-loss model? (flag) [unused when WakeMod=0]
true           TanInd         - Include tangential induction in BEMT calculations? (flag) [unused when WakeMod=0]
False          AIDrag         - Include the drag term in the axial-induction calculation? (flag) [unused when WakeMod=0]
False          TIDrag         - Include the drag term in the tangential-induction calculation? (flag) [unused when WakeMod=0 or TanInd=FALSE]
"Default"      IndToler       - Convergence tolerance for BEMT nonlinear solve residual equation {or "default"} (-) [unused when WakeMod=0]
      100      MaxIter        - Maximum number of iteration steps (-) [unused when WakeMod=0]
======  Dynamic Blade-Element/Momentum Theory Options  =================================== [used only when WakeMod=2]
        2      DBEMT_Mod      - Type of dynamic BEMT (DBEMT) model {1=constant tau1, 2=time-dependent tau1} (-) [used only when WakeMod=2]
        4      tau1_const     - Time constant for DBEMT (s) [used only when WakeMod=2 and DBEMT_Mod=1]
```

```
====== Beddoes-Leishman Unsteady Airfoil Aerodynamics Options  ======================================= [used only when AFAeroMod=2]
        3    UAMod                  - Unsteady Aero Model Switch (switch) {1=Baseline model (Original), 2=Gonzalez's variant (changes in Cn,Cc,Cm), 3=Minemma/Pierce variant (changes in Cc and Cm)}
True         FLookup                - Flag to indicate whether a lookup for f' will be calculated (TRUE) or whether best-fit exponential equations will be used (FALSE); if FALSE S1-S4 must be provi:
====== Airfoil Information =====================================================================
        1    InCol_Alfa             - The column in the airfoil tables that contains the angle of attack (-)
        2    InCol_Cl               - The column in the airfoil tables that contains the lift coefficient (-)
        3    InCol_Cd               - The column in the airfoil tables that contains the drag coefficient (-)
        4    InCol_Cm               - The column in the airfoil tables that contains the pitching-moment coefficient; use zero if there is no Cm column (-)
        0    InCol_Cpmin            - The column in the airfoil tables that contains the Cpmin coefficient; use zero if there is no Cpmin column (-)
        8    NumAFfiles             - Number of airfoil files used (-)
"../5MW_Baseline/Airfoils/Cylinder1.dat"    AFNames             - Airfoil file names (NumAFfiles lines) (quoted strings)
"../5MW_Baseline/Airfoils/Cylinder2.dat"
"../5MW_Baseline/Airfoils/DU40_A17.dat"
"../5MW_Baseline/Airfoils/DU35_A17.dat"
"../5MW_Baseline/Airfoils/DU30_A17.dat"
"../5MW_Baseline/Airfoils/DU25_A17.dat"
"../5MW_Baseline/Airfoils/DU21_A17.dat"
"../5MW_Baseline/Airfoils/NACA64_A17.dat"
====== Rotor/Blade Properties  =====================================================================
True         UseBlCm                - Include aerodynamic pitching moment in calculations?  (flag)
"../5MW_Baseline/NRELOffshrBsline5MW_AeroDyn_blade.dat"    ADBlFile(1)      - Name of file containing distributed aerodynamic properties for Blade #1 (-)
"../5MW_Baseline/NRELOffshrBsline5MW_AeroDyn_blade.dat"    ADBlFile(2)      - Name of file containing distributed aerodynamic properties for Blade #2 (-) [unused if NumBl < 2]
"../5MW_Baseline/NRELOffshrBsline5MW_AeroDyn_blade.dat"    ADBlFile(3)      - Name of file containing distributed aerodynamic properties for Blade #3 (-) [unused if NumBl < 3]
====== Tower Influence and Aerodynamics =========================================================== [used only when TwrPotent/=0, TwrShadow=True, or TwrAero=True]
       11    NumTwrNds              - Number of tower nodes used in the analysis  (-) [used only when TwrPotent/=0, TwrShadow=True, or TwrAero=True]
TwrElev       TwrDiam      TwrCd
(m)            (m)          (-)
1.0000000E+01  6.5000000E+00  1.0000000E+00
1.7760000E+01  6.2400000E+00  1.0000000E+00
2.5520000E+01  5.9700000E+00  1.0000000E+00
3.3280000E+01  5.7100000E+00  1.0000000E+00
4.1040000E+01  5.4500000E+00  1.0000000E+00
4.8800000E+01  5.1800000E+00  1.0000000E+00
5.6560000E+01  4.9200000E+00  1.0000000E+00
6.4320000E+01  4.6600000E+00  1.0000000E+00
7.2080000E+01  4.4000000E+00  1.0000000E+00
7.9840000E+01  4.1300000E+00  1.0000000E+00
8.7600000E+01  3.8700000E+00  1.0000000E+00
```

A.0.4 Moordyn file

```
--------------------- MoorDyn Input File ---------------------------------
Mooring system for OC4-DeepCwind Semi
FALSE    Echo      - echo the input file data (flag)
--------------------- LINE TYPES -----------------------------------------
1        NTypes    - number of LineTypes
Name     Diam      MassDen      EA    BA/-zeta  Can   Cat   Cdn   Cdt
(-)      (m)       (kg/m)       (N)   (N-s/-)   (-)   (-)   (-)   (-)
main     0.0766    113.35    7.536E8  -1.0      0.8   0.25  2.0   0.4
--------------------- CONNECTION PROPERTIES ------------------------------
6        NConnects - number of connections including anchors and fairleads
Node  Type     X        Y        Z       M     V     FX   FY   FZ   CdA    CA
(-)   (-)      (m)      (m)      (m)     (kg)  (m^3) (kN) (kN) (kN) (m^2)  (-)
1     Fixed    418.8    725.383  -200.0   0     0     0    0    0    0      0
2     Fixed   -837.6      0.0    -200.0   0     0     0    0    0    0      0
3     Fixed    418.8   -725.383  -200.0   0     0     0    0    0    0      0
4     Vessel   20.434   35.393   -14.0    0     0     0    0    0    0      0
5     Vessel  -40.868    0.0     -14.0    0     0     0    0    0    0      0
6     Vessel   20.434  -35.393   -14.0    0     0     0    0    0    0      0
--------------------- LINE PROPERTIES ------------------------------------
3        NLines    - number of line objects
Line  LineType UnstrLen  NumSegs   NodeAnch  NodeFair  Flags/Outputs
(-)   (-)      (m)       (-)       (-)       (-)       (-)
1     main     835.35    20        1         4         -
2     main     835.35    20        2         5         -
3     main     835.35    20        3         6         -
--------------------- SOLVER OPTIONS -------------------------------------
0.001    dtM       - time step to use in mooring integration (s)
3.0e6    kbot      - bottom stiffness (Pa/m)
3.0e5    cbot      - bottom damping (Pa-s/m)
2.0      dtIC      - time interval for analyzing convergence during IC gen (s)
60.0     TmaxIC    - max time for ic gen (s)
4.0      CdScaleIC - factor by which to scale drag coefficients during dynamic relaxation (-)
0.01     threshIC  - threshold for IC convergence (-)
```

A.0.5   Elastodyn file

```
------- ELASTODYN v1.03.* INPUT FILE ------------------------------------------
NREL 5.0 MW Baseline Wind Turbine for Use in Offshore Analysis. Properties from Dutch Offshore Wind Energy Converter (DOWEC) 6MW Pre-Design (10046_009.pdf) and REpower 5M 5MW
---------------------- SIMULATION CONTROL --------------------------------------
False         Echo        - Echo input data to "<RootName>.ech" (flag)
        3     Method      - Integration method: {1: RK4, 2: AB4, or 3: ABM4} (-)
"DEFAULT"     DT          - Integration time step (s)
---------------------- ENVIRONMENTAL CONDITION ---------------------------------
    9.80665   Gravity     - Gravitational acceleration (m/s^2)
---------------------- DEGREES OF FREEDOM --------------------------------------
true          FlapDOF1    - First flapwise blade mode DOF (flag)
true          FlapDOF2    - Second flapwise blade mode DOF (flag)
true          EdgeDOF     - First edgewise blade mode DOF (flag)
true          TeetDOF     - Rotor-teeter DOF (flag) [unused for 3 blades]
true          DrTrDOF     - Drivetrain rotational-flexibility DOF (flag)
true          GenDOF      - Generator DOF (flag)
true          YawDOF      - Yaw DOF (flag)
true          TwFADOF1    - First fore-aft tower bending-mode DOF (flag)
true          TwFADOF2    - Second fore-aft tower bending-mode DOF (flag)
true          TwSSDOF1    - First side-to-side tower bending-mode DOF (flag)
true          TwSSDOF2    - Second side-to-side tower bending-mode DOF (flag)
true          PtfmSgDOF   - Platform horizontal surge translation DOF (flag)
true          PtfmSwDOF   - Platform horizontal sway translation DOF (flag)
true          PtfmHvDOF   - Platform vertical heave translation DOF (flag)
true          PtfmRDOF    - Platform roll tilt rotation DOF (flag)
true          PtfmPDOF    - Platform pitch tilt rotation DOF (flag)
true          PtfmYDOF    - Platform yaw rotation DOF (flag)
---------------------- INITIAL CONDITIONS -------------------------------------
        0     OoPDefl     - Initial out-of-plane blade-tip displacement (meters)
        0     IPDefl      - Initial in-plane blade-tip deflection (meters)
        0     BlPitch(1)  - Blade 1 initial pitch (degrees)
        0     BlPitch(2)  - Blade 2 initial pitch (degrees)
        0     BlPitch(3)  - Blade 3 initial pitch (degrees) [unused for 2 blades]
        0     TeetDefl    - Initial or fixed teeter angle (degrees) [unused for 3 blades]
        0     Azimuth     - Initial azimuth angle for blade 1 (degrees)
        0     RotSpeed    - Initial or fixed rotor speed (rpm)
        0     NacYaw      - Initial or fixed nacelle-yaw angle (degrees)
        0     TTDspFA     - Initial fore-aft tower-top displacement (meters)
        0     TTDspSS     - Initial side-to-side tower-top displacement (meters)
        0     PtfmSurge   - Initial or fixed horizontal surge translational displacement of platform (meters)
        0     PtfmSway    - Initial or fixed horizontal sway translational displacement of platform (meters)
        0     PtfmHeave   - Initial or fixed vertical heave translational displacement of platform (meters)
        0     PtfmRoll    - Initial or fixed roll tilt rotational displacement of platform (degrees)
        0     PtfmPitch   - Initial or fixed pitch tilt rotational displacement of platform (degrees)
        0     PtfmYaw     - Initial or fixed yaw rotational displacement of platform (degrees)
```

```
---------------------- TURBINE CONFIGURATION ------------------------------------------
         3   NumBl        - Number of blades (-)
        63   TipRad       - The distance from the rotor apex to the blade tip (meters)
       1.5   HubRad       - The distance from the rotor apex to the blade root (meters)
      -2.5   PreCone(1)   - Blade 1 cone angle (degrees)
      -2.5   PreCone(2)   - Blade 2 cone angle (degrees)
      -2.5   PreCone(3)   - Blade 3 cone angle (degrees) [unused for 2 blades]
         0   HubCM        - Distance from rotor apex to hub mass [positive downwind] (meters)
         0   UndSling     - Undersling length [distance from teeter pin to the rotor apex] (meters) [unused for 3 blades]
         0   Delta3       - Delta-3 angle for teetering rotors (degrees) [unused for 3 blades]
         0   AzimB1Up     - Azimuth value to use for I/O when blade 1 points up (degrees)
   -5.0191   OverHang     - Distance from yaw axis to rotor apex [3 blades] or teeter pin [2 blades] (meters)
     1.912   ShftGagL     - Distance from rotor apex [3 blades] or teeter pin [2 blades] to shaft strain gages [positive for upwind rotors] (meters)
        -5   ShftTilt     - Rotor shaft tilt angle (degrees)
       1.9   NacCMxn      - Downwind distance from the tower-top to the nacelle CM (meters)
         0   NacCMyn      - Lateral  distance from the tower-top to the nacelle CM (meters)
      1.75   NacCMzn      - Vertical distance from the tower-top to the nacelle CM (meters)
  -3.09528   NcIMUxn      - Downwind distance from the tower-top to the nacelle IMU (meters)
         0   NcIMUyn      - Lateral  distance from the tower-top to the nacelle IMU (meters)
   2.23336   NcIMUzn      - Vertical distance from the tower-top to the nacelle IMU (meters)
   1.96256   Twr2Shft     - Vertical distance from the tower-top to the rotor shaft (meters)
      87.6   TowerHt      - Height of tower above ground level [onshore] or MSL [offshore] (meters)
        10   TowerBsHt    - Height of tower base above ground level [onshore] or MSL [offshore] (meters)
         0   PtfmCMxt     - Downwind distance from the ground level [onshore] or MSL [offshore] to the platform CM (meters)
         0   PtfmCMyt     - Lateral distance from the ground level [onshore] or MSL [offshore] to the platform CM (meters)
   -8.6588   PtfmCMzt     - Vertical distance from the ground level [onshore] or MSL [offshore] to the platform CM (meters)
         0   PtfmRefzt    - Vertical distance from the ground level [onshore] or MSL [offshore] to the platform reference point (meters)
---------------------- MASS AND INERTIA -------------------------------------------
         0   TipMass(1)   - Tip-brake mass, blade 1 (kg)
         0   TipMass(2)   - Tip-brake mass, blade 2 (kg)
         0   TipMass(3)   - Tip-brake mass, blade 3 (kg) [unused for 2 blades]
     56780   HubMass      - Hub mass (kg)
    115926   HubIner      - Hub inertia about rotor axis [3 blades] or teeter axis [2 blades] (kg m^2)
   534.116   GenIner      - Generator inertia about HSS (kg m^2)
    240000   NacMass      - Nacelle mass (kg)
2.60789E+06  NacYIner     - Nacelle inertia about yaw axis (kg m^2)
         0   YawBrMass    - Yaw bearing mass (kg)
3.85218E+06  PtfmMass     - Platform mass (kg)
2.56193E+09  PtfmRIner    - Platform inertia for roll tilt rotation about the platform CM (kg m^2)
2.56193E+09  PtfmPIner    - Platform inertia for pitch tilt rotation about the platform CM (kg m^2)
4.24265E+09  PtfmYIner    - Platform inertia for yaw rotation about the platform CM (kg m^2)
---------------------- BLADE --------------------------------------------------
        17   BldNodes     - Number of blade nodes (per blade) used for analysis (-)
"../5MW_Baseline/NRELOffshrBsline5MW_Blade.dat"    BldFile(1)   - Name of file containing properties for blade 1 (quoted string)
"../5MW_Baseline/NRELOffshrBsline5MW_Blade.dat"    BldFile(2)   - Name of file containing properties for blade 2 (quoted string)
"../5MW_Baseline/NRELOffshrBsline5MW_Blade.dat"    BldFile(3)   - Name of file containing properties for blade 3 (quoted string) [unused for 2 blades]
```

```
---------------------- ROTOR-TEETER -----------------------------------------------
         0   TeetMod    - Rotor-teeter spring/damper model {0: none, 1: standard, 2: user-defined from routine UserTeet} (switch) [unused for 3 blades]
         0   TeetDmpP   - Rotor-teeter damper position (degrees) [used only for 2 blades and when TeetMod=1]
         0   TeetDmp    - Rotor-teeter damping constant (N-m/(rad/s)) [used only for 2 blades and when TeetMod=1]
         0   TeetCDmp   - Rotor-teeter rate-independent Coulomb-damping moment (N-m) [used only for 2 blades and when TeetMod=1]
         0   TeetSStP   - Rotor-teeter soft-stop position (degrees) [used only for 2 blades and when TeetMod=1]
         0   TeetHStP   - Rotor-teeter hard-stop position (degrees) [used only for 2 blades and when TeetMod=1]
         0   TeetSSSp   - Rotor-teeter soft-stop linear-spring constant (N-m/rad) [used only for 2 blades and when TeetMod=1]
         0   TeetHSSp   - Rotor-teeter hard-stop linear-spring constant (N-m/rad) [used only for 2 blades and when TeetMod=1]
---------------------- DRIVETRAIN -------------------------------------------------
       100   GBoxEff    - Gearbox efficiency (%)
        97   GBRatio    - Gearbox ratio (-)
8.67637E+08  DTTorSpr   - Drivetrain torsional spring (N-m/rad)
  6.215E+06  DTTorDmp   - Drivetrain torsional damper (N-m/(rad/s))
---------------------- FURLING ----------------------------------------------------
False        Furling    - Read in additional model properties for furling turbine (flag) [must currently be FALSE]
"unused"     FurlFile   - Name of file containing furling properties (quoted string) [unused when Furling=False]
---------------------- TOWER ------------------------------------------------------
        20   TwrNodes   - Number of tower nodes used for analysis (-)
"NRELOffshrBsline5MW_OC4DeepCwindSemi_ElastoDyn_Tower.dat"    TwrFile    - Name of file containing tower properties (quoted string)
```

A.0.6 Elastodyn tower file

```
------- ELASTODYN V1.00.* TOWER INPUT FILE -------------------------------------
NREL 5.0 MW offshore baseline tower input properties for the OC4-DeepCwind Semi.
---------------------- TOWER PARAMETERS -----------------------------------------
        11    NTwInpSt    - Number of input stations to specify tower geometry
         1    TwrFADmp(1) - Tower 1st fore-aft mode structural damping ratio (%)
         1    TwrFADmp(2) - Tower 2nd fore-aft mode structural damping ratio (%)
         1    TwrSSDmp(1) - Tower 1st side-to-side mode structural damping ratio (%)
         1    TwrSSDmp(2) - Tower 2nd side-to-side mode structural damping ratio (%)
---------------------- TOWER ADJUSTMUNT FACTORS ---------------------------------
         1    FAStTunr(1) - Tower fore-aft modal stiffness tuner, 1st mode (-)
         1    FAStTunr(2) - Tower fore-aft modal stiffness tuner, 2nd mode (-)
         1    SSStTunr(1) - Tower side-to-side stiffness tuner, 1st mode (-)
         1    SSStTunr(2) - Tower side-to-side stiffness tuner, 2nd mode (-)
         1    AdjTwMa     - Factor to adjust tower mass density (-)
         1    AdjFASt     - Factor to adjust tower fore-aft stiffness (-)
         1    AdjSSSt     - Factor to adjust tower side-to-side stiffness (-)
---------------------- DISTRIBUTED TOWER PROPERTIES -----------------------------
  HtFract        TMassDen         TwFAStif          TwSSStif
   (-)            (kg/m)           (Nm^2)            (Nm^2)
0.0000000E+000  4.6670000E+003   6.0390300E+011    6.0390300E+011
1.0000000E-001  4.3452800E+003   5.1764400E+011    5.1764400E+011
2.0000000E-001  4.0347600E+003   4.4092500E+011    4.4092500E+011
3.0000000E-001  3.7354400E+003   3.7302200E+011    3.7302200E+011
4.0000000E-001  3.4473200E+003   3.1323600E+011    3.1323600E+011
5.0000000E-001  3.1704000E+003   2.6089700E+011    2.6089700E+011
6.0000000E-001  2.9046900E+003   2.1536500E+011    2.1536500E+011
7.0000000E-001  2.6501800E+003   1.7602800E+011    1.7602800E+011
8.0000000E-001  2.4068800E+003   1.4230100E+011    1.4230100E+011
9.0000000E-001  2.1747700E+003   1.1363000E+011    1.1363000E+011
1.0000000E+000  1.9538700E+003   8.9488000E+010    8.9488000E+010
---------------------- TOWER FORE-AFT MODE SHAPES -------------------------------
    1.1533    TwFAM1Sh(2) - Mode 1, coefficient of x^2 term
   -0.8622    TwFAM1Sh(3) -         , coefficient of x^3 term
    1.8042    TwFAM1Sh(4) -         , coefficient of x^4 term
   -1.5035    TwFAM1Sh(5) -         , coefficient of x^5 term
    0.4082    TwFAM1Sh(6) -         , coefficient of x^6 term
   19.1169    TwFAM2Sh(2) - Mode 2, coefficient of x^2 term
   -6.8956    TwFAM2Sh(3) -         , coefficient of x^3 term
   -8.185     TwFAM2Sh(4) -         , coefficient of x^4 term
   -5.1085    TwFAM2Sh(5) -         , coefficient of x^5 term
    2.0722    TwFAM2Sh(6) -         , coefficient of x^6 term
---------------------- TOWER SIDE-TO-SIDE MODE SHAPES ---------------------------
    1.1438    TwSSM1Sh(2) - Mode 1, coefficient of x^2 term
   -0.874     TwSSM1Sh(3) -         , coefficient of x^3 term
    1.8388    TwSSM1Sh(4) -         , coefficient of x^4 term
   -1.5306    TwSSM1Sh(5) -         , coefficient of x^5 term
    0.422     TwSSM1Sh(6) -         , coefficient of x^6 term
   11.2222    TwSSM2Sh(2) - Mode 2, coefficient of x^2 term
   -3.2615    TwSSM2Sh(3) -         , coefficient of x^3 term
   -5.1208    TwSSM2Sh(4) -         , coefficient of x^4 term
   -0.86      TwSSM2Sh(5) -         , coefficient of x^5 term
   -0.9798    TwSSM2Sh(6) -         , coefficient of x^6 term
```

Appendix B

Hydrodynamic and hydrostatic coefficients

An example for a period of about 628 s is given (when applied). The files with the full period range are not included due to their size.

B.0.1   Added-mass and damping coefficients

The first column provides the period; second and third columns provide the coefficients indexes; the fourth column the added-mass coefficients value; last column provides the damping coefficients value.

```
0.628319E+03    1    1   8.527234E+03   1.604159E-02
0.628319E+03    1    3  -9.061793E-03   5.969791E-04
0.628319E+03    1    5  -1.049620E+05  -1.030536E-01
0.628319E+03    2    2   8.527046E+03   1.606951E-02
0.628319E+03    2    4   1.049601E+05   1.023084E-01
0.628319E+03    2    6   4.576264E+00   4.414072E-06
0.628319E+03    3    1   1.177539E-02  -1.062250E-03
0.628319E+03    3    3   1.499195E+04   1.805970E+02
0.628319E+03    3    5  -3.530985E-01  -1.602945E-02
0.628319E+03    4    2   1.049543E+05   1.022840E-01
0.628319E+03    4    4   7.440688E+06   6.528001E-01
0.628319E+03    4    6   9.926791E+01  -2.577802E-03
0.628319E+03    5    1  -1.049591E+05  -1.004758E-01
0.628319E+03    5    3   1.033527E+00   2.604080E-01
0.628319E+03    5    5   7.440624E+06   5.748485E-01
0.628319E+03    6    2   2.810983E+00   1.265747E-05
0.628319E+03    6    4  -2.732847E+01   4.441947E-04
0.628319E+03    6    6   6.273284E+06   8.495479E-04
```

B.0.2   Excitation coefficients

The first column provides the period; the second column provides the incoming wave direction; the third column provides the coefficient index; the fourth provides the complex wave excitation module; the fifth, sixth and seventh columns provide the phase, real and imaginary part, respectively.

```
0.628319E+03 -0.180000E+03    1  5.067605E+00 -9.019937E+01 -1.763335E-02 -5.067575E+00
0.628319E+03 -0.180000E+03    2  1.233244E-07 -9.000932E+01 -2.006745E-11 -1.233244E-07
0.628319E+03 -0.180000E+03    3  3.798033E+02  2.810586E-04  3.798033E+02  1.863086E-03
0.628319E+03 -0.180000E+03    4  7.850422E-07 -9.020444E+01 -2.801196E-09 -7.850372E-07
0.628319E+03 -0.180000E+03    5  3.225916E+01  9.032115E+01 -1.808175E-01  3.225865E+01
0.628319E+03 -0.180000E+03    6  7.692402E-11 -9.000000E+01  1.013979E-13 -7.692395E-11
```

B.0.3 Hydrostatic restoring coefficients

The first, second, fourth and fifth columns provide the hydrostatic restoring matrix indexes. Third and and sixth columns the coefficients values.

1	1	0,00E+00	4	1	0,00E+00
1	2	0,00E+00	4	2	0,00E+00
1	3	0,00E+00	4	3	0,00E+00
1	4	0,00E+00	4	4	-3,79E+04
1	5	0,00E+00	4	5	0,00E+00
1	6	0,00E+00	4	6	0,00E+00
2	1	0,00E+00	5	1	0,00E+00
2	2	0,00E+00	5	2	0,00E+00
2	3	0,00E+00	5	3	-1,53E-02
2	4	0,00E+00	5	4	0,00E+00
2	5	0,00E+00	5	5	-3,79E+04
2	6	0,00E+00	5	6	0,00E+00
3	1	0,00E+00	6	1	0,00E+00
3	2	0,00E+00	6	2	0,00E+00
3	3	3,80E+02	6	3	0,00E+00
3	4	0,00E+00	6	4	0,00E+00
3	5	-1,53E-02	6	5	0,00E+00
3	6	0,00E+00	6	6	0,00E+00